UNIVERSITY OF CALIFORNIA SAN DIEGO

Orbitofrontal Cortex Mediates Action and Outcome Information and is Disrupted in Alcohol Dependence

A dissertation submitted in partial satisfaction of the requirements for the degree

Doctor of Philosophy

in

Neurosciences

by

Christian Cazares

Committee in Charge:

Professor Christina Gremel, Chair
Professor Edward Callaway
Professor Eran Mukamel
Professor Kay Tye
Professor Bradley Voytek

2022

The dissertation of Christian Cazares is approved, and it is acceptable in quality and form for publication on microfilm and electronically.

University of California San Diego

2022

DEDICATION

Dedicated to my parents, Patricia and Ernesto Cazares, who made a lot of sacrifices to ensure my access to education, my brother Ernesto Cazares and my sister-in-law Priscilla Garcia, who always made themselves available whenever I needed life advice, my partner Maribel Patiño, whose love and companionship made carrying out this research possible, and my two cats Kira and L, who provided a lot of warmth at night.

EPIGRAPH

All moments, past, present, and future, always have existed, always will exist.

Kurt Vonnegut
“Slaughterhouse-Five”
Delacorte Publishing, 1969

TABLE OF CONTENTS

LIST OF ABBREVIATIONS

AUD	Alcohol use disorder
OFC	orbitofrontal cortex
M2	Secondary motor cortex
CIE	Chronic Intermittent Ethanol
CamKII	Calcium/calmodulin-dependent protein kinase II
PV, Pvalb	Parvalbumin
BEC	Blood ethanol concentration
RT	random time schedule
CRF	Continuous Reinforcement Schedule
PETH	Peri-event time histogram
TTL	transitor-transitor logic
RR	Response rate
DS	Dorsal striatum

LIST OF SUPPLEMENTAL FILES

1. Supplemental Tables: Tables 2.S1-2.S10

LIST OF FIGURES

ACKNOWLEDGEMENTS

I would like to acknowledge and thank all members of the Gremel lab for fostering a supportive and fun learning environment. I thank my advisor Professor Christina M. Gremel for her scientific mentorship and unwavering support for my extracurricular outreach. I thank Dr. Drew Schreiner for humoring my questions about code, Dr. Rafael Renteria for the gaming sessions, Dr. Ege Yalcinbas for the singing lessons, Emily Baltz for the hangouts, and Chloe Shields for her financial advice, and all of them together for their discussions, thoughtful input, and guidance in putting together these studies. I also thank my thesis committee for their critical input and constructive feedback regarding this work at our meetings.

I am grateful to my family and friends for providing an incredible support network while I pursued my PhD. Special thanks my parents Ernesto and Patricia, literally none of this would've been possible without their emotional support and continuous encouragement. Thanks to my brother Ernesto and my sister-in-law Pricscilla, who were willing to talk me through some tough times these past few years. Thank you to all of my friends in the program, with a special mention to Marley and Kevin as members of my class who stuck by as friends as we got busier and busier with graduate responsibilities. I especially want to thank Maribel Patiño for her unwavering support. Maribel is the smartest person I know and I am proud to be her sidekick as she goes on to achieve great things. I also thank Kira and L the cats for being funny little dudes.

Finally, I would like to thank all the diversity initiatives that have supported me throughout my academic career including the UC Berkeley Minority Access to Research Careers Program, NIH PREP, NINDS Blueprint DSPAN and the SFN Neuroscience

Scholars Program. They were so instrumental to my success that I went off to start my own with Maribel and others. Who knew Colors of the Brain would grow into what it is now.

Chapter 1, in full, is a reprint of the material as it appears in: Cazares C., Schreiner D., Gremel, C.M. (2021) Different Effects of Alcohol Exposure on Action and Outcome Related Orbitofrontal Cortex Activity. eNeuro. 2021 Mar. The dissertation author was the primary investigator and author of this paper. This work was supported by National Institute on Alcohol Abuse and Alcoholism Grants R00AA021780 and R01AA026077 (to C.M.G.) and F31AA027439 (to D.C.S.), Whitehall and Brain and Behavior Foundations (C.M.G.), and the National Science Foundation GRFP Grant DGE-1650112 (to C.C.).

Chapter 2, in full, is currently being prepared for submission for publication and will include Drew Schreiner as a co-author and Professor Christina M. Gremel as the senior author. The dissertation author will be the first author of this work. This work was funded by F99-NS120434 (C.C.), F31AA027439 (D.C.S.), R01AA026077 (C.M.G.), and a Whitehall Foundation Award (C.M.G).

VITA

2014 Bachelor of Arts, Cognitive Science
University of California Berkeley, Berkeley, CA, USA

2022 Doctor of Philosophy, Neurosciences
University of California San Diego, La Jolla, CA, USA

PUBLICATIONS

Schreiner D., Cazares C., Renteria R., Gremel, C.M. (2022). Information normally considered task-irrelevant drives decision-making and affects premotor circuit recruitment. Nature Communications 13, 2134

Yalcinbas, E. A., Cazares C**.**, Gremel, C.M. (2021). Call For A More Balanced Approach to Understanding Orbital Frontal Cortex Function. Beh. Neuro. 2021 Apr

Cazares C., Schreiner D., Gremel, C.M. (2021). Different Effects of Alcohol Exposure on Action and Outcome Related Orbitofrontal Cortex Activity. eNeuro. 2021 Mar

Renteria R**.,** Cazares C., Baltz E.T., Schreiner D.C., Yalcinbas E.A., Stainkellner T., Hnasko T.S., Gremel, C.M. (2021). Mechanism for differential recruitment of orbitostriatal transmission during actions and outcomes following chronic alcohol exposure. Elife. 2021 Mar 17;10:e67065. doi: 10.7554/eLife.67065. PMID: 33729155.

Renteria R., Cazares C., Gremel, C.M. (2020). Habitual Ethanol Seeking and Licking Microstructure of Enhanced Ethanol Self-Administration in Ethanol-Dependent Mice. Alcohol Clin Exp Res. 2020 Apr;44(4):880-891

Labruna, L., Tischler C., Cazares C., Greenhouse I., Duque J., Lebon F., Ivry RB.(2019). Planning face, hand, and leg movements: anatomical constraints on preparatory inhibition. J. Neurophysiol. 121, 1609:1620

Ung H., Cazares C., Nanivadekar A., Kini, L. Wagenaar J., Becker D., Kahana M., Sperling M., Sharan A. Lucas T., Baltuch G., Litt B., Davis K.A. (2017). Interictal Epileptiform Activity outside the Seizure Onset Zone Impacts Cognition. Brain, Volume 140, Issue 8, 1 August 2017, 2157:2168

Duque J., Labruna L., Cazares C., Ivry R. (2014). Dissociating the influence of response selection and task anticipation on corticospinal suppression during response preparation. Neuropsychologia 65:287:296

Labruna L., Lebon F., Duque Julie., Klein P-A., Cazares C., Ivry R. (2014). Generic inhibition of the selected movement and constrained inhibition of non-selected movements during response preparation. Journal of Cognitive Neuroscience 26:2, 269:278

ABSTRACT OF DISSERTATION

Orbitofrontal Cortex Mediates Action and Outcome Information and is Disrupted in Alcohol Dependence

by

Christian Cazares

Doctor of Philosophy in Neurosciences

University of California San Diego, 2022

Professor Christina Gremel, Chair

Alcohol use disorder (AUD) is characterized by cognitive deficits thought to escalate maladaptive behaviors that increase the vulnerability to relapse. Neurobiological investigations have identified a key role for orbitofrontal cortex (OFC) computations in control of adaptive behavior. OFC-based computations and their

underlying circuits have been shown to disrupted in alcohol addiction and other disorders characterized by repetitive behaviors. However, little is known about how these changes manifest *in vivo* when behaviors are self-initiated and reliant on inferences shaped by action-related information. In this dissertation, I used a mouse neural circuit-dissection approach in conjunction with an unconstrained lever-pressing task to investigate OFC computations made during adaptive behavior and their disruption in alcohol dependence. Chapter 1 explored how alcohol dependence induced changes in OFC neural activity correlates of self-initiated actions and their associated outcomes. Results suggested that chronic alcohol exposure induces long-lasting disruptions to OFC function such that activity associated with volitional actions was enhanced, but OFC activity contributions to outcome-related information was diminished. Chapter 2 investigated how different OFC populations support action-related computations, including computations relating to prior action information. Results identified a novel role for OFC excitatory and inhibitory neurons in the continuous integration of action information for behavioral control. These studies showed that OFC populations differentially encode action-related information in a dynamic manner, and that these cortical representations are significantly altered in alcohol dependence. Overall, this dissertation revealed some of the complexity of OFC's contributions to adaptive behavior and further support the OFC as a target brain region for the intervention of AUD.

INTRODUCTION

Voluntary actions are essential to survival and are indispensable to our daily lives. Voluntary actions are motor acts that are generated internally and involve decision processes consisting of deciding when to act, what action to perform, and when to perform it (Haggard, 2008). These behaviors rarely occur in isolation, rather they are made in consideration of prior experiences that may be similar in nature (Schreiner et al., 2021, 2022). Within the passage of time, relevant experiences continuously accumulate, and a vast array of information from those experiences is internalized, evaluated, and used to control behavior and achieve desired goals (Balleine and Dickinson, 1998; Balleine and O'Doherty, 2010; Bradfield et al., 2013; Dickinson, 1985; Lak et al., 2014; Niv, 2019; Rangel et al., 2008; Schreiner et al., 2022; Schuck et al., 2016).

Behavioral experiences can shape contextual knowledge and inform associations between actions and outcomes that can serve as internal sources of information used to guide adaptive behavior. In other words, inferences made about the state of the world are molded by relevant experiences. Information derived from experience includes historical, contextual, associative, and other internal factors that are subjective (Schreiner et al., 2021). New experiences can influence how inferences are used to adapt behavior, such as when task contingencies change (Balleine and Dickinson, 1998; Balleine and O'Doherty, 2010; Bradfield et al., 2013; Corbit et al., 2002). A failure to appropriately use information to update inferences about the task-at-hand are thought to underlie behavioral inflexibility, compulsivity, and impulsivity, which are all hallmarks of decision-making disorders, including AUD (Izquierdo and Jentsch, 2012; Lüscher et

al., 2020; Milad and Rauch, 2012; Pauls et al., 2014; Winstanley et al., 2010). These disorders are harmful not only to the health of individuals, but also create significant economic and societal burden. Progress towards developing effective treatments for these disorders has been hampered by a lack of fundamental understanding of the underlying neural circuitry governing action control and the types of action-related information these circuits integrate and use to guide adaptive behavior.

Our brains can integrate information derived from our experiences to create abstract representations of the rules governing the world around us (Niv, 2019). These representations can be influenced by observable contextual information, such as whether an external stimulus is present (are the lights on or off in the room?), and by information that is not readily available in the environment, but rather retrieved from memory or other internal sources. Such experiential information is thought to be integrated in real-time and continuously recruited during adaptive behavior (Aoi et al., 2020; Barron et al., 2020; Lak et al., 2014; Schreiner et al., 2021, 2022; Yoo et al., 2021). However, disentangling exactly what types of information derived from experiences is critical to guiding adaptive behavior can prove difficult, as animals can not only show high variability of responses within the same task, but can also show ostensibly similar responses that may in actuality reflect different behavioral controllers and associated neural circuits (Balleine, 2019; Balleine and Dickinson, 1998). In addition, studies investigating adaptive behavior have largely imposed rigid structures to their tasks, such as requiring limited choice behaviors that are elicited via immediately observable stimuli. While this may be advantageous to isolating aspects of behavior for ease of analysis, this rigidity neglects the unstructured nature of how voluntary actions

are carried out in the open world (Yoo et al., 2021). When acting on our own to achieve a goal, what information does the brain use to guide these voluntary actions? And how does disrupting the underlying circuitry responsible for integrating experiential information impact how these actions are adapted? This dissertation addresses these questions by using a rodent model of alcohol dependence and an unconstrained behavioral task to investigate the neural circuits governing adaptive voluntary actions.

Alcohol dependence is associated with decision-making dysfunctions that are thought to drive a relapsing cycle of intoxication, binging, withdrawal and craving that promotes excessive alcohol use despite negative consequences (Goldstein and Volkow, 2011; Gremel and Lovinger, 2017). Findings from preclinical and non-human animal models suggest that alcohol dependence results in long-lasting deficits in behavioral flexibility, including changes in action control (Renteria et al., 2018; Sjoerds et al., 2013). Drug-dependence is hypothesized to disrupt action control processes such that drug-seeking and drug-taking behaviors are biased towards habits (Belin et al., 2013). Often in these models, outcome devaluation procedures are used to probe the ability to update and infer a value representation to guide adaptive behavior (Ersche et al., 2016; Renteria et al., 2018). However, these approaches have been limited in understanding how alcohol dependence affects more unconstrained behaviors that do not rely on immediately observable stimuli to inform decisions and choices. Indeed, compulsive drug use in real-world scenarios occurs in contexts where individuals are faced with a wide-variety of choices, the vast majority which are not cued by environmental triggers (Hogarth, 2020).

A region known to implement behavioral control of actions is the OFC (Bradfield et al., 2015; Gremel and Costa, 2013; Gremel et al., 2016; Rhodes and Murray, 2013; Stalnaker et al., 2015). OFC behavioral control processes are thought to rely on information received by interconnected structures known to regulate emotion, memory, learning, and other functions critical for guiding adaptive behavior (Barreiros et al., 2021; Cavada et al., 2000; Rolls, 2004; Zhang et al., 2016). For example, reciprocal connections between the OFC and the basolateral amygdala (BLA) transmit and encode reward-related information critical for adapting behavior (Lichtenberg et al., 2017; Schoenbaum et al., 1998, 2003; Sias et al., 2021). Indeed, prior works have shown that intact OFC circuits functionally contribute to outcome re-evaluation and contingency updating processes necessary for shifts in behavior (Balleine et al., 2011; Baltz et al., 2018; Gremel and Costa, 2013; Groman et al., 2019; Izquierdo et al., 2004; Malvaez et al., 2019; Rhodes and Murray, 2013; Stalnaker et al., 2006). This function has been shown to be mediated in part by representations of contextual information inferred from memory, such as the expected outcome value of choices and expected contingencies of the ongoing task (Bradfield et al., 2015; Namboodiri et al., 2019; Niv, 2019; Padoa-Schioppa and Assad, 2006a; Stalnaker et al., 2014; Wallis, 2007, 2018; Young and Shapiro, 2011).

OFC processing of associative information led to the idea that OFC can represent abstract representations of perceptual and memory-related information that is critical to meeting task demands. In other words, OFC is through to form a “cognitive map” of task space that integrates information related to previous stimuli and choices to support ongoing decision-making processes (Gardner and Schoenbaum, 2021;

Sadacca et al., 2018; Schuck et al., 2016; Wilson et al., 2014; Yalcinbas et al., 2021). In support of this function, past investigations have shown that OFC can represent inferred value, reward and sensory-related information from prior choices before an upcoming choice is made (Hocker et al., 2021; Nogueira et al., 2017; Riceberg and Shapiro, 2017). These OFC-based contributions are critical, as OFC lesions have been shown to spare learning and decision-making behavior that relies on immediately observable stimuli, while performance becomes impaired as task rules get more abstract and being to rely more on inferred, unobservable information for success (Wilson et al., 2014). Yet little is known about how action-related information, beyond its outcome associations, is actively recruited by OFC to shape inferences critical for guiding future behavior. On the contrary, some lines of evidence suggests that action information is processed elsewhere in the cortex during behaviors guided by inferred value representations (Grattan and Glimcher, 2014; Padoa-Schioppa and Assad, 2006b; Padoa-Schioppa and Cai, 2011; Padoa-Schioppa and Conen, 2017). In addition, what is known about how OFC supports adaptive behaviors has largely ignored the rich diversity of cell types in the region (Yalcinbas et al., 2021), such as GABAergic interneurons that can shape and influence local network rhythmicity and local pyramidal neuron firing (Ferguson and Cardin, 2020; Kepecs and Fishell, 2014).

OFC structure, function and neurophysiology is disrupted in diseases characterized by repetitive behaviors, such as addiction and obsessive compulsive disorder (Badanich et al., 2011; Beck et al., 2012; Lüscher et al., 2020; Milad and Rauch, 2012; Nimitvilai et al., 2016, 2017; Pauls et al., 2014; Renteria et al., 2018; Robbins et al., 2019; Sjoerds et al., 2013). Specifically, OFC has been widely

associated with dysfunction induced by alcohol-dependence (Gremel and Costa, 2013; McGuier et al., 2015; Renteria et al., 2018). For example, studies on alcoholic patient have reported dependence-related hypoactivity in OFC during adaptive behavior tasks as well as abnormal output connectivity and widespread grey matter volume loss in this region compared to healthy controls (Beck et al., 2012; Reiter et al., 2016; Sjoerds et al., 2013; Tanabe et al., 2009). Animal models of alcohol dependence corroborate these findings, showing that prolonged drinking alters the structure and intrinsic function of OFC excitatory projection populations (McGuier et al., 2015; Nimitvilai et al., 2017; Renteria et al., 2018). As a result, dependence-induced deficits of goal-directed behavior are thought to involve a breakdown of OFC computations critical for shaping inferred representations of the state of the world, especially when observable information about ongoing processes and future consequences are not readily available (Schreiner et al., 2021; Wilson et al., 2014). Indeed, while neurobiological investigations have identified a key role for OFC computations in action control, the specific neural mechanisms underlying these computations and their disruption in addiction remain poorly understood.

An increased understanding of the neurobiological disruptions seen in decision-making disorders, such as AUD, has the potential to direct new strategies aimed at restoring appropriate behavior in these patient populations. Repeated transcranial magnetic stimulation studies targeting OFC have been proven effective at treating compulsivity in neuropsychiatric disorders (Nauczyciel et al., 2014; Price et al., 2021), thus there is a need to understand the types of information used to control self-initiated and un-cued behaviors within this circuit in health and disease. By using rodent models

of alcohol dependence, Chapter 1 of this dissertation directly assesses how neuronal populations supporting adaptive behavior are functionally disrupted by chronic alcohol exposure. To do so, we used a well-validated model of alcohol dependence, chronic intermittent ethanol (CIE), and performed in vivo extracellular recordings as mice performed an instrumental lever-pressing task in which they self-initiated lever-press responses and were required to hold down the lever past a minimum duration to earn a food reward. We found that 1) alcohol dependence disrupted goal-directed action control of task performance, 2) increased OFC activity associated with lever-pressing actions, and 3) decreased OFC activity during outcome-related epochs. Our results suggested that chronic alcohol exposure induced long-lasting disruptions to OFC function such that activity associated with actions was enhanced, but OFC activity contributions to outcome-related information was diminished. Overall our findings identified some of the complexity in how OFC's contributions to decision-making computations are altered following alcohol exposure and further supported the OFC as a target brain region for the intervention of AUD.

While the findings from Chapter 1 implicated OFC in representing self-initiated actions, it remained unknown whether OFC populations supported the use of action-related information to shape future behavior. Given that OFC has been hypothesized as key for inference-based Pavlovian behavior, Chapter 2 of this dissertation aimed to investigate whether OFC populations contributed to action-related inferences. To do so, we took advantage of our self-paced lever-press hold down task to probe how ongoing and prior lever press durations guided subsequent lever press performance. We found that 1) calcium activity of genetically identified OFC subpopulations differentially

instantiated ongoing and prior action information during ongoing and future behavior, 2) transient activity disruptions to OFC activity left mice unable to use recently executed durations to guide ongoing action performance, and that 3) a chronic functional loss of OFC circuit activity resulted in a compensatory mechanisms of repetitive action control, increasing behavioral reliance on the action that had just been completed. Thus our Chapter 2 results identified a novel role for OFC in the continuous integration of action information in guiding adaptive behavior.

Altogether, the two chapters of this dissertation provide insights of how alcohol dependence changes OFC support of adaptive behavior (Chapter 1), as well as how adaptive behaviors are influenced by action information processed within OFC circuits (Chapter 2). Importantly, we show that the use of tasks in which animals are free to initiate behavior when they wish to do so is helpful to understanding how circuits are continuously recruited to process information from prior experiences. Through an interdisciplinary approach to neural circuit dissection, our results suggest a more active role for OFC in processing information related to actions, which further highlights its relevance for therapeutic targeting in neuropsychiatric disorders characterized by repetitive behaviors.

References

Aoi, M.C., Mante, V., and Pillow, J.W. (2020). Prefrontal cortex exhibits multidimensional dynamic encoding during decision-making. Nat Neurosci *23*, 1410–1420. https://doi.org/10.1038/s41593-020-0696-5.

Badanich, K.A., Becker, H.C., and Woodward, J.J. (2011). Effects of chronic intermittent ethanol exposure on orbitofrontal and medial prefrontal cortex-dependent behaviors in mice. Behav Neurosci *125*, 879–891. https://doi.org/10.1037/a0025922.

Balleine, B.W. (2019). The Meaning of Behavior: Discriminating Reflex and Volition in the Brain. Neuron *104*, 47–62. https://doi.org/10.1016/j.neuron.2019.09.024.

Balleine, B.W., and Dickinson, A. (1998). Goal-directed instrumental action: contingency and incentive learning and their cortical substrates. Neuropharmacology *37*, 407–419. https://doi.org/10.1016/s0028-3908(98)00033-1.

Balleine, B.W., and O'Doherty, J.P. (2010). Human and rodent homologies in action control: corticostriatal determinants of goal-directed and habitual action. Neuropsychopharmacology *35*, 48–69. https://doi.org/10.1038/npp.2009.131.

Balleine, B.W., Leung, B.K., and Ostlund, S.B. (2011). The orbitofrontal cortex, predicted value, and choice. Annals of the New York Academy of Sciences *1239*, 43–50. https://doi.org/10.1111/j.1749-6632.2011.06270.x.

Baltz, E.T., Yalcinbas, E.A., Renteria, R., and Gremel, C.M. (2018). Orbital frontal cortex updates state-induced value change for decision-making. ELife *7*, e35988. https://doi.org/10.7554/eLife.35988.

Barreiros, I., Ishii, H., Walton, M., and Panagi, M.C. (2021). Defining an orbitofrontal compass: functional and anatomical heterogeneity across anterior-posterior and medial-lateral axes. Behavioral Neuroscience.

Barron, H.C., Reeve, H.M., Koolschijn, R.S., Perestenko, P.V., Shpektor, A., Nili, H., Rothaermel, R., Campo-Urriza, N., O'Reilly, J.X., Bannerman, D.M., et al. (2020). Neuronal Computation Underlying Inferential Reasoning in Humans and Mice. Cell *0*. https://doi.org/10.1016/j.cell.2020.08.035.

Beck, A., Wüstenberg, T., Genauck, A., Wrase, J., Schlagenhauf, F., Smolka, M.N., Mann, K., and Heinz, A. (2012). Effect of Brain Structure, Brain Function, and Brain Connectivity on Relapse in Alcohol-Dependent Patients. Arch Gen Psychiatry *69*, 842–852. https://doi.org/10.1001/archgenpsychiatry.2011.2026.

Belin, D., Belin-Rauscent, A., Murray, J.E., and Everitt, B.J. (2013). Addiction: failure of control over maladaptive incentive habits. Current Opinion in Neurobiology *23*, 564–572. https://doi.org/10.1016/j.conb.2013.01.025.

Bradfield, L.A., Bertran-Gonzalez, J., Chieng, B., and Balleine, B.W. (2013). The thalamostriatal pathway and cholinergic control of goal-directed action: interlacing new with existing learning in the striatum. Neuron *79*, 153–166. https://doi.org/10.1016/j.neuron.2013.04.039.

Bradfield, L.A., Dezfouli, A., van Holstein, M., Chieng, B., and Balleine, B.W. (2015). Medial Orbitofrontal Cortex Mediates Outcome Retrieval in Partially Observable Task Situations. Neuron *88*, 1268–1280. https://doi.org/10.1016/j.neuron.2015.10.044.

Cavada, C., Compañy, T., Tejedor, J., Cruz-Rizzolo, R.J., and Reinoso-Suárez, F. (2000). The Anatomical Connections of the Macaque Monkey Orbitofrontal Cortex. A Review. Cereb Cortex *10*, 220–242. https://doi.org/10.1093/cercor/10.3.220.

Corbit, L.H., Ostlund, S.B., and Balleine, B.W. (2002). Sensitivity to instrumental contingency degradation is mediated by the entorhinal cortex and its efferents via the dorsal hippocampus. J Neurosci *22*, 10976–10984.

Dickinson, A. (1985). Actions and Habits: The Development of Behavioural Autonomy. Philosophical Transactions of the Royal Society of London Series B *308*, 67. https://doi.org/10.1098/rstb.1985.0010.

Ersche, K.D., Gillan, C.M., Jones, P.S., Williams, G.B., Ward, L.H.E., Luijten, M., Wit, S. de, Sahakian, B.J., Bullmore, E.T., and Robbins, T.W. (2016). Carrots and sticks fail to change behavior in cocaine addiction. Science *352*, 1468–1471. https://doi.org/10.1126/science.aaf3700.

Ferguson, K.A., and Cardin, J.A. (2020). Mechanisms underlying gain modulation in the cortex. Nat Rev Neurosci *21*, 80–92. https://doi.org/10.1038/s41583-019-0253-y.

Gardner, M.P.H., and Schoenbaum, G. (2021). The orbitofrontal cartographer. Behav Neurosci *135*, 267–276. https://doi.org/10.1037/bne0000463.

Goldstein, R.Z., and Volkow, N.D. (2011). Dysfunction of the prefrontal cortex in addiction: neuroimaging findings and clinical implications. Nat Rev Neurosci *12*, 652–669. https://doi.org/10.1038/nrn3119.

Grattan, L.E., and Glimcher, P.W. (2014). Absence of Spatial Tuning in the Orbitofrontal Cortex. PLOS ONE *9*, e112750. https://doi.org/10.1371/journal.pone.0112750.

Gremel, C.M., and Costa, R.M. (2013). Orbitofrontal and striatal circuits dynamically encode the shift between goal-directed and habitual actions. Nature Communications *4*, 2264. https://doi.org/10.1038/ncomms3264.

Gremel, C.M., and Lovinger, D.M. (2017). Associative and sensorimotor cortico-basal ganglia circuit roles in effects of abused drugs. Genes, Brain and Behavior *16*, 71–85. https://doi.org/10.1111/gbb.12309.

Gremel, C.M., Chancey, J.H., Atwood, B.K., Luo, G., Neve, R., Ramakrishnan, C., Deisseroth, K., Lovinger, D.M., and Costa, R.M. (2016). Endocannabinoid Modulation of Orbitostriatal Circuits Gates Habit Formation. Neuron *90*, 1312–1324. https://doi.org/10.1016/j.neuron.2016.04.043.

Groman, S.M., Keistler, C., Keip, A.J., Hammarlund, E., DiLeone, R.J., Pittenger, C., Lee, D., and Taylor, J.R. (2019). Orbitofrontal Circuits Control Multiple Reinforcement-Learning Processes. Neuron *103*, 734-746.e3. https://doi.org/10.1016/j.neuron.2019.05.042.

Haggard, P. (2008). Human volition: towards a neuroscience of will. Nat Rev Neurosci *9*, 934–946. https://doi.org/10.1038/nrn2497.

Hocker, D.L., Brody, C.D., Savin, C., and Constantinople, C.M. (2021). Subpopulations of neurons in lOFC encode previous and current rewards at time of choice. ELife *10*, e70129. https://doi.org/10.7554/eLife.70129.

Hogarth, L. (2020). Addiction is driven by excessive goal-directed drug choice under negative affect: translational critique of habit and compulsion theory. Neuropsychopharmacol. *45*, 720–735. https://doi.org/10.1038/s41386-020-0600-8.

Izquierdo, A., and Jentsch, J.D. (2012). Reversal learning as a measure of impulsive and compulsive behavior in addictions. Psychopharmacology *219*, 607–620. https://doi.org/10.1007/s00213-011-2579-7.

Izquierdo, A., Suda, R.K., and Murray, E.A. (2004). Bilateral Orbital Prefrontal Cortex Lesions in Rhesus Monkeys Disrupt Choices Guided by Both Reward Value and Reward Contingency. J Neurosci *24*, 7540–7548. https://doi.org/10.1523/JNEUROSCI.1921-04.2004.

Kepecs, A., and Fishell, G. (2014). Interneuron cell types are fit to function. Nature *505*, 318–326. https://doi.org/10.1038/nature12983.

Lak, A., Costa, G.M., Romberg, E., Koulakov, A.A., Mainen, Z.F., and Kepecs, A. (2014). Orbitofrontal Cortex Is Required for Optimal Waiting Based on Decision Confidence. Neuron *84*, 190–201. https://doi.org/10.1016/j.neuron.2014.08.039.

Lichtenberg, N.T., Pennington, Z.T., Holley, S.M., Greenfield, V.Y., Cepeda, C., Levine, M.S., and Wassum, K.M. (2017). Basolateral Amygdala to Orbitofrontal Cortex Projections Enable Cue-Triggered Reward Expectations. J. Neurosci. *37*, 8374–8384. https://doi.org/10.1523/JNEUROSCI.0486-17.2017.

Lüscher, C., Robbins, T.W., and Everitt, B.J. (2020). The transition to compulsion in addiction. Nat Rev Neurosci *21*, 247–263. https://doi.org/10.1038/s41583-020-0289-z.

Malvaez, M., Shieh, C., Murphy, M.D., Greenfield, V.Y., and Wassum, K.M. (2019). Distinct cortical-amygdala projections drive reward value encoding and retrieval. Nat Neurosci *22*, 762–769. https://doi.org/10.1038/s41593-019-0374-7.

McGuier, N.S., Padula, A.E., Lopez, M.F., Woodward, J.J., and Mulholland, P.J. (2015). Withdrawal from chronic intermittent alcohol exposure increases dendritic spine density in the lateral orbitofrontal cortex of mice. Alcohol *49*, 21–27. https://doi.org/10.1016/j.alcohol.2014.07.017.

Milad, M.R., and Rauch, S.L. (2012). Obsessive-compulsive disorder: beyond segregated cortico-striatal pathways. Trends Cogn Sci *16*, 43–51. https://doi.org/10.1016/j.tics.2011.11.003.

Namboodiri, V.M.K., Otis, J.M., van Heeswijk, K., Voets, E.S., Alghorazi, R.A., Rodriguez-Romaguera, J., Mihalas, S., and Stuber, G.D. (2019). Single-cell activity tracking reveals that orbitofrontal neurons acquire and maintain a long-term memory to guide behavioral adaptation. Nat Neurosci *22*, 1110–1121. https://doi.org/10.1038/s41593-019-0408-1.

Nauczyciel, C., Le Jeune, F., Naudet, F., Douabin, S., Esquevin, A., Vérin, M., Dondaine, T., Robert, G., Drapier, D., and Millet, B. (2014). Repetitive transcranial magnetic stimulation over the orbitofrontal cortex for obsessive-compulsive disorder: a double-blind, crossover study. Transl Psychiatry *4*, e436. https://doi.org/10.1038/tp.2014.62.

Nimitvilai, S., Lopez, M.F., Mulholland, P.J., and Woodward, J.J. (2016). Chronic Intermittent Ethanol Exposure Enhances the Excitability and Synaptic Plasticity of Lateral Orbitofrontal Cortex Neurons and Induces a Tolerance to the Acute Inhibitory Actions of Ethanol. Neuropsychopharmacology *41*, 1112–1127. https://doi.org/10.1038/npp.2015.250.

Nimitvilai, S., Uys, J.D., Woodward, J.J., Randall, P.K., Ball, L.E., Williams, R.W., Jones, B.C., Lu, L., Grant, K.A., and Mulholland, P.J. (2017). Orbitofrontal Neuroadaptations and Cross-Species Synaptic Biomarkers in Heavy-Drinking Macaques. J. Neurosci. *37*, 3646–3660. https://doi.org/10.1523/JNEUROSCI.0133-17.2017.

Niv, Y. (2019). Learning task-state representations. Nat Neurosci *22*, 1544–1553. https://doi.org/10.1038/s41593-019-0470-8.

Nogueira, R., Abolafia, J.M., Drugowitsch, J., Balaguer-Ballester, E., Sanchez-Vives, M.V., and Moreno-Bote, R. (2017). Lateral orbitofrontal cortex anticipates choices and integrates prior with current information. Nat Commun *8*, 1–13. https://doi.org/10.1038/ncomms14823.

Padoa-Schioppa, C., and Assad, J.A. (2006a). Neurons in the orbitofrontal cortex encode economic value. Nature *441*, 223–226. https://doi.org/10.1038/nature04676.

Padoa-Schioppa, C., and Assad, J.A. (2006b). Neurons in the orbitofrontal cortex encode economic value. Nature *441*, 223–226. https://doi.org/10.1038/nature04676.

Padoa-Schioppa, C., and Cai, X. (2011). The orbitofrontal cortex and the computation of subjective value: consolidated concepts and new perspectives. Ann N Y Acad Sci *1239*, 130–137. https://doi.org/10.1111/j.1749-6632.2011.06262.x.

Padoa-Schioppa, C., and Conen, K.E. (2017). Orbitofrontal Cortex: A Neural Circuit for Economic Decisions. Neuron *96*, 736–754. https://doi.org/10.1016/j.neuron.2017.09.031.

Pauls, D.L., Abramovitch, A., Rauch, S.L., and Geller, D.A. (2014). Obsessive-compulsive disorder: an integrative genetic and neurobiological perspective. Nat Rev Neurosci *15*, 410–424. https://doi.org/10.1038/nrn3746.

Price, R.B., Gillan, C.M., Hanlon, C., Ferrarelli, F., Kim, T., Karim, H.T., Renard, M., Kaskie, R., Degutis, M., Wears, A., et al. (2021). Effect of Experimental Manipulation of the Orbitofrontal Cortex on Short-Term Markers of Compulsive Behavior: A Theta Burst Stimulation Study. Am J Psychiatry *178*, 459–468. https://doi.org/10.1176/appi.ajp.2020.20060821.

Rangel, A., Camerer, C., and Montague, P.R. (2008). Neuroeconomics: The neurobiology of value-based decision-making. Nat Rev Neurosci *9*, 545–556. https://doi.org/10.1038/nrn2357.

Reiter, A.M.F., Deserno, L., Kallert, T., Heinze, H.-J., Heinz, A., and Schlagenhauf, F. (2016). Behavioral and Neural Signatures of Reduced Updating of Alternative Options in Alcohol-Dependent Patients during Flexible Decision-Making. J Neurosci *36*, 10935–10948. https://doi.org/10.1523/JNEUROSCI.4322-15.2016.

Renteria, R., Baltz, E.T., and Gremel, C.M. (2018). Chronic alcohol exposure disrupts top-down control over basal ganglia action selection to produce habits. Nature Communications *9*, 211. https://doi.org/10.1038/s41467-017-02615-9.

Rhodes, S.E.V., and Murray, E.A. (2013). Differential Effects of Amygdala, Orbital Prefrontal Cortex, and Prelimbic Cortex Lesions on Goal-Directed Behavior in Rhesus Macaques. J Neurosci *33*, 3380–3389. https://doi.org/10.1523/JNEUROSCI.4374-12.2013.

Riceberg, J.S., and Shapiro, M.L. (2017). Orbitofrontal Cortex Signals Expected Outcomes with Predictive Codes When Stable Contingencies Promote the Integration of Reward History. J. Neurosci. *37*, 2010–2021. https://doi.org/10.1523/JNEUROSCI.2951-16.2016.

Robbins, T.W., Vaghi, M.M., and Banca, P. (2019). Obsessive-Compulsive Disorder: Puzzles and Prospects. Neuron *102*, 27–47. https://doi.org/10.1016/j.neuron.2019.01.046.

Rolls, E.T. (2004). The functions of the orbitofrontal cortex. Brain Cogn *55*, 11–29. https://doi.org/10.1016/S0278-2626(03)00277-X.

Sadacca, B.F., Wied, H.M., Lopatina, N., Saini, G.K., Nemirovsky, D., and Schoenbaum, G. (2018). Orbitofrontal neurons signal sensory associations underlying model-based inference in a sensory preconditioning task. ELife *7*, e30373. https://doi.org/10.7554/eLife.30373.

Schoenbaum, G., Chiba, A.A., and Gallagher, M. (1998). Orbitofrontal cortex and basolateral amygdala encode expected outcomes during learning. Nature Neuroscience *1*, 155–159. https://doi.org/10.1038/407.

Schoenbaum, G., Setlow, B., Saddoris, M.P., and Gallagher, M. (2003). Encoding Predicted Outcome and Acquired Value in Orbitofrontal Cortex during Cue Sampling Depends upon Input from Basolateral Amygdala. Neuron *39*, 855–867. https://doi.org/10.1016/S0896-6273(03)00474-4.

Schreiner, D.C., Yalcinbas, E.A., and Gremel, C.M. (2021). A Push For Examining Subjective Experience in Value-Based Decision-Making. Curr Opin Behav Sci *41*, 45–49. https://doi.org/10.1016/j.cobeha.2021.03.020.

Schreiner, D.C., Cazares, C., Renteria, R., and Gremel, C.M. (2022). Information normally considered task-irrelevant drives decision-making and affects premotor circuit recruitment. Nat Commun *13*, 2134. https://doi.org/10.1038/s41467-022-29807-2.

Schuck, N.W., Cai, M.B., Wilson, R.C., and Niv, Y. (2016). Human Orbitofrontal Cortex Represents a Cognitive Map of State Space. Neuron *91*, 1402–1412. https://doi.org/10.1016/j.neuron.2016.08.019.

Sias, A.C., Morse, A.K., Wang, S., Greenfield, V.Y., Goodpaster, C.M., Wrenn, T.M., Wikenheiser, A.M., Holley, S.M., Cepeda, C., Levine, M.S., et al. (2021). A bidirectional corticoamygdala circuit for the encoding and retrieval of detailed reward memories. Elife *10*, e68617. https://doi.org/10.7554/eLife.68617.

Sjoerds, Z., de Wit, S., van den Brink, W., Robbins, T.W., Beekman, A.T.F., Penninx, B.W.J.H., and Veltman, D.J. (2013). Behavioral and neuroimaging evidence for overreliance on habit learning in alcohol-dependent patients. Transl Psychiatry *3*, e337. https://doi.org/10.1038/tp.2013.107.

Stalnaker, T.A., Roesch, M.R., Franz, T.M., Burke, K.A., and Schoenbaum, G. (2006). Abnormal associative encoding in orbitofrontal neurons in cocaine-experienced rats during decision-making. European Journal of Neuroscience *24*, 2643–2653. https://doi.org/10.1111/j.1460-9568.2006.05128.x.

Stalnaker, T.A., Cooch, N.K., McDannald, M.A., Liu, T.-L., Wied, H., and Schoenbaum, G. (2014). Orbitofrontal neurons infer the value and identity of predicted outcomes. Nature Communications *5*, 3926. https://doi.org/10.1038/ncomms4926.

Stalnaker, T.A., Cooch, N.K., and Schoenbaum, G. (2015). What the orbitofrontal cortex does not do. Nature Neuroscience *18*, 620–627. https://doi.org/10.1038/nn.3982.

Tanabe, J., Tregellas, J.R., Dalwani, M., Thompson, L., Owens, E., Crowley, T., and Banich, M. (2009). Medial orbitofrontal cortex gray matter is reduced in abstinent substance-dependent individuals. Biol. Psychiatry *65*, 160–164. https://doi.org/10.1016/j.biopsych.2008.07.030.

Wallis, J.D. (2007). Orbitofrontal cortex and its contribution to decision-making. Annu Rev Neurosci *30*, 31–56. https://doi.org/10.1146/annurev.neuro.30.051606.094334.

Wallis, J.D. (2018). Decoding Cognitive Processes from Neural Ensembles. Trends in Cognitive Sciences *22*, 1091–1102. https://doi.org/10.1016/j.tics.2018.09.002.

Wilson, R.C., Takahashi, Y.K., Schoenbaum, G., and Niv, Y. (2014). Orbitofrontal cortex as a cognitive map of task space. Neuron *81*, 267–279. https://doi.org/10.1016/j.neuron.2013.11.005.

Winstanley, C.A., Olausson, P., Taylor, J.R., and Jentsch, J.D. (2010). Insight into the relationship between impulsivity and substance abuse from studies using animal models. Alcohol Clin Exp Res *34*, 1306–1318. https://doi.org/10.1111/j.1530-0277.2010.01215.x.

Yalcinbas, E.A., Cazares, C., and Gremel, C.M. (2021). Call for a more balanced approach to understanding orbital frontal cortex function. Behav Neurosci *135*, 255–266. https://doi.org/10.1037/bne0000450.

Yoo, S.B.M., Hayden, B.Y., and Pearson, J.M. (2021). Continuous decisions. Philosophical Transactions of the Royal Society B: Biological Sciences *376*, 20190664. https://doi.org/10.1098/rstb.2019.0664.

Young, J.J., and Shapiro, M.L. (2011). The orbitofrontal cortex and response selection. Annals of the New York Academy of Sciences *1239*, 25–32. https://doi.org/10.1111/j.1749-6632.2011.06279.x.

Zhang, S., Xu, M., Chang, W.-C., Ma, C., Hoang Do, J.P., Jeong, D., Lei, T., Fan, J.L., and Dan, Y. (2016). Organization of long-range inputs and outputs of frontal cortex for top-down control. Nat Neurosci *19*, 1733–1742. https://doi.org/10.1038/nn.4417.

CHAPTER ONE

Different Effects of Alcohol Exposure on Action and Outcome-Related Orbitofrontal Cortex Activity

Christian Cazares[1], Drew C. Schreiner[2] and Christina M. Gremel[1, 2]

[1]Neurosciences Graduate Program, University of California, San Diego, La Jolla, California, 92093

[2]Department of Psychology, University of California San Diego, La Jolla, California, 92093

Chapter One is a reprint of material that appeared in *eNeuro*, Vol. 8, Issue 2, 2021.

Abstract

Alcohol dependence can result in long-lasting deficits to decision-making and action control. Neurobiological investigations have identified orbitofrontal cortex (OFC) as important for outcome-related contributions to goal-directed actions during decision-making. Prior work has shown that alcohol dependence induces long-lasting changes to OFC function that persist into protracted withdrawal and disrupts goal-directed control over actions. However, it is unclear whether these changes in function alter representation of action and outcome-related neural activity in OFC. Here, we used the well-validated chronic intermittent ethanol (CIE) exposure and withdrawal procedure to model alcohol dependence in mice and performed in vivo extracellular recordings during an instrumental task in which lever-press actions made for a food outcome. We found alcohol dependence disrupted goal-directed action control and increased OFC activity associated with lever-pressing but decreased OFC activity during outcome-related epochs. The ability to decode outcome-related information, but not action information, from OFC activity following CIE exposure was reduced. Hence, chronic alcohol exposure induced a long-lasting disruption to OFC function such that activity associated with actions was enhanced, but OFC activity contributions to outcome-related information was diminished. This has important implications for hypotheses regarding compulsive and habitual phenotypes observed in addiction.

Introduction

Alcohol use disorder (AUD) can result in decision-making deficits that can persist into protracted abstinence. In those suffering from AUDs, these deficits are thought to contribute to habitual and compulsive alcohol-seeking, a persistent vulnerability to relapse, and decrements in daily cognitive function (Stephens and Duka, 2008; Berre et al., 2012; Reich and Goldman, 2015; Le Berre et al., 2017; Sebold et al., 2017; Bickel et al., 2018). With reports of alcohol dependence-induced functional and structural alterations across the cortex (Volkow et al., 1994, 1997; Laakso et al., 2002; Cardenas et al., 2011; Durazzo et al., 2011; Beck et al., 2012; Sjoerds et al., 2013; Thayer et al., 2016), it is highly likely that a broad array of computations normally contributing to efficacious decision-making are also altered. Identifying which computations are disrupted along with any corresponding aberrant activity patterns would offer a starting point for mechanistic investigations into cortical circuit alterations that produce these long-lasting impairments in decision-making.

One such cortical circuit that often shows long-lasting dependence-induced disruptions is the orbitofrontal cortex (OFC). Abstinent AUD patient studies generally report a hypoactive OFC both at baseline and during adaptive decision-making (Volkow et al., 1994, 1997; Boettiger et al., 2007; Sjoerds et al., 2013; Reiter et al., 2016) but also report OFC hyperactivity to stimuli and related approach behaviors (Wrase et al., 2002; Hermann et al., 2006; Reinhard et al., 2015), reminiscent of OFC hyperactivity reported in patients with other psychiatric conditions, including obsessive compulsive disorder (Milad and Rauch, 2012; Pauls et al., 2014; Robbins et al., 2019; Lüscher et al., 2020). This dichotomy of effects suggests that long-lasting perturbations to OFC

circuitry induced by alcohol dependence may differentially alter the computations performed by OFC neurons in response to information coming into OFC. Hence, initial investigations into computations performed by OFC during decision-making and their long-lasting disruption in alcohol dependence would provide a framework with which to investigate broader circuit mechanisms contributing to observed OFC dysfunction.

Several lines of evidence implicate the OFC as a key contributor to computations that can contribute to value-based decision-making processes (Fellows, 2007; Wallis, 2007; Gremel and Costa, 2013; Stalnaker et al., 2015; Padoa-Schioppa and Conen, 2017) as well as to compulsive control (Milad and Rauch, 2012; Pauls et al., 2014; Robbins et al., 2019; Lüscher et al., 2020). OFC neurons will modulate firing rate when subjects make a lever press (Gremel and Costa, 2013) and when presented with an appetitive outcome (Rolls et al., 1996; Wallis, 2011). Functional manipulations to OFC activity have generally supported a role for OFC in using outcome-related information to control decision-making (Gremel and Costa, 2013; Rhodes and Murray, 2013; Baltz et al., 2018; Malvaez et al., 2019). Interestingly, increased OFC activity has also been functionally implicated in contributing to compulsive control over behavior (Ahmari et al., 2013; Burguière et al., 2013; Pascoli et al., 2015, 2018), with previous work showing that increased OFC activity and downstream output supports compulsive lever pressing for dopamine neuron stimulation (Pascoli et al., 2018).

Likewise, animal models of alcohol dependence have revealed long-lasting dependence-induced disruptions to OFC-dependent processes, including behavioral flexibility and outcome devaluation (Badanich et al., 2011; Kroener et al., 2012; Lopez et al., 2014; Fernandez et al., 2017; Renteria et al., 2018, 2020). Chronic heavy alcohol

consumption in non-human primates, as well as prior chronic alcohol exposure in mice, results in long-lasting changes to OFC intrinsic excitability, synaptic transmission, and increases in dendritic spine density of OFC neurons (Badanich et al., 2013; McGuier et al., 2015; Nimitvilai et al., 2016, 2017; Renteria et al., 2018). Similar to findings in chronically drinking non-human primates (Nimitvilai et al., 2017), previous work has reported that chronic intermittent ethanol (CIE) vapor exposure and withdrawal procedures in mice led to a reduction in OFC excitability (Renteria et al., 2018). CIE-exposed mice also showed an insensitivity to outcome devaluation in protracted withdrawal, characterized as a reduction in goal-directed control and an increased reliance on habitual control over lever pressing for food. Notably, artificially increasing the activity of OFC projection neurons was sufficient to restore sensitivity to outcome devaluation in CIE-exposed mice (Renteria et al., 2018). To this end, the observed dependence-induced deficits in decision-making are hypothesized to include alterations to OFC activity critical for decision-making processes. However, whether this includes alterations to OFC activity during actions and outcome-related epochs is unknown.

Here, we examined CIE exposure-induced disruptions to OFC activity during protracted withdrawal in an instrumental task where actions are made for a food outcome. We used an adapted action contingency task, historically termed action differentiation (Platt et al., 1973; Kuch, 1974; Yin, 2009; Fan et al., 2012). In this task, mice must learn to press and hold a lever down beyond a fixed minimum duration to earn a food reward. The structure of the task allows us to look at OFC activity at the onset, during, and offset of lever presses, as well as during outcome-related epochs. Prior works have found that alcohol-exposed rats and mice show similar acquisition of

lever-press performance compared with naive controls, but outcome devaluation and contingency degradation procedures (Corbit et al., 2012; Lopez et al., 2014; Morisot et al., 2019; Renteria et al., 2018; Barker et al., 2020) have shown that such lever pressing is controlled by habitual, instead of goal-directed, processes. Thus, in a subset of mice, we performed outcome devaluation testing procedures after acquisition. Replicating previous findings, we show that air and CIE mice acquire similar lever pressing performance. However, subsequent outcome devaluation testing showed that such lever pressing was under habitual control in CIE mice and goal-directed control in air mice. When we examined OFC activity during behavioral acquisition, we found that prior induction of alcohol dependence led to higher OFC firing rates related to lever-pressing, but reduced firing rates during periods associated with outcome delivery. Decoder analyses on OFC activity showed reduced accuracy to classify outcome related information in CIE-exposed mice compared with controls. Thus, while CIE led to increased activity related to actions, it reduced OFCs normal representation of outcome-related information that may be important for goal-directed decision-making.

Results

Induction of ethanol dependence disrupts goal-directed control over lever pressing

We employed a well-validated model of CIE vapor exposure and repeated withdrawal (Becker and Hale, 1993; Becker and Lopez, 2004; Lopez and Becker, 2005; Griffin et al., 2009). Mice were exposed to periods of ethanol (CIE) or air (air) vapor and subsequent withdrawal over a period of four weeks (six vapor cohorts; air: n = 17, CIE: n = 16; Figure 1.1A). CIE procedures produced mean BECs in ethanol-exposed mice in line with previous reports (29.53 ± 2.36 mm; Lopez and Becker, 2005; Renteria et al.,

2018). Alcohol withdrawal has been delineated into two phases; an immediate acute withdrawal period (2–3 d), followed by a protracted period extending at least three months (Heilig et al., 2010). To examine OFC activity and related behavior during this protracted withdrawal period, food-restricted mice began instrumental training and testing procedures 5 d after their last vapor exposure.

To examine the effects of prior CIE procedures on OFC activity during action and outcome-related epochs in decision-making, we adapted an instrumental task examining action differentiation (Figure 1.1A), where a mouse must learn to press and hold a lever down beyond a fixed minimum duration to earn a reward (Yin, 2009; Fan et al., 2012). Throughout training, mice learned to press and hold down a lever beyond a predetermined minimum duration to earn a food pellet on release of the lever. Mice self-initiated and self-terminated every lever press in the absence of any extrinsic cues signaling lever press duration. Importantly, reward delivery occurred only at the offset of a lever press that exceeded the duration criteria (Figure 1.1B-C), preventing the use of reward presence to signal lever press termination. Thus, this task produces discretized behavior epochs conducive to neural activity analysis (e.g., lever-press onset, during the lever-press, lever-press offset, and outcome delivery).

Following vapor procedures, air and CIE mice underwent action differentiation training, with the initial criterion for lever press duration set at 800-ms for five daily sessions, followed by five daily sessions of a 1600-ms criterion (see Materials and Methods). Representative sessions from one air and one CIE mouse on a 1600-ms criteria day are shown in Figure 1.1C, suggesting that mice show a distribution of lever press durations that approximate the duration criterion. This distribution of lever presses

Figure 1.1

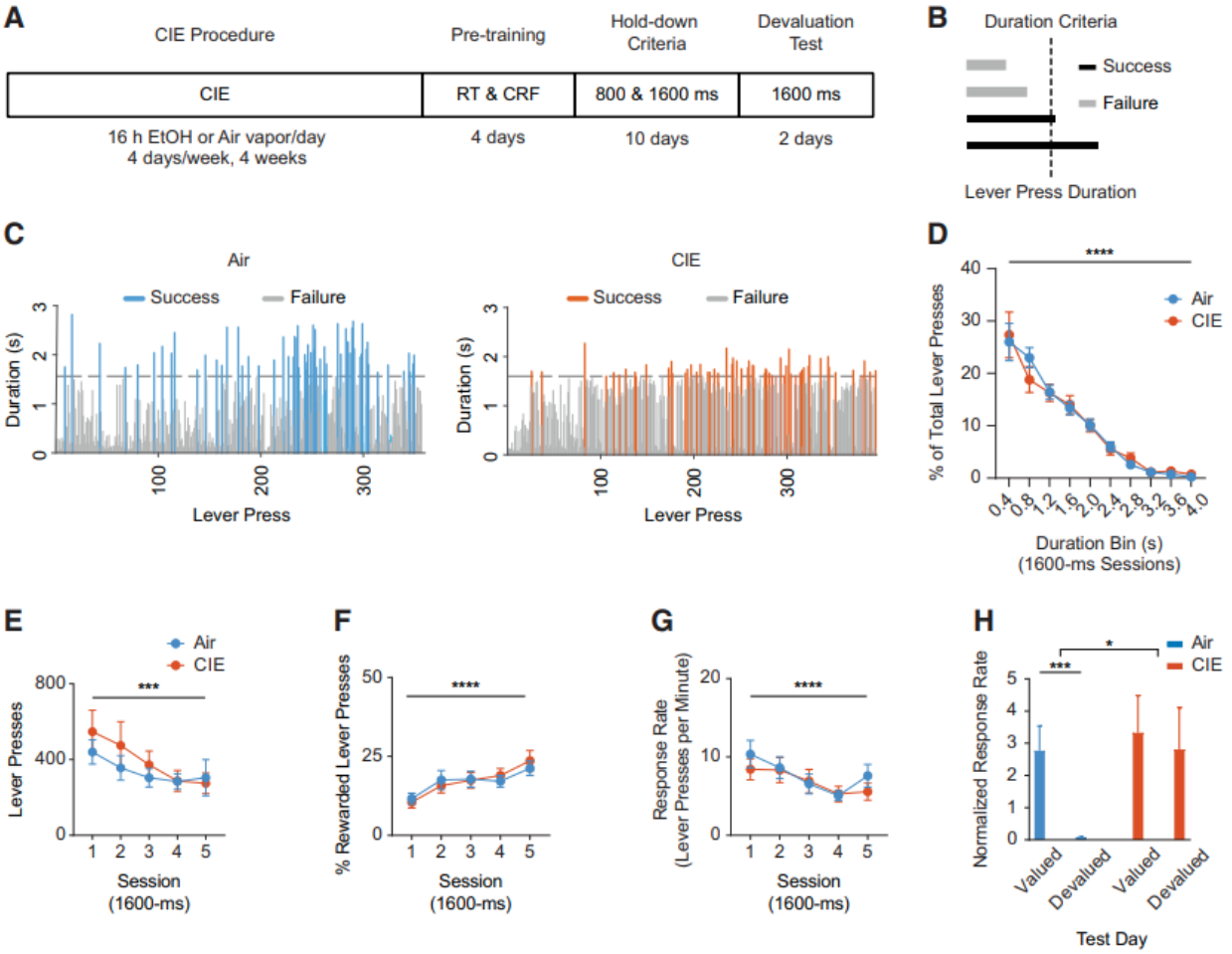

Figure 1.1. Effects of alcohol dependence on lever press acquisition (**A–G**) and outcome devaluation (**H**). A, Experimental timeline starting with the CIE procedure, subsequent RT delivery of outcome, fixed-ratio CRF on lever press, five daily sessions of 800-ms, and then five daily sessions of 1600-ms, lever press duration criterion sessions and, lastly, two subsequent days of outcome devaluation (DV) testing. **B**, Schematic of lever press duration performance. Lever presses exceeding the session's minimum hold-down duration criterion were rewarded only at the offset of the lever press. **C**, Example lever press performance from individual air (left) and CIE (right) mice during a 1600-ms hold-down duration criterion session late in training. Distribution of lever press durations (**D**), average total lever presses (**E**), average percentage of rewarded lever presses (**F**), and average response rate through 1600-ms lever press duration criterion sessions (**G**). **H**, Average normalized response rate in valued and devalued states throughout devaluation testing. Lever press duration distributions throughout acquisition and predevaluation test food consumption are shown in Figure 1.S1. Data points represent mean ± SEM; *p < 0.05, ***p < 0.001, ****p < 0.0001.

Figure 1.S1

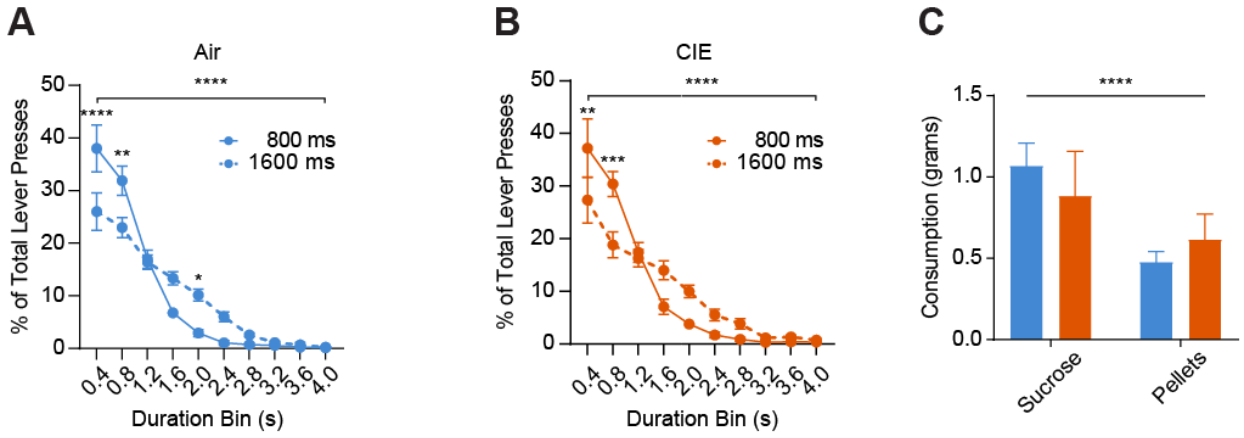

Figure 1.S1. ***A–C***, Lever press performance throughout acquisition and predevaluation test food consumption. ***A***, Distribution of the percentage of total lever presses binned by duration for 800- and 1600-ms criteria days for air and (***B***) CIE groups. In the air group, a two-way repeated measures ANOVA (bin × criteria) on the lever press duration distribution revealed an interaction: $F_{(9,270)} = 6.21$, $p < 0.0001$, and a main effect of bin: $F_{(9,270)} = 87.73$, $p < 0.0001$ (*post hoc* comparisons, $p < 0.05$). In the CIE group, a two-way repeated measures ANOVA (bin × criteria) on the lever press duration distribution revealed an interaction: $F_{(9,261)} = 4.37$, $p < 0.0001$, and a main effect of bin only: $F_{(9,261)} = 57.03$, $p < 0.0001$ (*post hoc* comparisons $p < 0.05$). ***C***, Total grams of food pellet and 20% sucrose solution consumed during each 1-h *ad libitum* access feeding period before each 10-min outcome devaluation test session. A two-way repeated measures ANOVA (food type × treatment) on grams consumed during this period found no interaction, but a main effect of food type: $F_{(1,20)} = 25.2$, $p > 0.0001$. Data points represent mean ± SEM; $^{**}p < 0.01$, $^{***}p < 0.001$, $^{****}p < 0.0001$.

was similar between air and CIE mice (1600-ms criteria training sessions, two-way repeated measures ANOVA (bin × treatment); no interaction; main effect of bin: $F_{(9,252)} = 53.56$, $p < 0.0001$), and importantly, each group showed evidence of learning with rightward shifts in their corresponding lever press duration distributions following the switch from 800- to 1600-ms training criteria (Figure 1.S1A-B). We focused our examinations on behavior throughout the 1600-ms criterion sessions, after mice had learned the action differentiation rule and had shifted to a longer duration contingency. Air and CIE mice showed similar levels of lever pressing that increased across sessions (mixed-effects repeated measures ANOVA (session × treatment); no interaction; main effect of session only: $F_{(4,121)} = 5.36$, $p < 0.0001$; Figure 1.1E). This task was similarly challenging for air and CIE mice, and only ~25% of total lever presses in air and CIE mice exceeded the duration criterion within each session (mixed-effects repeated measures ANOVA (session × treatment); no interaction; main effect of session: $F_{(4,121)} = 12.28$, $p < 0.0001$; Figure 1.1F). Further, CIE treatment did not alter response rates, which increased across sessions for both air and CIE mice (mixed-effects repeated measures ANOVA (session × treatment); no interaction; main effect of session: $F_{(4,121)} = 12.28$, $p < 0.0001$). Thus, as expected, CIE and air mice show similar lever press acquisition for food reward.

Examination of lever press performance as discussed above, however, cannot distinguish whether lever press is under goal-directed of habitual control. To examine whether the observed lever pressing was under different action controllers in CIE compared with air mice, we performed outcome devaluation procedures and testing following training on the 1600-ms duration criterion. In outcome devaluation testing, a

reduction in response rates following prefeeding with the outcome normally earned through lever pressing has been defined as a measure of goal-directed control (Dickinson, 1985). Prior work has found that alcohol dependence reduces the contribution of goal-directed control to lever pressing for food (Dickinson, 1985; Lopez et al., 2014; Renteria et al., 2018) within the time frame examined in the present experiment (Renteria et al., 2018). We subjected a subset of air and CIE mice to sensory-specific satiation of food pellets previously earned by lever pressing or to a previously habituated control outcome (20% sucrose solution). In each of the two consecutive test days, mice had ad libitum access to either pellets (devalued state) or sucrose solution (valued state) for 1 h before measuring non-reinforced lever press responses in the operant chamber throughout each 10-min 1600-ms duration criterion session. While air mice clearly reduced response rates (normalized to the response rate during last two days of acquisition) in the devalued state compared with valued state, CIE mice did not. A two-way repeated measures ANOVA (value × treatment) revealed different patterns of responding in treatment groups (interaction: $F_{(1,22)} = 6.961$, $p = 0.015$; main effect of value only: $F_{(1,22)} = 12.54$, $p = 0.001$). Post hoc analysis on normalized response rates revealed a difference between valued and devalued test sessions in air mice ($p = 0.0002$), but not in CIE mice ($p > 0.5$). As air and CIE mice consumed similar amounts of both outcomes during the prefeeding periods (Figure 1.S1C), the data show that lever press performance in CIE mice was not controlled by goal-directed processes.

OFC populations differentially encode lever-pressing and outcome-related components

Given that the deficits in outcome devaluation observed in CIE mice have been shown to involve OFC (Gourley et al., 2013; Gremel and Costa, 2013; Rhodes and Murray, 2013; Gremel et al., 2016; Renteria et al., 2018), and OFC modulates activity during outcome-related epochs (Rolls et al., 1996; Wallis, 2011), we hypothesized that alcohol exposure would disrupt OFC neural activity related to lever press and outcome-related epochs in our task. We examined OFC activity in relation to task epochs in a subset of the mice that had been implanted with chronic indwelling micro-electrode arrays into the OFC before the start of CIE procedures (five vapor cohorts; air $n = 9$, CIE $n = 9$; Figure 1.2A).

We focused on OFC activity data collected during the last two sessions of the 1600-ms duration criterion, a time point during which animals from both groups most proficiently performed the task. Putative single OFC unit spike activity was aligned to timestamps collected each time a lever press onset, offset, or pellet reward delivery occurred (see Materials and Methods). Importantly, there was no effect of CIE exposure on average baseline firing rates ($p > 0.05$; Figure 1.2B). More OFC units in CIE mice (67%) than air mice (54%) showed significantly altered firing rates during any task-related epochs (Figure 1.2C; $\chi^2_{1,667} = 10.21$, $p < 0.002$; see Materials and Methods). However, in both groups, we found similar proportions of OFC units that significantly up-modulated (increased firing rate) or down-modulated (decreased firing rate) across lever press onset, lever press offset, and outcome delivery epochs (χ^2s < 3.76, ps > 0.05; Figure 1.2D). Furthermore, we found that in both air and CIE mice, individual OFC units usually altered activity across multiple epochs (e.g., both the onset and offset of a lever press; Figure 1.2E; $\chi^2_{6,394} = 8.04$, $p < 0.24$), with relative high percentages of OFC units

Figure 1.2

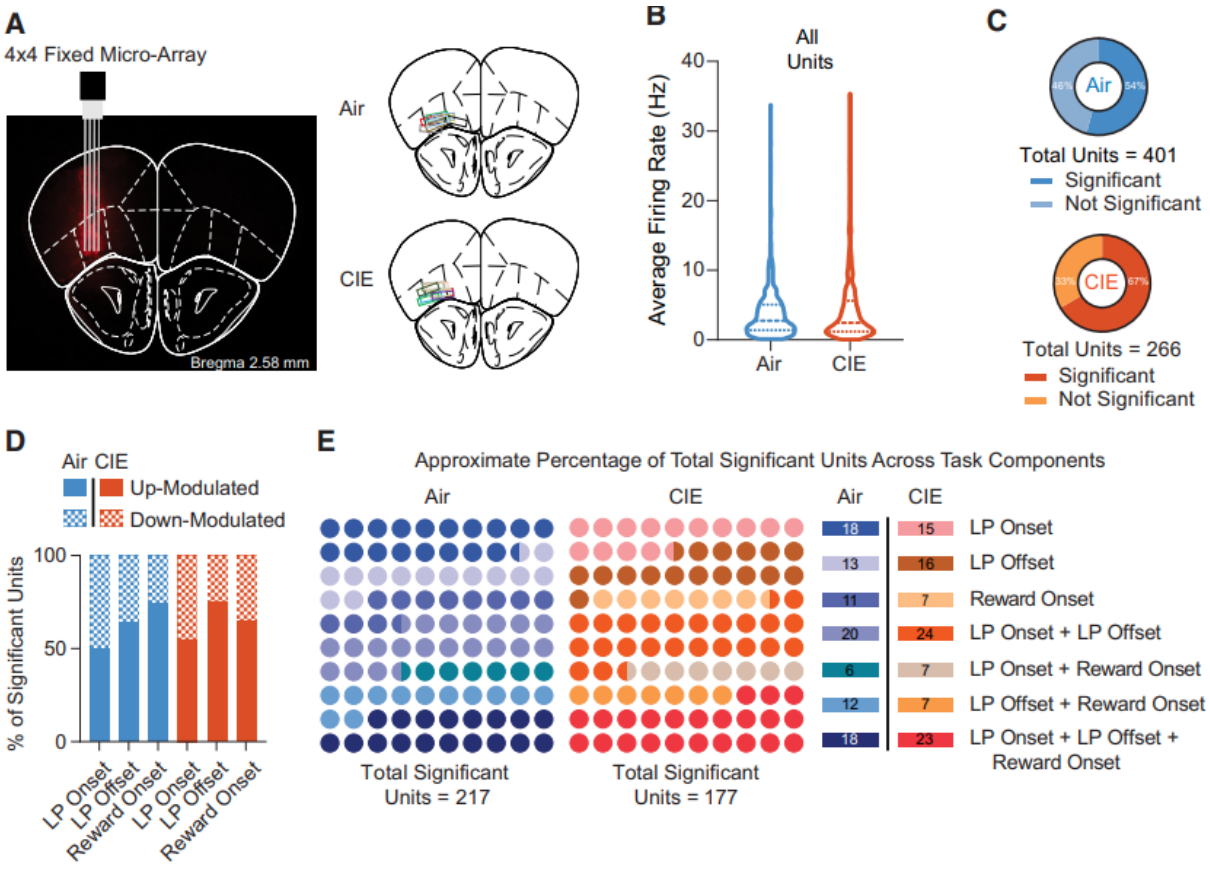

Figure 1.2. ***A–E***, OFC activity correlates of lever pressing and outcome delivery. ***A***, Representative image of fixed micro-array implant over the orbitofrontal cortex. Implant locations segmented by air and CIE groups. A subset of micro-arrays was dyed with a 25 mg/ml DiI solution in 200 proof ethanol for placement verification. ***B***, Average firing rates from all captured units during a baseline period (−5 to −2 s before lever press onset) for air and CIE cohorts. ***C***, Proportion of all captured units in which firing rates significantly deviated from a baseline period (−5 to −2 s before lever press onset) for air (~54%) and CIE (~66%) groups. ***D***, Percentage of units that significantly increased or decreased their firing rates from baseline in relation to lever press onset, offset, and food pellet reward delivery. ***E***, Percentage of units that significantly changed their firing rates from baseline in relation to discrete task events (lever press onset: air: ~18%, CIE: ~15%; lever press offset: air: ~13%, CIE: ~16%; reward delivery: air: ~11%, CIE: ~7%) as well as multiple task components (lever press onset and offset: air: ~20%, CIE: ~24%; lever press onset and reward delivery: air: ~6%, CIE: ~7%; lever press offset and reward delivery: air: ~12%, CIE: ~7%; lever press onset, offset, and reward delivery: ~18%, CIE: ~23%).

encoding action onset, action offset, and reward (air = 18%; CIE = 23%). Air and CIE mice showed similar numbers of significantly modulated units/mouse across events (lever press onset (air = 7.83 ± 1.8, CIE = 7.3 ± 1.8); lever press offset (air = 8.06 ± 1.6, CIE = 7.11 ± 1.7), reinforcement delivery (air = 6.11 ± 2.3, CIE = 4.61 ± 1.33). Altogether, this suggests that the OFC populations normally recruited during this instrumental task were largely not altered following the induction of alcohol dependence.

Prior CIE procedures enhances OFC lever press-related activity

While we observed similar recruitment of OFC populations during behavior, it may be that the magnitude and patterns of OFC activity during task-related epochs are different between the two groups. We first asked whether CIE would alter OFC activity associated with the initiation of lever pressing. We examined the firing rate activity of all significantly modulated units during the 1000-ms period preceding lever press onset, as shown in the normalized activity peri-event heatmaps in both air and CIE animals (Figure 1.3A). We found greater increases in baseline normalized OFC firing rates before the onset of lever pressing in CIE mice compared with air mice (Figure 1.3C). A two-way repeated measures ANOVA (250-ms bin × treatment) showed no interaction, but a main effect of treatment only ($F_{(1,1032)} = 17.39$, $p < 0.0001$). This increase in firing rates was also present when we examined up-modulated and down-modulated CIE populations separately (Figure 1.S2A-B), suggesting an overall increase in action-related OFC activity in CIE mice.

We next asked whether activity associated with lever press initiation reflected future performance outcomes, i.e., were firing rates different for lever presses that were eventually rewarded? To this end, we grouped lever press durations by whether they

Figure 1.3

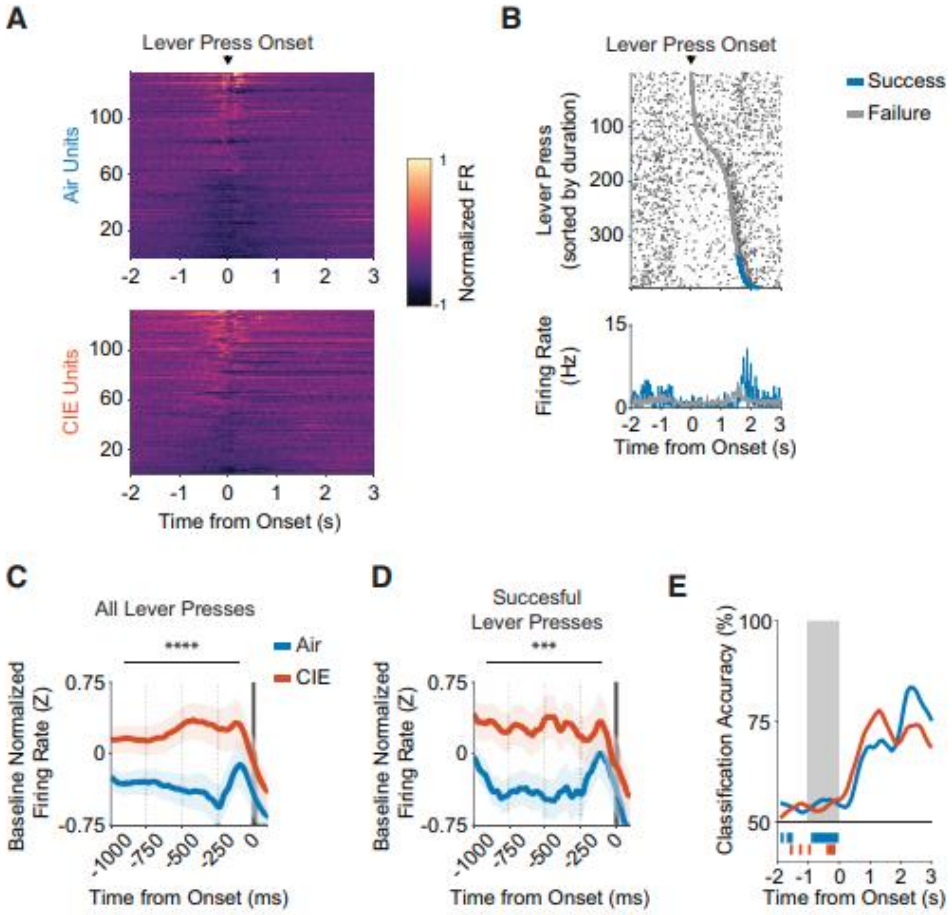

Figure 1.3. ***A–E***, Ethanol dependence alters OFC activity correlates of lever pressing initiation. ***A***, Heat map of normalized firing rates for units that significantly increased or decreased from baseline, displayed relative to lever press onset. Units are sorted by activity from a 1-s window around lever press onset. ***B***, Raster plot of a representative unit's firing rate relative to lever press onset, sorted from shortest to longest durations within a 1600-ms lever press criterion session that occurred late in training. Gray and blue markers indicate the end of lever presses that failed or succeeded in exceeding the 1600-ms lever press criterion, respectively. ***C***, Average z-scored firing rate changes from baseline for all lever presses and (***D***) successful lever presses only. Firing rate changes were compared across four 250-ms bins relative to lever press onset. ***E***, SVM classification accuracy of task performance outcomes (i.e., did lever press exceed 1600-ms hold-down criterion?) from all captured air and CIE units, displayed relative to lever press onset. Bars underneath traces indicate time points before the onset of the lever press in which classification accuracy was significantly different compared with the null distribution. Shaded region indicates time points in which classification accuracy comparisons were made between air and CIE groups. OFC activity correlates of lever pressing initiation are shown by significantly up-modulated and down-modulated unit averages in Figure 2.3-1. Data points represent mean ± SEM; ***$p < 0.001$, ****$p < 0.0001$.

Figure 1.S2. ***A–D***, OFC activity correlates of lever pressing initiation are altered by ethanol dependence but do not reflect future outcomes. ***A***, Average z-scored firing rate changes from all lever presses for significantly up-modulated and (***B***) down-modulated units from air and CIE groups, displayed relative to lever press onset. In up-modulated units, a two-way repeated measures ANOVA (bin × treatment) on activity prior to lever press onset revealed no interactions, but main effects of bin: $F_{(3,564)} = 12.34$, $p < 0.0001$ and treatment: $F_{(1,564)} = 5.878$, $p = 0.016$. In down-modulated units, a two-way repeated measures ANOVA (bin × treatment) on activity prior to lever press onset revealed no interactions, but main effects of bin: $F_{(3,508)} = 25.11$, $p < 0.0001$ and treatment: $F_{(1,508)} = 38.84$, $p < 0.0001$. *Post hoc* comparisons on down-modulated unit activity found differences between air and CIE groups in the 2nd ($p = 0.036$), 3rd ($p < 0.001$), and 4th ($p = 0.0045$) bins. ***C***, Air (left) and CIE (right) group's average z-scored firing rate changes of up-modulated and (***D***) down-modulated units, segmented by whether a lever press successfully exceeded the 1600-ms duration criterion or not, and displayed relative to lever press onset. For the air group, individual two-way repeated measures ANOVAs (bin × outcome) on activity prior to lever press onset revealed no interactions, but main effect of bin only for up-modulated ($F_{(3,560)} = 14.47$, $p < 0.0001$) and down-modulated ($F_{(3,552)} = 37.13$, $p < 0.0001$) units. Similarly, for the CIE group, individual two-way repeated measures ANOVAs (bin × outcome) on activity prior to lever press onset revealed no interactions, but main effect of bin only for up-modulated ($F_{(3,568)} = 4.19$, $p = 0.006$) and down-modulated ($F_{(3,464)} = 9.77$, $p < 0.0001$) units. Average z-scored firing rate changes were compared between treatment groups or outcomes across four 250-ms bins relative to lever press initiation. Data points represent mean ± SEM; *$p < 0.05$, **$p < 0.01$, ***$p < 0.001$, ****$p < 0.0001$.

Figure 1.S2

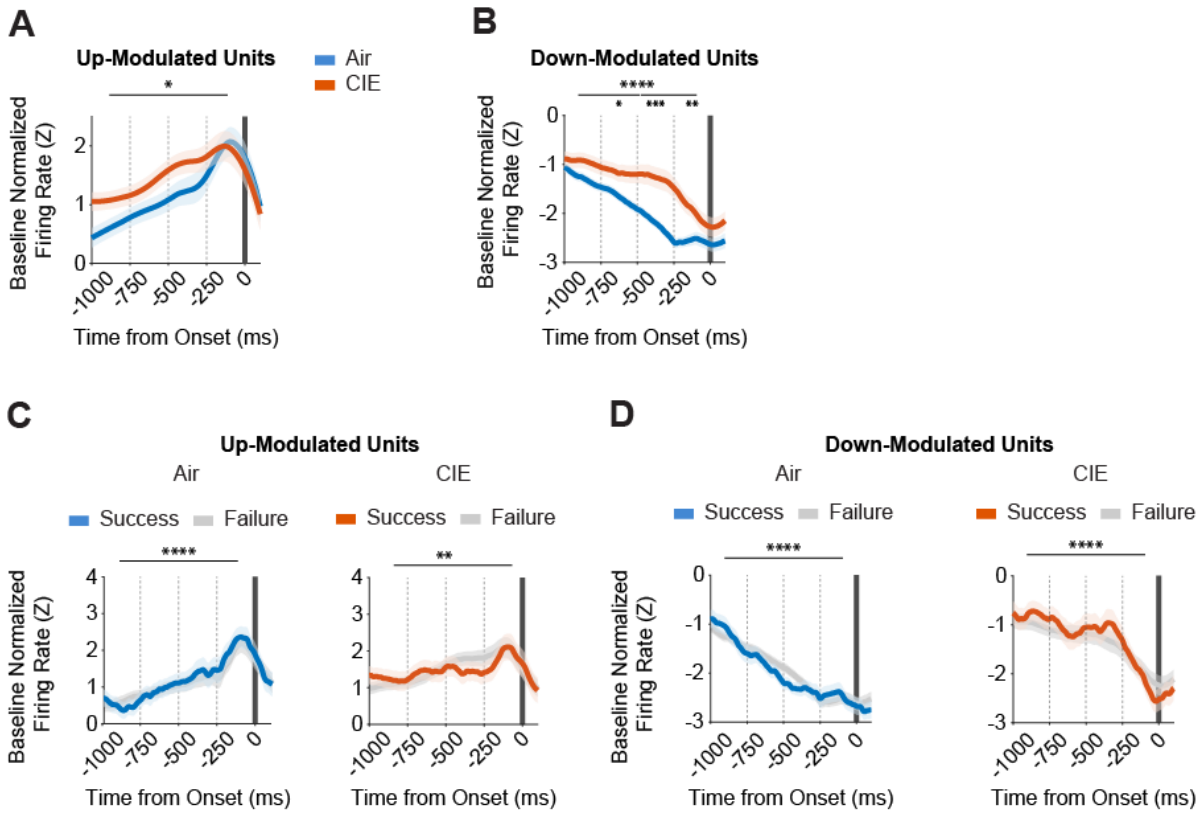
A
Up-Modulated Units
Air
CIE
Baseline Normalized Firing Rate (Z)
Time from Onset (ms)
B
Down-Modulated Units
Baseline Normalized Firing Rate (Z)
Time from Onset (ms)
C
Up-Modulated Units
Air
CIE
Success
Failure
Baseline Normalized Firing Rate (Z)
Time from Onset (ms)
D
Down-Modulated Units
Air
CIE
Success
Failure
Baseline Normalized Firing Rate (Z)
Time from Onset (ms)

successfully exceeded the lever press duration criterion or not (Figure 1.3B). We did not find evidence of predictive coding of successful performance in either air or CIE mice (Figure 1.S2C-D). In addition, when we examined only lever presses that were successful, the increased firing rate observed in CIE mice was still present (two-way repeated measures ANOVA (bin × treatment): main effect of treatment only ($F_{(1,1032)} = 14.58$, $p = 0.0001$; Figure 1.3D). We then trained a support vector machine (SVN) model with the peri-event firing rate activity of all captured (including significant and non-significant activity modulation in relation to behavioral epochs) units to directly test whether firing rates could accurately classify whether an individual lever press exceeded the 1600-ms duration criterion. In line with the lack of predictive coding, we found overall low classification performance that did not differ between air and CIE mice. A two-way repeated measures ANOVA (bin × treatment) comparisons of temporally binned classification performance between air and CIE mice revealed no significant differences within the 1000-ms period preceding lever press onset ($p > 0.29$). Thus, prior CIE procedures increased OFC activity associated with action onset; however, this activity, as well as activity in air control mice, was not predictive of impending lever-press success.

Prior CIE procedures have little effect on OFC activity during lever press execution

We next asked whether the increased OFC activity observed in CIE mice before lever-press onset would persist as mice held down the lever. Our analysis focused solely on units that were significantly modulated before the onset of a lever press. When we examined individual unit activity raster plots (Figure 1.3B), we often observed broad reductions in OFC activity as mice held down the lever. Indeed, we found on average

only ~38% of total lever presses made had at least one putative action potential occur during lever press execution, and this was not different in CIE mice (air mice = 37.85 ± 2%; CIE mice = 38.25± 2%; unpaired t test with Welch's correction: $t_{(257.4)} = 0.15$, $p = 0.88$).

As there was a distribution of lever press durations in each session, we next examined whether this relative reduction in OFC activity was different depending on the duration of the lever press being executed. We also examined whether prior CIE procedures would alter any potential change in activity during the lever press itself. To examine this, for a given mouse on a given day, we first divided lever presses within a session into four quartiles (see Materials and Methods; Figure 1.4A). Mean quartile distribution boundaries were similar between groups (Figure 1.S3A-C). Then, for each of the lever presses made in those quartiles, spike activity that happened while the mouse was holding down the lever (duration of the press) was z-scored normalized to baseline and divided into four equal segments spanning the lever press duration. This segment z-scored activity was then averaged within air and CIE groups. As shown by baseline normalized z-scored activity from a representative unit in Figure 1.4B, this allowed us to examine activity changes across the duration of the lever press based on the relative length of the final lever press duration.

We found OFC firing rates during the execution of the lever press did differ depending on the duration of the lever press; however, prior CIE exposure had very little effect on these patterns. As exemplified by Figure 1.4B, longer lever presses showed lower firing rates during the lever press, with an increase in firing rate occurring close to the release of the lever press. In air mice, a two-way repeated measures ANOVA

Figure 1.4

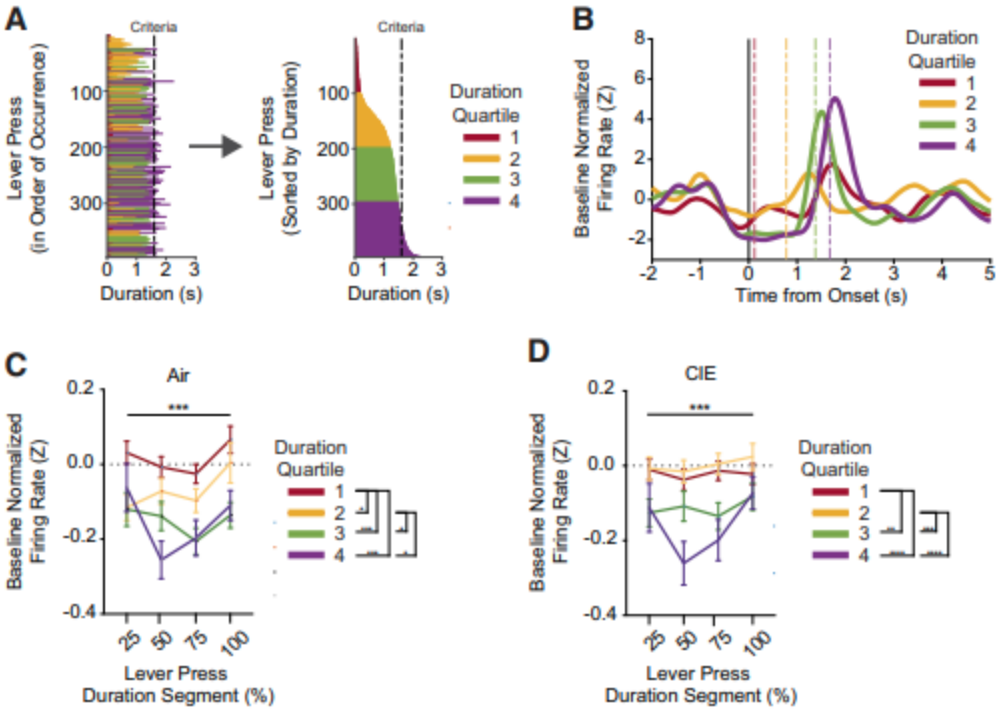

Figure 1.4. ***A–D***, OFC reduces firing while mice hold down the lever. ***A***, Lever presses were segmented into four quartiles determined by the distribution of lever press durations within each individual session. ***B***, Representative unit's mean baseline normalized z-scored firing rate changes displayed relative to lever press onset. Dashed lines indicate the mean lever press duration for each respective duration quartile within the session. ***C***, Mean baseline normalized z-scored firing rate changes across equidistant duration segments (i.e., 0–25%, 25–50%, 50–75%, 75–100% of lever press duration) of lever presses belonging to each duration quartile for air and (***D***) CIE groups. Quartile boundaries determined by within-session lever press duration distributions are shown in Extended Data Figure 4-1. Data points represent mean ± SEM; *$p < 0.05$, **$p < 0.01$, ***$p < 0.001$, ****$p < 0.0001$.

Figure 1.S3

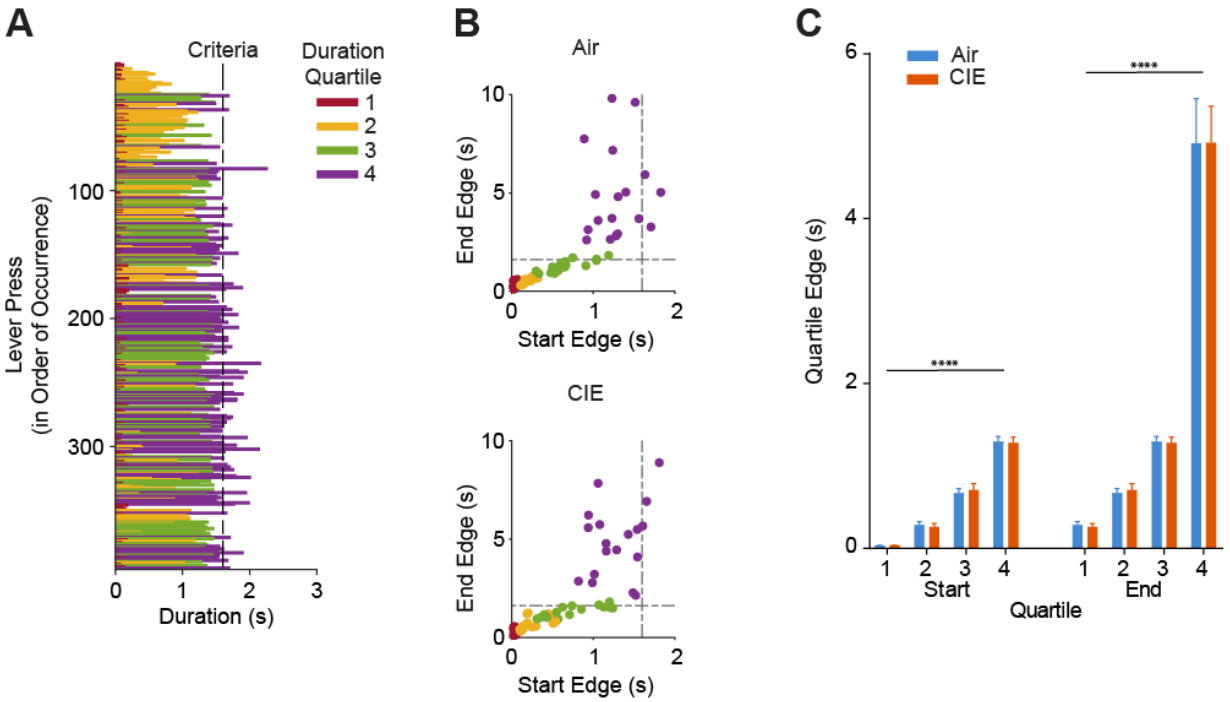

Figure 1.S3. ***A–C***, Quartile boundaries were determined by within-session lever press duration distributions and do not differ between air and CIE groups. ***A***, Examples session in which lever press durations were binned into four quartiles determined by the distribution of lever press durations. ***B***, ***C***, Duration quartile bin boundaries were similar between groups across the last two 1600-ms hold down criteria sessions that were included in our firing rate analyses. Dashed lines indicate 1600-ms duration criterion. For the starting edges of these bin boundaries, a two-way ANOVA (quartile × treatment) found no interaction, but a main effect of quartile only: $F_{(3,136)} = 226.5$, $p < 0.0001$). For the ending edges of these bin boundaries, a two-way ANOVA (quartile × treatment) found no interaction, but a main effect of quartile only: $F_{(3,136)} = 141.8$, $p < 0.0001$). Data points represent mean ± SEM; ****$p < 0.0001$.

(quartile × segment) revealed a main effect of quartile ($F_{(3,2176)} = 15.87$, $p < 0.0001$), a main effect of segment ($F_{(3,2176)} = 4.18$, $p < 0.005$), but no interaction. Follow-up main effect analyses on quartile effects showed that baseline normalized averaged z-scored activity within a quartile largely differed from activity in other quartiles. The exception being activity in the longest two quartiles which did not differ from each other (Figure 1.4C). The same analyses in CIE mice showed similar differences (main effect of quartile: $F_{(3,1952)} = 15.19$, $p < 0.0001$), but no effect of segment or interaction ($p > 0.05$). In addition, air mice also had similar baseline activity during the first and second (i.e., the shortest lever presses) quartiles (Figure 1.4D). Follow-up analyses on main effects of segments showed few differences, except in air mice where the last quarter of the lever press differed from the preceding quarter ($p = 0.01$), as represented by the increase in firing rate during the last portion of a lever press in Figure 1.4B. Together, the above data suggest that OFC overall reduces its firing rate activity during the execution of the lever press in a manner that reflects the future duration, with longer lever presses showing greater reductions in firing rate, and that CIE does not drastically alter the ability of OFC to do so.

Prior CIE procedures decrease OFC activity during outcomes

OFC neurons have long been reported to increase their activity in anticipation of and during outcome delivery (Wallis, 2007; Stalnaker et al., 2014, 2018). In the present task, reward delivery cannot occur until the lever is released. Thus, we defined an action offset epoch (1000 ms), and in some cases an outcome-related epoch (3000 ms) following a reward delivery, that encompassed moving to the food receptacle and potentially reward consumption. As the reward is readily visible without mice having to

insert their heads into the food receptacle, it is likely that reward perception happens earlier than consumption. As seen in the normalized activity peri-event heatmaps (Figure 1.5A) and in an example from a representative OFC unit (Figure 1.5B), OFC firing rates changed significantly during the action offset and outcome-related epochs of the task. We observed similar percentages of OFC units recorded between air and CIE mice where significant activity changes were associated with action offset only (air = 13.5%, CIE = 16.5%) and outcome-related only (air = 11.5%, CIE = 7.5%), as well as OFC units that had activity associated with both action offset and outcome evaluation (air 12%, CIE 7%) or action onset, action offset, and outcome-related (air = 18%; CIE = 23%; Figure 1.2E).

When we examined modulation of OFC activity following lever press offset, we found that CIE mice showed greater increases in baseline normalized z-scored OFC firing rates compared with air controls (two-way repeated measures ANOVA (bin × treatment); no interaction; main effect of bin: $F_{(3,1044)} = 6.612$, $p = 0.0002$; main effect of treatment: $F_{(1,1044)} = 22.63$, $p < 0.0001$; Figure 1.5C; Figure 1.S4A-B). We also found that OFC activity changes at lever press offset reflected performance outcomes in both air and CIE mice (Figure 1.S4E-F); however, it is important to note that this OFC activity was comprised of all lever presses, including those that were rewarded. Thus, we examined OFC firing rate changes aligned to outcome-related epochs following only successful lever presses and asked whether CIE procedures would change the magnitude of these increases. We found large increases in OFC firing rate changes during outcome-related epochs. In contrast to the increase in activity related to lever-pressing in CIE mice, we found air mice had greater increases in OFC firing rates during

Figure 1.5

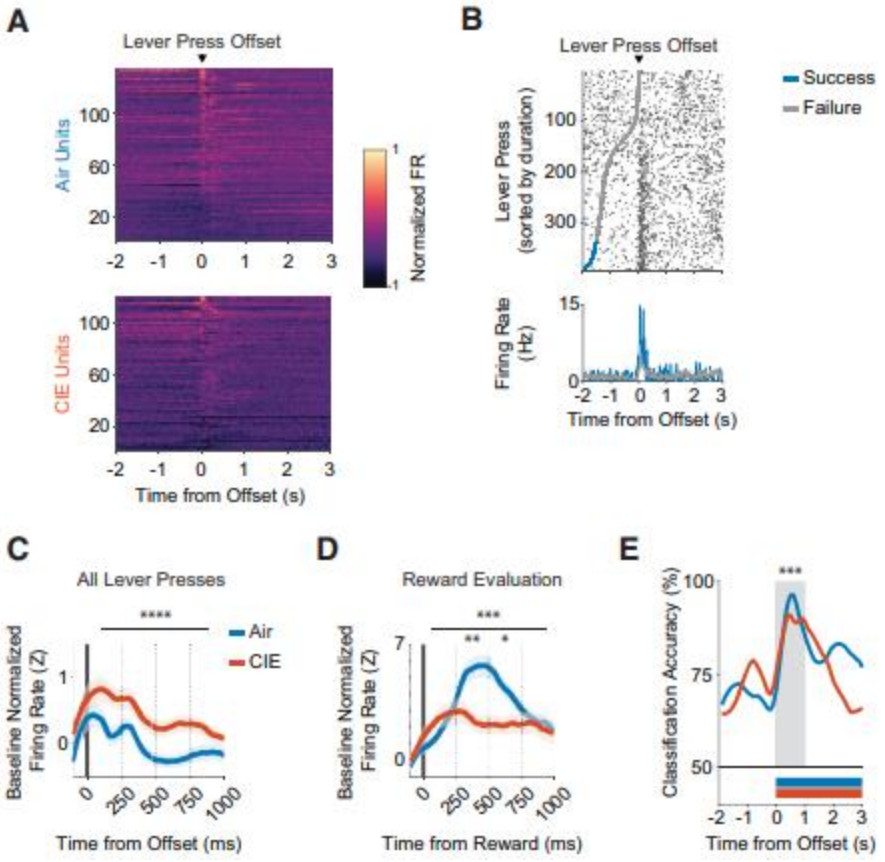

Figure 1.5. ***A–E***, Ethanol dependence alters OFC activity correlates of outcome delivery. ***A***, Heat map of normalized firing rates for units that significantly increased or decreased from baseline, displayed relative to lever press offset. Units are sorted by activity from a 1-s window around lever press offset. ***B***, Raster plot of a representative unit's firing rate relative to lever press offset, sorted from shortest to longest durations within a 1600-ms lever press criterion session that occurred late in training. Gray and blue markers indicate the start of a lever presses that failed or succeeded in exceeding the 1600-ms lever press criterion, respectively. ***C***, Average z-scored firing rate changes from baseline for all lever presses and (***D***) rewarded lever presses only. Firing rate changes were compared across four 250-ms bins relative to lever press offset. ***E***, SVM classification accuracy of task performance outcomes (i.e., did lever press exceed 1600-ms hold-down criterion?) from all captured air and CIE units, displayed relative to lever press offset. Bars underneath traces indicate time points after the offset of the lever press in which classification accuracy was significantly different compared with the null distribution. Shaded region indicates time points in which classification accuracy comparisons were made between air and CIE groups. OFC activity correlates of lever pressing termination and reward delivery are shown by significantly up-modulated and down-modulated unit averages in Figure 1.S4. Data points represent mean ± SEM; *$p < 0.05$, **$p < 0.01$, ***$p < 0.001$.

Figure 1.S4. ***A–F***, OFC activity correlates of outcome delivery are altered by ethanol dependence and reflect successful performance. ***A***, Average z-scored firing rate changes from all lever presses for significantly up-modulated and (***B***) down-modulated units from air and CIE groups, displayed relative to lever press offset. In up-modulated units, a two-way repeated measures ANOVA (bin × treatment) on activity prior to lever press offset revealed no interactions, but main effects of bin: $F_{(3,748)} = 21.82$, $p < 0.0001$ and treatment: $F_{(1,748)} = 8.159$, $p = 0.004$. In down-modulated units, a two-way repeated measures ANOVA (bin × treatment) on activity prior to lever press offset revealed no differences ($p > 0.08$). ***C***, Average z-scored firing rate changes from rewarded lever presses for significantly up-modulated and (***D***) down-modulated units from air and CIE groups, displayed relative to reward delivery. In up-modulated units, a two-way repeated measures ANOVA (bin × treatment) on activity prior to reward delivery revealed an interaction: $F_{(3,532)} = 4.508$, $p = 0.004$, and a main effect of bin: $F_{(3,532)} = 7.199$, $p < 0.0001$. *Post hoc* comparisons on up-modulated unit activity found differences between air and CIE groups in the 2nd ($p < 0.03$) bin. In down-modulated units, a two-way repeated measures ANOVA (bin × treatment) on activity prior to reward delivery revealed no differences ($p > 0.2$). ***E***, Air (left) and CIE (right) group's average z-scored firing rate changes of up-modulated and (***F***) down-modulated units, segmented by whether a lever press successfully exceeded the 1600-ms duration criterion or not, and displayed relative to lever press offset. For up-modulated units, individual two-way repeated measures ANOVAs (bin × outcome) on activity after to lever press offset revealed no interactions, but main effects of bin: $F_{(3,736)} = 5.406$, $p = 0.0011$, and outcome: $F_{(1,736)} = 46.77$, $p < 0.0001$ for the air group and no interactions, but main effects of bin: $F_{(3,760)} = 8.816$, $p < 0.0001$, and outcome: $F_{(1,760)} = 31.08$, $p < 0.0001$ for the CIE group. For down-modulated units, individual two-way repeated measures ANOVAs (bin × outcome) on activity after to lever press offset revealed an interaction: $F_{(3,408)} = 3.916$, $p = 0.009$, and main effects of bin: $F_{(3,408)} = 4.523$, $p = 0.004$, and outcome: $F_{(1,408)} = 81.83$, $p < 0.0001$ for the air group, and an interaction: $F_{(3,248)} = 3.412$, $p = 0.02$, and main effects of bin: $F_{(3,248)} = 4.540$, $p = 0.004$, and outcome: $F_{(1,248)} = 12.79$, $p = 0.0004$ for the CIE group. *Post hoc* comparisons on down-modulated unit activity found differences between successful and failed lever presses in the 2nd ($p < 0.0001$), 3rd ($p < 0.0001$), and 4th ($p = 0.0002$) bins for the air group and in the 4th ($p = 0.0002$) bin only for the CIE group. Average z-scored firing rate changes were compared between treatment groups or outcomes across four 250-ms bins relative to the end of the lever press or reward delivery. Data points represent mean ± SEM; *$p < 0.05$, **$p < 0.01$, ***$p < 0.001$, ****$p < 0.0001$.

Figure 1.S4.

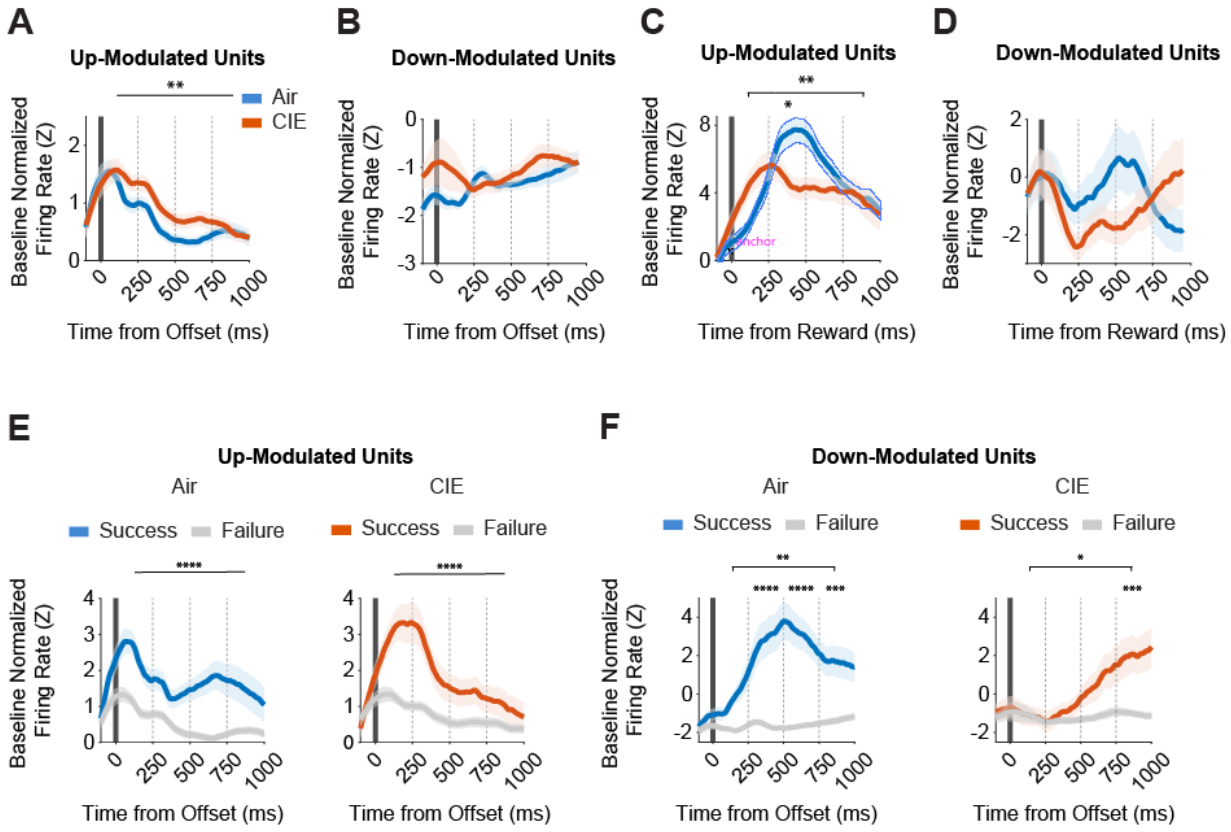
A
Up-Modulated Units
Air
CIE
Baseline Normalized Firing Rate (Z)
Time from Offset (ms)
B
Down-Modulated Units
Time from Offset (ms)
C
Up-Modulated Units
Time from Reward (ms)
D
Down-Modulated Units
Time from Reward (ms)
E
Up-Modulated Units
Air
CIE
Success
Failure
Time from Offset (ms)
F
Down-Modulated Units
Time from Offset (ms)

outcome-related epochs compared with CIE mice (two-way repeated measures ANOVA (bin × treatment); interaction: $F_{(3,724)} = 4.04$, $p = 0.007$; main effect of bin: $F_{(3,724)} = 4.43$, $p = 0.004$; main effect of treatment: $F_{(1,724)} = 8.66$, $p = 0.003$; Figure 1.5D; Figure 1.S4C-D). Given the overall robust increases in OFC activity during outcome-related epochs, as well as the differences in magnitude induced by CIE procedures, we asked whether a support vector machine (SVM) model trained with the peri-event activity of all captured OFC units could accurately classify whether an individual lever press exceeded the 1600-ms duration criterion during the action offset and outcome-related epochs. We found high classification accuracy during the outcome-related epochs, especially within the first 1000 ms of reward delivery. Furthermore, classification accuracy was lower in OFC units from CIE mice during this period (two-way repeated measures ANOVA (bin × treatment); interaction: ($F_{(9,180)} = 3.33$, $p = 0.0009$; main effect of bin: $F_{(9,180)} = 5.11$, $p < 0.0001$). A post hoc Benjamini and Hochberg multiple comparison test revealed that decoder accuracy differences were pronounced in the 1st ($p = 0.005$), 3rd ($p = 0.006$), and 4th ($p = 0.0086$) 100-ms bins of the outcome related epoch. Thus, CIE mice show greater OFC activity associated with lever pressing, but reduced OFC activity during outcome-related epochs, with OFC activity being less predictive of rewarded lever presses.

Discussion

Alcohol dependence is associated with impairments to OFC function and aberrant decision-making, thereby increasing the vulnerability to relapse and maladaptive alcohol consumption (Zinn et al., 2004; Chanraud et al., 2007; Loeber et al., 2009; Berre et al., 2012; Reiter et al., 2016; Le Berre et al., 2017). Here, we

uncovered neural correlates of actions and outcomes and found them perturbed by prior chronic alcohol exposure and withdrawal. Our results suggest alcohol exposure induces long-lasting perturbations to OFC activity in a bidirectional manner, dependent on the computation being performed. CIE mice showed a modulation of OFC activity that suggests overall increases in OFC activity associated with actions (i.e., lever press onset and offset), and a blunting of OFC activity during outcome-related epochs. This raises the hypothesis that alcohol dependence does not result in a loss of OFC recruitment, but rather induces a change in how computations performed by OFC circuits may contribute to decision-making.

In the present data, CIE-exposed animals acquired and performed the lever pressing at similar levels compared with alcohol naive controls (Figure 1.1). However, outcome devaluation testing showed that such lever pressing was not under goal-directed control as it was in air mice. Thus, CIE mice were able to acquire lever pressing for food relying on neural mechanisms supporting habit learning. Recent findings corroborate the observed lack of goal-directed control in CIE mice (Lopez et al., 2014; Renteria et al., 2018, 2020; Barker et al., 2020) and with the disruption to decision-making control observed under different instrumental tasks and varied tests of goal-directed control. Our work adds to an ever-growing body of research on such decision-making deficits and highlights the importance of examining alcohol-induced alterations to neural circuits and mechanisms controlling goal-directed processes.

Clinical studies have previously shown that alcohol dependence alters representation of decision-making within OFC circuits, albeit not always in the same manner. The OFC is widely found to be hypoactive in alcohol dependence (Volkow et

al., 1994, 1997; Boettiger et al., 2007; Sjoerds et al., 2013; Reiter et al., 2016), but there have also been reports of hyperactivity (Wrase et al., 2002; Tapert et al., 2003; Myrick et al., 2004, 2008; Hermann et al., 2006; Ernst et al., 2014; Reinhard et al., 2015). We find that to be the case in our data as well, such that alcohol exposure altered decision-making representations in the OFC in a variety of ways. Prior CIE exposure and withdrawal changed OFC computations in a way that suggests an overall increase in activity during actions (Figure 1.3). This dependence-induced change could suggest an increased contribution of OFC processes to action-related processes. We should emphasize that the action contingency in the present task is the duration of the lever press, and that it is inferred from prior experience. This suggests that alcohol dependence increases OFC activity related to the retrieval and execution of inferred action association. In this context, it is important to note that a hyperactive OFC has also been observed in those with obsessive compulsive disorder and increased activity of OFC neurons during actions has been linked to compulsive action phenotypes (Milad and Rauch, 2012; Pauls et al., 2014; Robbins et al., 2019; Lüscher et al., 2020). Whether this increased OFC activity related to actions that we find in CIE mice plays a role in compulsive phenotypes in alcohol dependence is not currently known.

A hallmark of OFC function is its contribution to reward evaluation and updating, with increases in OFC activity observed during outcome anticipation and presentation (Rolls et al., 1996; Wallis, 2011; Jones et al., 2012; Stalnaker et al., 2014, 2015, 2018). Recent works have shown that inhibition of OFC activity during periods of outcome presentation prevent outcome evaluation and updating (Baltz et al., 2018; Malvaez et al., 2019). Further, recent work in humans has suggested that OFC encodes reward

identity expectations (Howard and Kahnt, 2018), which contribute to the generation of prediction errors even when there is no change in value (Stalnaker et al., 2018). Here, we observed large increases in OFC activity during outcome-evaluation periods and this increase was reduced following alcohol exposure (Figure 1.5). SVM modeling showed reduced accuracy in classifying rewarded lever presses following alcohol exposure. Furthermore, CIE affected OFC computations made only after successful lever presses. Thus, in addition to action-associated OFC activity, the data above strongly suggests that OFC's contribution to outcome retrieval, evaluation, or identification is altered following alcohol exposure. Further, results of from decoder analysis showed that OFC activity during outcome-related epochs normally carries information about whether the lever press was successful or not. CIE reduced this OFC representation. Combined with the insensitivity to outcome devaluation, our data support the hypothesis that alcohol dependence leads to reduced contribution of OFC to outcome-related decision-making. Further, the observed bidirectional alcohol exposure effects on OFC computations support the hypothesized complexity of alcohol dependence effects on OFC decision-making circuitry. For instance, previous accounts on the modulatory influence of alcohol dependence on OFC activity have differed (Volkow et al., 1994, 1997; Boettiger et al., 2007; Sjoerds et al., 2013; Reiter et al., 2016), which in conjunction with our findings suggests a divergent effect of alcohol dependence that may be dependent on decision-making demands and information in OFC. While the critical role for the OFC in regulating the ability to adapt behavior when outcome value or identity changes has been largely established, here we present new evidence on the specificity of dependence-induced effects on the computations supporting these processes.

The self-paced nature of our task allowed us to investigate the dynamics of OFC computations made during ongoing decision-making that relies solely on internal representations or retrieval of learned duration contingencies, rather than a reliance on predictive external sensory information. Here, we show with in vivo electrophysiology data that the OFC activity was modulated during the lever press itself. OFC activity decreased while mice held down the lever, with OFC activity in air controls resembling a U-shaped pattern during longer presses (Figure 1.4). The continuous nature of holding down the lever revealed an activity pattern of an initial decrease in activity relative to baseline that subsequently increases before the release of the lever press and before when outcomes are expected. The increase in activity before lever press release may correspond to a greater confidence in outcome delivery, something previously shown for OFC activity in cued tasks (Kepecs et al., 2008; Masset et al., 2020). Another possibility stems from prior data from OFC lesioned patients suggesting a potential role for OFC activity in evaluating the passing of time (Berlin et al., 2004; Berlin and Rolls, 2004). Considering reports of increased OFC activity during actions and its association with compulsive action phenotypes similar to those seen in drug studies (Milad and Rauch, 2012; Pauls et al., 2014; Robbins et al., 2019; Lüscher et al., 2020), another hypothesis could be that we would observe larger increases in OFC activity at some point during the duration of lever presses and that CIE may enhance this. Overall, prior alcohol exposure had very minor effects on duration-related activity patterns, although the increase before lever press release was absent in CIE mice. Thus, future experiments aimed at investigating the above hypotheses are warranted.

The dichotomy of CIE effects on the different behavioral components of our task suggests a combination of OFC circuitry changes that could manifest in a variety of ways. In the future, it will be of interest to examine how CIE perturbs OFC function and output that relies on information received by interconnected structures. For example, chronic alcohol exposure and withdrawal may be perturbing the excitability and transmission of local OFC circuitry via cell-type-specific changes (Badanich et al., 2013; McGuier et al., 2015; Nimitvilai et al., 2017; Renteria et al., 2018), such that the integration of incoming information from other associative regions necessary to guide decision-making is disrupted. Additional difficulties in parsing the effects of alcohol dependence on decision-making processes arise from a fundamental lack of structural and functional input-output mapping of the highly complex neural circuits that support decision-making. While in general the areas projecting to OFC have been identified, the relative proportions of inputs across brain regions, as well as the connectivity, strength, and pattern of inputs onto excitatory and inhibitory OFC populations is unknown in naive circumstances, much less following alcohol dependence. It may be that alcohol dependence results in a redistribution of inputs across OFC excitatory and inhibitory populations and/or alters input transmission onto OFC circuits, thereby altering their ability to contribute to decision-making. We should note that it is not clear whether effects observed on neural activity in the present study differ depending on sex. Because of difficulties in female mice maintaining and carrying electrodes and associated head-caps, we were not powered in our in vivo recording experiments to examine whether there were any sex differences in our neural data that could

differentially mediate contingency and expected outcome value control (Barker et al., 2010).

As with all brain areas, the capacity to contribute to decision-making computations is going to depend on the afferent inputs as well as local capabilities. Alcohol dependence is likely to affect both across the brain. Here, we identified some of the complexity in how OFC's contributions to decision-making computations are altered following alcohol exposure. These findings will hopefully shed light on the behavioral and OFC-based perturbations previously reported and provide insight into the therapeutic treatment of alcohol dependence.

Methods

Animals

Male and female C57BL/6J mice (n = 15, 9 males, 6 females or non-recording experiments; n = 18, 17 males, 1 female for recording experiments) were housed two to five per cage under a 14/10 h light/dark cycle with access to food (Labdiet 5015) and water ad libitum unless stated otherwise. C57BL/6J (The Jackson Laboratory) mice were at least six weeks of age before intracranial micro-array implant and at least 52 d of age before vapor procedures or behavioral training. Investigators were not blind to the experimental groups. The Animal Care and Use Committee of the University of California, San Diego approved all experiments and experiments were conducted according to the NIH guidelines.

Surgical procedures

Animals under isoflurane anesthesia were implanted with a stereotaxically guided fixed micro-array consisting of four-rows of four platinum-plated tungsten electrodes

(35-μm tip, Innovative Neurophysiology), with electrodes spaced 150 μm apart, and rows 150 μm apart. The dearth of female mice in the recording study was because of problems with female mice not being able to maintain and carry the electrode implant through CIE procedures and behavioral testing. To maximize targeting of the OFC, arrays were centered at the following coordinates from bregma: A, 2.5 mm; M/L, 1.3 mm; V, 2.0 mm. An additional bilateral craniotomy was made over the posterior cerebellum for placement of screws wrapped with the electrical reference wire attached to the micro-array. After testing, mice were euthanized, and brains extracted and fixed in 4% paraformaldehyde. Micro-array placement was qualified by examining tracts in 50- to 100-μm-thick brain slices under a macro fluorescence microscope (Olympus MVX10). A subset of micro-arrays was dyed with a 25 mg/ml 1,1′-dioctadecyl-3,3,3′,3′-tetramethylindocarbocyanine perchlorate (Dil) solution in 200 proof ethanol (Sigma) for placement verification. All surgical and behavioral experiments were performed during the light portion of the cycle.

CIE exposure and repeated withdrawal

One to two weeks after micro-array implant surgeries for recording mice, all mice were exposed to four rounds of ethanol vapor or air (Becker and Hale, 1993; Becker and Lopez, 2004; Lopez and Becker, 2005; Griffin et al., 2009; Renteria et al., 2018). Each round consisted of 16 h of vapor exposure followed by an 8-h withdrawal period, repeated for four consecutive days. The CIE procedure is designed to repeatedly induce alcohol withdrawal syndrome after long periods of alcohol exposure, a key criterion in the diagnosis of alcohol dependence (Lopez and Becker, 2005). Ethanol was volatilized by bubbling air through a flask containing 95% ethanol at a rate of 2–3 l/min. The

resulting ethanol vapor was combined with a separate air stream to give a total flow rate of ~10 l/min, which was delivered to the mice housed in Plexiglas chambers (Plas Labs Inc). Mice were not pretreated with a loading dose of ethanol or pyrazole to avoid confounding effects of stress that can bias reliance on habitual control, as well as to avoid the effects of pyrazole on neural activity, including actions at the NMDA receptor (Pereira et al., 1992; Becker and Lopez, 2004; Dias-Ferreira et al., 2009). Blood ethanol concentrations (BECs) were collected at the end of each round from separate, non-experimental mice to avoid previously reported stress effects on decision-making from blood extraction on air mice (mean ± SEM BEC = 29.53 ± 2.36 mm). BEC assays that experienced technical errors were excluded from this measurement.

Behavioral task

We adapted a lever press hold down task previously used to assay the timing of decision-making actions in mice (Yin, 2009; Fan et al., 2012). Mice were trained in standard operant chambers with one lever extended to the left (or right) of a food magazine and a house light on the opposite wall within sound-attenuating boxes (Med-Associates). Two days before training, mice were food restricted and maintained at 85−90% of their baseline body weight throughout training and testing.

Magazine training

On the first day, mice were trained to retrieve pellets from the food magazine (no levers present) on a random time (RT) schedule, with a pellet outcome delivered on average every 120 s for 60 min.

Continuous reinforcement

The next 3 d the left (or right) lever was present the entire duration of the session. Lever presses were rewarded on a continuous reinforcement (CRF) schedule for up to 15 (CRF day 1), 30 (CRF day 2), or 60 (CRF day 3) pellet deliveries or until 60–90 min had passed. For electrode-implanted animals, an additional CRF training day (4 d total) was administered with the implant connected to the amplifier board to habituate the animal to the tethered connection.

Lever press hold down training

The action differentiation task required lever press durations to exceed a duration criterion assigned before the start of the daily session. This criterion was the minimum duration of time the animal was required to hold the lever in a depressed position to receive a reward. Each session began with the house light turning on and the left (or right) lever being extended for the duration of the session. Lever pressing was self-initiated and self-paced without an imposed trial structure (i.e., the lever was never retracted until the session was complete). Reward delivery occurred at the offset of the lever press only if the hold down timer exceeded the session's assigned duration criterion. Sessions were completed when 30 outcomes (non-recording animals) or 60 outcomes (recording animals) were earned or after 90 min, whichever came first. The lever press duration criterion for the first 5 d was 800 ms, followed by 5 d (4 d in three animals because of loss of head-cap implant) of a lever press duration requirement of 1600 ms.

Devaluation testing

Following the last day of hold down testing in the behavioral cohort, mice were habituated to a novel cage and 20% sucrose solution for 1 h each. Devaluation testing

through sensory-specific satiation was conducted across 2 d and consisted of a valued day and a devalued day. For the valued day, the mice were allowed to prefeed for 1 h on 20% sucrose solution. For the devalued day, mice could prefeed for 1 h on the pellet outcome previously earned in the lever press hold down task. Mice that did not consume enough pellets (<0.1 g) or sucrose (<0.1 ml) during prefeeding were excluded from subsequent analysis (CIE cohort, n = 1). Each day immediately following prefeeding, mice were placed into their respective operant chamber for 10 min, where the number and duration of lever presses made were recorded, but no outcome was delivered. Investigators were not blind to the experimental groups. Valued and devalued days were counterbalanced and run across consecutive days. Response rate comparisons between valued and devaluated days were made by normalizing each mouse's test day response rate to the average response rate of their corresponding last 2 d of 1600-ms duration criterion sessions using the following formula:

$RR_{Test\ Day} \div \text{mean}(RR_{1600ms4}+RR_{1600ms5})$

Electrophysiological recordings and spike sorting

Spike activity and local field potentials were recorded using an RHD2000 USB interface board system connected to an amplifier board via a serial peripheral interface (SPI) cable (Intan Technologies). Electrode signals were amplified, digitized at 30 kHz and filtered between 0.1 Hz and 6 kHz for spikes and 0.1 and 600 Hz for local field potentials. Initial sorting occurred before each testing session using an online-sorting algorithm (OpenEphys; Siegle et al., 2017). Behavior events that occurred inside the operant boxes were timestamped in synchronization in OpenEphys with neural activity using transistor-transistor logic (TTL) pulses collected at a 10-ms resolution from Med

Associates SuperPort Output cards. Spike data were re-sorted offline (Offline Sorter, Plexon) using a T-Distribution Expectation-Maximization Scan algorithm in 3D feature space (Shoham et al., 2003). This allowed for the identification of neuronal activity units based on waveform, amplitude, and inter spike interval histogram (no spikes during a refractory period of 1.4 ms). After sorting, each isolated cluster of waveforms was then manually inspected, and biologically implausible waveform clusters were removed from further analysis. To ensure high signal-to-noise quality of each waveform cluster, waveforms 2 standard deviations (SDs) greater than the clustered population mean were excluded from the analyses. Units with <1000 spike waveforms captured within an entire recording session or that did not show consistent activity across a recording session were not included in our analyses. Before each recording session, mice were exposed to a brief (10–20 s) bout of low-dose isoflurane anesthesia to connect the implant with the recording cable. To avoid confounding effects of anesthesia on brain activity, mice were then moved into the procedure room and monitored for a minimum of 30 min before placing them in the operant chamber and initiating the session.

Identification of significantly modulated units

To initially examine task-related neural activity, for each previously isolated recorded unit we constructed a peri-event histogram (PETH) around time-stamped lever-press and reward delivery events, such that neural activity was binned into 20-ms bins and averaged across events to analyze amplitude and latency during the recorded behaviors. Per-unit PETHs were then smoothed using a Gaussian-weighted moving average over three bins (60 ms). Using the distribution of the PETH from 10,000 to 2000 ms before lever press onset as baseline activity, we focused our analysis on a

period 2000 ms before to 10,000 ms after task-related events. A task-related neuron was up-modulated if it had a significant increase in firing rate defined as at least four bins (80 ms) with a firing rate larger than a threshold of 95% confidence interval above baseline activity during the period from 2000 before to 3000 ms after each task event. A task-related neuron was down-modulated if it had a significant decrease in firing rate if at least four consecutive bins (80 ms) had a firing rate smaller than a threshold of 95% confidence interval below baseline activity during the period from 2000 before to 3000 ms after each task event (Jin and Costa, 2010). The onset of significantly modulated task-related activity was defined as the first of these four-consecutive significant PETH bins. To examine the net effect of CIE on OFC activity as animals performed the task, we combined these up-modulated and down-modulated unit populations for subsequent population analyses.

Population analyses

Performance-related spike activity

To investigate differences in peri-event spike activity between lever presses that were rewarded or not, spike timestamps occurring 10,000 ms before to 10,000 ms after individual lever press events were split into successes (lever press duration exceeded session's criterion duration) and failures (lever press duration did not exceed session's criterion duration). Performance segmented neural activity was then binned into 20-ms bins, averaged across events, and then smoothed using a Gaussian-weighted moving average over three bins (60 ms), resulting in two PETHs per unit (successes or failures). Individual PETHs were then converted to z-scores using the mean and SD of the firing rate during a baseline period occurring 10,000–2000 before lever press onset. Per-unit

z-scored PETHs were then averaged by treatment group to construct population response profiles for each group. Population spike activity from the last the two sessions of 1600-ms duration criteria was grouped such that a minimum of one session per animal was included. Population spike activity traces were then smoothed with MATLAB's Savitzky–Golay smoothdata method using a 400-sample sliding window for visual display purposes only.

Ongoing lever press-related spike activity

To investigate differences in spike activity during ongoing lever-presses, each lever press duration was first calculated by subtracting the lever press onset timestamp from lever press offset timestamp. Each lever press duration was then segmented into four equivalent segment bins (i.e., 0–25%, 25–50%, 50–75%, 75–100% of lever press duration), and all spikes occurring within each of these duration bins were counted and calculated as a proportion of all spikes that occurred during that entire lever press.

To investigate differences in firing rate changes between different lever press durations, lever presses were first grouped into four quartiles determined by the distribution of lever press durations within each individual recording session. Quartile-grouped spike activity occurring 10,000 ms before to 10,000 ms after lever press onset was then binned into 20-ms bins, averaged across lever presses, and then smoothed using a Gaussian-weighted moving average over three bins (60 ms), resulting in four PETHs per unit, one for each duration quartile. To account for variable lever press durations, PETHs were converted to z-scores using the mean and SD of activity occurring before the onset of the lever press proportionate in duration to the average lever press duration within each quartile. Individual lever press activity from these

PETHs were then segmented into four equivalent segment bins (i.e., 0–25%, 25–50%, 50–75%, 75–100% of lever press duration). Per-unit, baseline z-scored traces were then averaged across the four duration segments within quartile and treatment groups to construct population response profiles.

Neural decoding of task performance from spike activity

For all units from recording sessions in which a minimum of 10 lever presses exceeded the session's lever press duration criterion, spike timestamps occurring 2000 ms before to 10,000 ms after individual lever press events were binned into 1-ms bins and labeled by lever press outcome (success or failure to exceed the session's lever press duration criterion). These peri-event rasters were then segmented by treatment groups and task event (lever press onset or offset) and used to train a model to classify successful lever presses. The classifier, a support vector machine model implemented in MATLAB with the NDT toolbox, was trained and tested at 100-ms steps with a bin width of 200 ms (Meyers, 2013). For each of these time points, the classifier used 10 cross-validation splits to segment per-unit firing rates from randomly selected lever press events into training (90%) and testing (10%) sets for 500 resampling runs. Significance at each of these timepoints was tested by first creating 5 null distributions of decoding accuracy with 500 resampling runs each in which the performance labels were shuffled. The accuracy of our decoder was then compared with these null distributions across all time points.

Statistical procedures

Statistical significance was defined as an α of $p < 0.05$. Statistical analysis was performed using GraphPad Prism 8.3.0 (GraphPad Software) and custom MATLAB

R2019a (MathWorks) scripts using a PC desktop with Windows 10. Acquisition data, including lever presses, response rate, and proportion of lever presses that were rewarded were analyzed using two-way repeated measures ANOVA (session × treatment) unless otherwise noted. For outcome devaluation testing, two-way repeated measure ANOVAs (value × treatment) with preplanned post hoc Sidak's multiple comparison testing were performed to examine whether outcome devaluation reduced lever pressing on the devalued compared with valued day within each group. For peri-event spike activity comparisons, per-unit average z-scored firing rates were binned into four 250-ms bins before the lever press onset, or after lever press offset and after reward delivery, respectively. Within treatment groups, we performed two-way repeated measure ANOVAs (bin × outcome) to examine differences in spike activity between lever presses that failed or succeeded to exceed the session's lever press duration criteria, with post hoc Sidak's multiple comparison testing to determine bins in which differences were pronounced. Two-way repeated measure ANOVAs (bin x treatment) were performed to examine differences in spike activity between treatment groups, with post hoc Sidak's multiple comparison testing to determine bins in which differences were pronounced. Two-way repeated measure ANOVAs (segment × treatment) were performed to examine group differences in the proportions of spikes occurring between lever press duration segments. Between group comparisons of decoder accuracy were made with two-way repeated measure ANOVAs (bin × treatment), with post hoc Benjamini and Hochberg multiple comparison testing to examine in which of the 100-ms bins were differences pronounced. When appropriate, mixed-effect analyses were

conducted in lieu of repeated measures ANOVAs (e.g., when data points were missing because of loss of implant). Data are presented as mean ± SEM.

Code accessibility

The code/software described in the paper is freely available online at https://github.com/gremellab/CIEOFCHOLD. All data generated or analyzed during this study are available at https://doi.org/10.6084/m9.figshare.12605225.v1.

Conflict of Interest

The authors declare no competing financial interests.

Acknowledgments

Chapter 1 is, in full, a reprint of the material published in *eNeuro* (2020). Cazares C., Schreiner, D.C., Gremel, Christina M., 2020. The dissertation author was the primary investigator and author of this paper. This work was supported by National Institute on Alcohol Abuse and Alcoholism Grants R00AA021780 and R01AA026077 (to C.M.G.) and F31AA027439 (to D.C.S.), Whitehall and Brain and Behavior Foundations (C.M.G.), and the National Science Foundation GRFP Grant DGE-1650112 (to C.C.). We thank undergraduate research assistant Mariela Lopez Valencia for technical assistance and Roy Jungay for animal care assistance.

References

Ahmari, S. E., Spellman, T., Douglass, N. L., Kheirbek, M. A., Simpson, H. B., Deisseroth, K., Gordon, J. A., & Hen, R. (2013). Repeated cortico-striatal stimulation generates persistent OCD-like behavior. Science (New York, N.Y.), 340(6137), 1234–1239. https://doi.org/10.1126/science.1234733

Badanich, K. A., Becker, H. C., & Woodward, J. J. (2011). Effects of chronic intermittent ethanol exposure on orbitofrontal and medial prefrontal cortex-dependent behaviors in mice. Behavioral Neuroscience, 125(6), 879–891. https://doi.org/10.1037/a0025922

Badanich, K. A., Mulholland, P. J., Beckley, J. T., Trantham-Davidson, H., & Woodward, J. J. (2013). Ethanol Reduces Neuronal Excitability of Lateral Orbitofrontal Cortex Neurons Via a Glycine Receptor Dependent Mechanism. Neuropsychopharmacology, 38(7), 1176–1188. https://doi.org/10.1038/npp.2013.12

Baltz, E. T., Yalcinbas, E. A., Renteria, R., & Gremel, C. M. (2018). Orbital frontal cortex updates state-induced value change for decision-making. ELife, 7. https://doi.org/10.7554/eLife.35988

Barker, J. M., Bryant, K. G., Montiel-Ramos, A., Goldwasser, B., & Chandler, L. J. (2020). Selective Deficits in Contingency-Driven Ethanol Seeking Following Chronic Ethanol Exposure in Male Mice. Alcoholism: Clinical and Experimental Research, 44(9), 1896–1905. https://doi.org/10.1111/acer.14418

Barker, J. M., Torregrossa, M. M., Arnold, A. P., & Taylor, J. R. (2010). Dissociation of genetic and hormonal influences on sex differences in alcoholism-related behaviors. The Journal of Neuroscience: The Official Journal of the Society for Neuroscience, 30(27), 9140–9144. https://doi.org/10.1523/JNEUROSCI.0548-10.2010

Beck, A., Wüstenberg, T., Genauck, A., Wrase, J., Schlagenhauf, F., Smolka, M. N., Mann, K., & Heinz, A. (2012). Effect of Brain Structure, Brain Function, and Brain Connectivity on Relapse in Alcohol-Dependent Patients. Archives of General Psychiatry, 69(8), 842–852. https://doi.org/10.1001/archgenpsychiatry.2011.2026

Becker, H. C., & Hale, R. L. (1993). Repeated episodes of ethanol withdrawal potentiate the severity of subsequent withdrawal seizures: An animal model of alcohol withdrawal “kindling.” Alcoholism, Clinical and Experimental Research, 17(1), 94–98. https://doi.org/10.1111/j.1530-0277.1993.tb00731.x

Becker, Howard C., & Lopez, M. F. (2004). Increased ethanol drinking after repeated chronic ethanol exposure and withdrawal experience in C57BL/6 mice. Alcoholism, Clinical and Experimental Research, 28(12), 1829–1838.

Berre, A.-P. L., Vabret, F., Cauvin, C., Pinon, K., Allain, P., Pitel, A.-L., Eustache, F., & Beaunieux, H. (2012). Cognitive Barriers to Readiness to Change in Alcohol-Dependent Patients. Alcoholism: Clinical and Experimental Research, 36(9), 1542–1549. https://doi.org/10.1111/j.1530-0277.2012.01760.x

Bickel, W. K., Mellis, A. M., Snider, S. E., Athamneh, L. N., Stein, J. S., & Pope, D. A. (2018). 21st century neurobehavioral theories of decision making in addiction: Review and evaluation. Pharmacology Biochemistry and Behavior, 164, 4–21. https://doi.org/10.1016/j.pbb.2017.09.009

Boettiger, C. A., Mitchell, J. M., Tavares, V. C., Robertson, M., Joslyn, G., D'Esposito, M., & Fields, H. L. (2007). Immediate Reward Bias in Humans: Fronto-Parietal Networks and a Role for the Catechol-O-Methyltransferase 158Val/Val Genotype. Journal of Neuroscience, 27(52), 14383–14391. https://doi.org/10.1523/JNEUROSCI.2551-07.2007

Burguière, E., Monteiro, P., Feng, G., & Graybiel, A. M. (2013). Optogenetic Stimulation of Lateral Orbitofronto-Striatal Pathway Suppresses Compulsive Behaviors. Science, 340(6137), 1243–1246. https://doi.org/10.1126/science.1232380

Cardenas, V. A., Durazzo, T. C., Gazdzinski, S., Mon, A., Studholme, C., & Meyerhoff, D. J. (2011). Brain morphology at entry into treatment for alcohol dependence is related to relapse propensity. Biological Psychiatry, 70(6), 561–567. https://doi.org/10.1016/j.biopsych.2011.04.003

Chanraud, S., Martelli, C., Delain, F., Kostogianni, N., Douaud, G., Aubin, H.-J., Reynaud, M., & Martinot, J.-L. (2007). Brain Morphometry and Cognitive Performance in Detoxified Alcohol-Dependents with Preserved Psychosocial Functioning. Neuropsychopharmacology, 32(2), 429–438. https://doi.org/10.1038/sj.npp.1301219

Corbit, L. H., Nie, H., & Janak, P. H. (2012). Habitual alcohol seeking: Time course and the contribution of subregions of the dorsal striatum. Biological Psychiatry, 72(5), 389. https://doi.org/10.1016/j.biopsych.2012.02.024

Dias-Ferreira, E., Sousa, J. C., Melo, I., Morgado, P., Mesquita, A. R., Cerqueira, J. J., Costa, R. M., & Sousa, N. (2009). Chronic stress causes frontostriatal reorganization and affects decision-making. Science (New York, N.Y.), 325(5940), 621–625. https://doi.org/10.1126/science.1171203

Dickinson, A. (1985). Actions and Habits: The Development of Behavioural Autonomy. Philosophical Transactions of the Royal Society of London Series B, 308, 67. https://doi.org/10.1098/rstb.1985.0010

Durazzo, T. C., Tosun, D., Buckley, S., Gazdzinski, S., Mon, A., Fryer, S. L., & Meyerhoff, D. J. (2011). Cortical thickness, surface area, and volume of the brain reward system in alcohol dependence: Relationships to relapse and extended abstinence. Alcoholism, Clinical and Experimental Research, 35(6), 1187–1200. https://doi.org/10.1111/j.1530-0277.2011.01452.x

Ernst, L. H., Plichta, M. M., Dresler, T., Zesewitz, A. K., Tupak, S. V., Haeussinger, F. B., Fischer, M., Polak, T., Fallgatter, A. J., & Ehlis, A.-C. (2014). Prefrontal correlates of approach preferences for alcohol stimuli in alcohol dependence. Addiction Biology, 19(3), 497–508. https://doi.org/10.1111/adb.12005

Fan, D., Rossi, M. A., & Yin, H. H. (2012). Mechanisms of action selection and timing in substantia nigra neurons. The Journal of Neuroscience: The Official Journal of the Society for Neuroscience, 32(16), 5534–5548. https://doi.org/10.1523/JNEUROSCI.5924-11.2012

Fellows, L. K. (2007). The role of orbitofrontal cortex in decision making: A component process account. Annals of the New York Academy of Sciences, 1121, 421–430. https://doi.org/10.1196/annals.1401.023

Fernandez, G. M., Lew, B. J., Vedder, L. C., & Savage, L. M. (2017). Chronic intermittent ethanol exposure leads to alterations in brain-derived neurotrophic factor within the frontal cortex and impaired behavioral flexibility in both adolescent and adult rats. Neuroscience, 348, 324–334. https://doi.org/10.1016/j.neuroscience.2017.02.045

Gourley, S. L., Olevska, A., Zimmermann, K. S., Ressler, K. J., DiLeone, R. J., & Taylor, J. R. (2013). The orbitofrontal cortex regulates outcome-based decision-making via the lateral striatum. The European Journal of Neuroscience, 38(3). https://doi.org/10.1111/ejn.12239

Gremel, C. M., Chancey, J. H., Atwood, B. K., Luo, G., Neve, R., Ramakrishnan, C., Deisseroth, K., Lovinger, D. M., & Costa, R. M. (2016). Endocannabinoid Modulation of Orbitostriatal Circuits Gates Habit Formation. Neuron, 90(6), 1312–1324. https://doi.org/10.1016/j.neuron.2016.04.043

Gremel, C. M., & Costa, R. M. (2013). Orbitofrontal and striatal circuits dynamically encode the shift between goal-directed and habitual actions. Nature Communications, 4, 2264. https://doi.org/10.1038/ncomms3264

Griffin, W. C., Lopez, M. F., & Becker, H. C. (2009). Intensity and duration of chronic ethanol exposure is critical for subsequent escalation of voluntary ethanol drinking in mice. Alcoholism, Clinical and Experimental Research, 33(11), 1893–1900. https://doi.org/10.1111/j.1530-0277.2009.01027.x

Heilig, M., Egli, M., Crabbe, J. C., & Becker, H. C. (2010). REVIEW: Acute withdrawal, protracted abstinence and negative affect in alcoholism: are they linked? Addiction Biology, 15(2), 169–184. https://doi.org/10.1111/j.1369-1600.2009.00194.x

Hermann, D., Smolka, M. N., Wrase, J., Klein, S., Nikitopoulos, J., Georgi, A., Braus, D. F., Flor, H., Mann, K., & Heinz, A. (2006). Blockade of cue-induced brain activation of abstinent alcoholics by a single administration of amisulpride as measured with fMRI. Alcoholism, Clinical and Experimental Research, 30(8), 1349–1354. https://doi.org/10.1111/j.1530-0277.2006.00174.x

Howard, J. D., & Kahnt, T. (2018). Identity prediction errors in the human midbrain update reward-identity expectations in the orbitofrontal cortex. Nature Communications, 9(1), 1611. https://doi.org/10.1038/s41467-018-04055-5

Jin, X., & Costa, R. M. (2010). Start/Stop Signals Emerge in Nigrostriatal Circuits during Sequence Learning. Nature, 466(7305), 457–462. https://doi.org/10.1038/nature09263

Jones, J. L., Esber, G. R., McDannald, M. A., Gruber, A. J., Hernandez, A., Mirenzi, A., & Schoenbaum, G. (2012). Orbitofrontal cortex supports behavior and learning using inferred but not cached values. Science (New York, N.Y.), 338(6109), 953–956. https://doi.org/10.1126/science.1227489

Kepecs, A., Uchida, N., Zariwala, H. A., & Mainen, Z. F. (2008). Neural correlates, computation and behavioural impact of decision confidence. Nature, 455(7210), 227–231. https://doi.org/10.1038/nature07200

Kroener, S., Mulholland, P. J., New, N. N., Gass, J. T., Becker, H. C., & Chandler, L. J. (2012). Chronic Alcohol Exposure Alters Behavioral and Synaptic Plasticity of the Rodent Prefrontal Cortex. PLOS ONE, 7(5), e37541. https://doi.org/10.1371/journal.pone.0037541

Kuch, D. O. (1974). Differentiation of Press Durations with Upper and Lower Limits on Reinforced Values. Journal of the Experimental Analysis of Behavior, 22(2), 275–283. https://doi.org/10.1901/jeab.1974.22-275

Laakso, M. P., Gunning-Dixon, F., Vaurio, O., Repo-Tiihonen, E., Soininen, H., & Tiihonen, J. (2002). Prefrontal volumes in habitually violent subjects with antisocial personality disorder and type 2 alcoholism. Psychiatry Research, 114(2), 95–102. https://doi.org/10.1016/s0925-4927(02)00005-7

Le Berre, A.-P., Fama, R., & Sullivan, E. V. (2017). Executive Functions, Memory, and Social Cognitive Deficits and Recovery in Chronic Alcoholism: A Critical Review to Inform Future Research. Alcoholism, Clinical and Experimental Research, 41(8), 1432–1443. https://doi.org/10.1111/acer.13431

Loeber, S., Duka, T., Welzel, H., Nakovics, H., Heinz, A., Flor, H., & Mann, K. (2009). Impairment of Cognitive Abilities and Decision Making after Chronic Use of Alcohol: The Impact of Multiple Detoxifications. Alcohol and Alcoholism, 44(4), 372–381. https://doi.org/10.1093/alcalc/agp030

Lopez, M. F., Becker, H. C., & Chandler, L. J. (2014). Repeated episodes of chronic intermittent ethanol promote insensitivity to devaluation of the reinforcing effect of ethanol. Alcohol (Fayetteville, N.Y.), 48(7), 639–645. https://doi.org/10.1016/j.alcohol.2014.09.002

Lopez, Marcelo F., & Becker, H. C. (2005). Effect of pattern and number of chronic ethanol exposures on subsequent voluntary ethanol intake in C57BL/6J mice. Psychopharmacology, 181(4), 688–696. https://doi.org/10.1007/s00213-005-0026-3

Lüscher, C., Robbins, T. W., & Everitt, B. J. (2020). The transition to compulsion in addiction. Nature Reviews Neuroscience, 21(5), 247–263. https://doi.org/10.1038/s41583-020-0289-z

Malvaez, M., Shieh, C., Murphy, M. D., Greenfield, V. Y., & Wassum, K. M. (2019). Distinct cortical–amygdala projections drive reward value encoding and retrieval. Nature Neuroscience, 22(5), 762–769. https://doi.org/10.1038/s41593-019-0374-7

Masset, P., Ott, T., Lak, A., Hirokawa, J., & Kepecs, A. (2020). Behavior- and Modality-General Representation of Confidence in Orbitofrontal Cortex. Cell, 0(0). https://doi.org/10.1016/j.cell.2020.05.022

McGuier, N. S., Padula, A. E., Lopez, M. F., Woodward, J. J., & Mulholland, P. J. (2015). Withdrawal from chronic intermittent alcohol exposure increases dendritic spine density in the lateral orbitofrontal cortex of mice. Alcohol, 49(1), 21–27. https://doi.org/10.1016/j.alcohol.2014.07.017

Meyers, E. M. (2013). The neural decoding toolbox. Frontiers in Neuroinformatics, 7. https://doi.org/10.3389/fninf.2013.00008

Milad, M. R., & Rauch, S. L. (2012). Obsessive-compulsive disorder: Beyond segregated cortico-striatal pathways. Trends in Cognitive Sciences, 16(1), 43–51. https://doi.org/10.1016/j.tics.2011.11.003

Morisot, N., Phamluong, K., Ehinger, Y., Berger, A. L., Moffat, J. J., & Ron, D. (2019). MTORC1 in the orbitofrontal cortex promotes habitual alcohol seeking. ELife, 8, e51333. https://doi.org/10.7554/eLife.51333

Myrick, H., Anton, R. F., Li, X., Henderson, S., Drobes, D., Voronin, K., & George, M. S. (2004). Differential brain activity in alcoholics and social drinkers to alcohol cues: Relationship to craving. Neuropsychopharmacology: Official Publication of the American College of Neuropsychopharmacology, 29(2), 393–402. https://doi.org/10.1038/sj.npp.1300295

Myrick, H., Anton, R. F., Li, X., Henderson, S., Randall, P. K., & Voronin, K. (2008). Effect of naltrexone and ondansetron on alcohol cue-induced activation of the ventral striatum in alcohol-dependent people. Archives of General Psychiatry, 65(4), 466–475. https://doi.org/10.1001/archpsyc.65.4.466

Nimitvilai, S., Lopez, M. F., Mulholland, P. J., & Woodward, J. J. (2016). Chronic Intermittent Ethanol Exposure Enhances the Excitability and Synaptic Plasticity of Lateral Orbitofrontal Cortex Neurons and Induces a Tolerance to the Acute Inhibitory Actions of Ethanol. Neuropsychopharmacology, 41(4), 1112–1127. https://doi.org/10.1038/npp.2015.250

Nimitvilai, S., Uys, J. D., Woodward, J. J., Randall, P. K., Ball, L. E., Williams, R. W., Jones, B. C., Lu, L., Grant, K. A., & Mulholland, P. J. (2017). Orbitofrontal Neuroadaptations and Cross-Species Synaptic Biomarkers in Heavy-Drinking Macaques. The Journal of Neuroscience: The Official Journal of the Society for Neuroscience, 37(13), 3646–3660. https://doi.org/10.1523/JNEUROSCI.0133-17.2017

Padoa-Schioppa, C., & Conen, K. E. (2017). Orbitofrontal Cortex: A Neural Circuit for Economic Decisions. Neuron, 96(4), 736–754. https://doi.org/10.1016/j.neuron.2017.09.031

Pascoli, V., Hiver, A., Van Zessen, R., Loureiro, M., Achargui, R., Harada, M., Flakowski, J., & Lüscher, C. (2018). Stochastic synaptic plasticity underlying compulsion in a model of addiction. Nature, 564(7736), 366–371. https://doi.org/10.1038/s41586-018-0789-4

Pascoli, V., Terrier, J., Hiver, A., & Lüscher, C. (2015). Sufficiency of Mesolimbic Dopamine Neuron Stimulation for the Progression to Addiction. Neuron, 88(5), 1054–1066. https://doi.org/10.1016/j.neuron.2015.10.017

Pauls, D. L., Abramovitch, A., Rauch, S. L., & Geller, D. A. (2014). Obsessive-compulsive disorder: An integrative genetic and neurobiological perspective. Nature Reviews. Neuroscience, 15(6), 410–424. https://doi.org/10.1038/nrn3746

Pereira, E. F., Aracava, Y., Aronstam, R. S., Barreiro, E. J., & Albuquerque, E. X. (1992). Pyrazole, an alcohol dehydrogenase inhibitor, has dual effects on N-methyl-D-aspartate receptors of hippocampal pyramidal cells: Agonist and noncompetitive antagonist. The Journal of Pharmacology and Experimental Therapeutics, 261(1), 331–340.

Platt, J. R., Kuch, D. O., & Bitgood, S. C. (1973). Rats' Lever-Press Durations as Psychophysical Judgments of Time1. Journal of the Experimental Analysis of Behavior, 19(2), 239–250. https://doi.org/10.1901/jeab.1973.19-239

Reich, R. R., & Goldman, M. S. (2015). Decision making about alcohol use: The case for scientific convergence. Addictive Behaviors, 44, 23–28. https://doi.org/10.1016/j.addbeh.2014.12.001

Reinhard, I., Leménager, T., Fauth-Bühler, M., Hermann, D., Hoffmann, S., Heinz, A., Kiefer, F., Smolka, M. N., Wellek, S., Mann, K., & Vollstädt-Klein, S. (2015). A comparison of region-of-interest measures for extracting whole brain data using survival analysis in alcoholism as an example. Journal of Neuroscience Methods, 242, 58–64. https://doi.org/10.1016/j.jneumeth.2015.01.001

Reiter, A. M. F., Deserno, L., Kallert, T., Heinze, H.-J., Heinz, A., & Schlagenhauf, F. (2016). Behavioral and Neural Signatures of Reduced Updating of Alternative Options in Alcohol-Dependent Patients during Flexible Decision-Making. The Journal of Neuroscience, 36(43), 10935–10948. https://doi.org/10.1523/JNEUROSCI.4322-15.2016

Renteria, R., Baltz, E. T., & Gremel, C. M. (2018). Chronic alcohol exposure disrupts top-down control over basal ganglia action selection to produce habits. Nature Communications, 9(1), 211. https://doi.org/10.1038/s41467-017-02615-9

Renteria, R., Cazares, C., & Gremel, C. M. (2020). Habitual Ethanol Seeking and Licking Microstructure of Enhanced Ethanol Self-Administration in Ethanol-Dependent Mice. Alcoholism: Clinical and Experimental Research, 44(4), 880–891. https://doi.org/10.1111/acer.14302

Rhodes, S. E. V., & Murray, E. A. (2013). Differential Effects of Amygdala, Orbital Prefrontal Cortex, and Prelimbic Cortex Lesions on Goal-Directed Behavior in Rhesus Macaques. The Journal of Neuroscience, 33(8), 3380–3389. https://doi.org/10.1523/JNEUROSCI.4374-12.2013

Robbins, T. W., Vaghi, M. M., & Banca, P. (2019). Obsessive-Compulsive Disorder: Puzzles and Prospects. Neuron, 102(1), 27–47. https://doi.org/10.1016/j.neuron.2019.01.046

Rolls, E. T., Everitt, B. J., & Roberts, A. (1996). The Orbitofrontal Cortex [and Discussion]. Philosophical Transactions: Biological Sciences, 351(1346), 1433–1444.

Sebold, M., Nebe, S., Garbusow, M., Guggenmos, M., Schad, D. J., Beck, A., Kuitunen-Paul, S., Sommer, C., Frank, R., Neu, P., Zimmermann, U. S., Rapp, M. A., Smolka, M. N., Huys, Q. J. M., Schlagenhauf, F., & Heinz, A. (2017). When

Habits Are Dangerous: Alcohol Expectancies and Habitual Decision Making Predict Relapse in Alcohol Dependence. Biological Psychiatry, 82(11), 847–856. https://doi.org/10.1016/j.biopsych.2017.04.019

Shoham, S., Fellows, M. R., & Normann, R. A. (2003). Robust, automatic spike sorting using mixtures of multivariate t-distributions. Journal of Neuroscience Methods, 127(2), 111–122. https://doi.org/10.1016/S0165-0270(03)00120-1

Siegle, J. H., López, A. C., Patel, Y. A., Abramov, K., Ohayon, S., & Voigts, J. (2017). Open Ephys: An open-source, plugin-based platform for multichannel electrophysiology. Journal of Neural Engineering, 14(4), 045003. https://doi.org/10.1088/1741-2552/aa5eea

Sjoerds, Z., de Wit, S., van den Brink, W., Robbins, T. W., Beekman, A. T. F., Penninx, B. W. J. H., & Veltman, D. J. (2013). Behavioral and neuroimaging evidence for overreliance on habit learning in alcohol-dependent patients. Translational Psychiatry, 3, e337. https://doi.org/10.1038/tp.2013.107

Stalnaker, T. A., Cooch, N. K., McDannald, M. A., Liu, T.-L., Wied, H., & Schoenbaum, G. (2014). Orbitofrontal neurons infer the value and identity of predicted outcomes. Nature Communications, 5, 3926. https://doi.org/10.1038/ncomms4926

Stalnaker, T. A., Cooch, N. K., & Schoenbaum, G. (2015). What the orbitofrontal cortex does not do. Nature Neuroscience, 18(5), 620–627. https://doi.org/10.1038/nn.3982

Stalnaker, T. A., Liu, T.-L., Takahashi, Y. K., & Schoenbaum, G. (2018). Orbitofrontal neurons signal reward predictions, not reward prediction errors. Neurobiology of Learning and Memory, 153(Pt B), 137–143. https://doi.org/10.1016/j.nlm.2018.01.013

Stephens, D. N., & Duka, T. (2008). Cognitive and emotional consequences of binge drinking: Role of amygdala and prefrontal cortex. Philosophical Transactions of the Royal Society B: Biological Sciences, 363(1507), 3169–3179. https://doi.org/10.1098/rstb.2008.0097

Tapert, S. F., Cheung, E. H., Brown, G. G., Frank, L. R., Paulus, M. P., Schweinsburg, A. D., Meloy, M. J., & Brown, S. A. (2003). Neural response to alcohol stimuli in adolescents with alcohol use disorder. Archives of General Psychiatry, 60(7), 727–735. https://doi.org/10.1001/archpsyc.60.7.727

Thayer, R. E., Hagerty, S. L., Sabbineni, A., Claus, E. D., Hutchison, K. E., & Weiland, B. J. (2016). Negative and interactive effects of sex, aging, and alcohol abuse on gray matter morphometry. Human Brain Mapping, 37(6), 2276–2292. https://doi.org/10.1002/hbm.23172

Volkow, N. D., Wang, G. J., Hitzemann, R., Fowler, J. S., Overall, J. E., Burr, G., & Wolf, A. P. (1994). Recovery of brain glucose metabolism in detoxified alcoholics. The American Journal of Psychiatry, 151(2), 178–183. https://doi.org/10.1176/ajp.151.2.178

Volkow, N. D., Wang, G. J., Overall, J. E., Hitzemann, R., Fowler, J. S., Pappas, N., Frecska, E., & Piscani, K. (1997). Regional brain metabolic response to lorazepam in alcoholics during early and late alcohol detoxification. Alcoholism, Clinical and Experimental Research, 21(7), 1278–1284.

Wallis, J. D. (2007). Orbitofrontal cortex and its contribution to decision-making. Annual Review of Neuroscience, 30, 31–56. https://doi.org/10.1146/annurev.neuro.30.051606.094334

Wallis, J. D. (2012). Cross-species studies of orbitofrontal cortex and value-based decision-making. Nature Neuroscience, 15(1), 13–19. https://doi.org/10.1038/nn.2956

Wrase, J., Grüsser, S. M., Klein, S., Diener, C., Hermann, D., Flor, H., Mann, K., Braus, D. F., & Heinz, A. (2002). Development of alcohol-associated cues and cue-induced brain activation in alcoholics. European Psychiatry: The Journal of the Association of European Psychiatrists, 17(5), 287–291. https://doi.org/10.1016/s0924-9338(02)00676-4

Yin, H. H. (2009). The role of the murine motor cortex in action duration and order. Frontiers in Integrative Neuroscience, 3, 23. https://doi.org/10.3389/neuro.07.023.2009

Zinn, S., Stein, R., & Swartzwelder, H. S. (2004). Executive Functioning Early in Abstinence From Alcohol. Alcoholism: Clinical and Experimental Research, 28(9), 1338–1346. https://doi.org/10.1097/01.ALC.0000139814.81811.62

CHAPTER TWO

Orbitofrontal Cortex Populations are Differentially Recruited to Support Actions

Christian Cazares[1], Drew C. Schreiner[2], Mariela Lopez Valencia[2] and Christina M. Gremel[1, 2]

[1]Neurosciences Graduate Program, University of California, San Diego, La Jolla, California, 92093

[2]Department of Psychology, University of California San Diego, La Jolla, California, 92093

Chapter Two is a reprint of material that was submitted to Neuron on May 3rd, 2022

Abstract

The ability to use information from prior actions is necessary for inference-guided behavior. While Orbitofrontal cortex (OFC) has been hypothesized as key for inferences made using Pavlovian and value-related information, whether OFC populations contribute to behavior by use of information from self-initiated actions is not clear. Here, we used a self-paced lever-press hold down task in which mice infer prior lever press durations to guide subsequent lever press performance. We show that activity of genetically identified lateral OFC subpopulations differentially instantiate current and prior action information during ongoing action execution. Transient state-dependent lOFC circuit disruptions of specified subpopulations reduced encoding of ongoing press durations and disrupted use of action-related information to guide future performance. In contrast, a chronic functional loss of lOFC circuit activity resulted in increased reliance on recently executed lever press durations and impaired contingency reversal, suggesting the recruitment of compensatory mechanisms that resulted in repetitive action-control. Our results identify a novel role for lOFC in the integration of action information to guide adaptive behavior.

Introduction

Flexible decision-making requires successful use of information derived from past experiences (Balleine & Dickinson, 1998; Bouton & Balleine, 2019; Balleine, 2019; Yoo et al., 2021). Orbitofrontal cortex (OFC) has been hypothesized to process inferred information relevant to ongoing task demands, integrating inferences into a "cognitive map" to support ongoing decision-making processes (Wilson et al., 2014; Schuck et al., 2016; Wikenheiser & Schoenbaum, 2016; Lopatina et al., 2017; Sadacca et al., 2018; Niv, 2019; Gardner & Schoenbaum, 2021). Past investigations have supported this hypothesis, showing OFC activity contributes to inferred information derived from external sources, such as with Pavlovian cues (e.g., Gallagher et al., 1999; Ostlund & Balleine, 2007a; Burke et al., 2009; Morrison & Salzman, 2011; Namboodiri et al., 2019), cued choices (e.g., Schoenbaum et al., 2003; Roesch et al., 2006; Rudebeck & Murray, 2008; Nogueira et al., 2017; Riceberg & Shapiro, 2017; Hocker et al., 2021), and outcome value (e.g., Izquierdo et al., 2004; Burke et al., 2008; Jones et al., 2012; Stalnaker et al., 2014; Bradfield et al., 2015; Rich & Wallis, 2016; Baltz et al., 2018; Malvaez et al., 2019). However, prior actions can also be used as information for inferences critical to adaptive control (Balleine, 2019; Klaus et al., 2019; Schreiner et al., 2021, 2022). Whether and which OFC populations are recruited for action-related information is less clear (Yalcinbas et al., 2021).

Volitional actions provide one the ability to dictate opportunities and achieve desired goals (Haggard, 2008). Depending on recent experiences, one can repeat actions to exploit a known rule, or modify an action to explore for new rules (Daw et al., 2006; Hogeveen et al., 2022), allowing one to adjust behavior from one decision to the

next. However, whether such action-related inferences recruit OFC-based contributions has been debated. On one hand, prior investigations have observed modulation of lateral OFC (lOFC) neurons during actions (e.g., Furuyashiki et al., 2008; Gremel & Costa, 2013; Simon et al., 2015; Cazares et al., 2021) and found disrupting lOFC activity perturbs actions sensitive to outcome devaluation (e.g., Gourley et al., 2013; Gremel et al., 2016; Gremel & Costa, 2013; Renteria et al., 2018; Rhodes & Murray, 2013). Additional work has suggested lOFC is recruited for goal-directed action control when action-outcome contingencies change during learning (Parkes et al., 2018). In contrast, studies have suggested that OFC populations may not participate in action processes per se, but instead are only recruited when Pavlovian-related, outcome-related, or value-related information is used to control behavior (Padoa-Schioppa & Assad, 2006; Ostlund & Balleine, 2007; Rudebeck et al., 2008; Camille et al., 2011; Fellows, 2011; Luk & Wallis, 2013; Cai & Padoa-Schioppa, 2014; Panayi & Killcross, 2018; Grattan & Glimcher, 2014). In support of the latter hypothesis, broad (i.e. not population specific) chemical-induced lOFC inactivation in marmosets was found to enhance choice sensitivity to changes in action-outcome contingencies (Duan et al., 2021). These latter findings support the hypothesis that lOFC activity is necessary when Pavlovian-related or outcome-related information contributes to inferences controlling behavior, but not behavior dependent upon inferences made using action-related information. However, action-outcome contingency degradation and outcome devaluation procedures often used to test these hypotheses do not provide a way to examine adjustments to the action itself, independently from adjustments based on the relationship between an action and its associated outcome. Furthermore, relatively

longer-term (i.e. lesions or whole-session manipulations) and non-specific lOFC activity disruptions found in these aforementioned studies may have facilitated compensatory mechanisms to assume responsibility for the observed behavioral disparities (Yin et al., 2006; Gremel et al., 2016; Li et al., 2016; Fresno et al., 2019; Inagaki et al., 2022). Thus, the specific contributions of lOFC to action-related information, if any, remain ambiguous.

Lateral OFC is widely innervated by cortical, thalamic, and subcortical areas (Cavada et al., 2000; Rolls, 2004; J. L. Price, 2007; Zhang et al., 2016; Murphy & Deutch, 2018; Barreiros et al., 2021), with incoming afferents synapsing onto various cortical cell types that include excitatory projection neurons and local interneuron populations that shape local network rhythmicity and neuronal firing (Sohal et al., 2009; Isaacson & Scanziani, 2011; Hu et al., 2014; Kepecs & Fishell, 2014; Ferguson & Cardin, 2020). Despite this vast interconnectivity, little is known about how information used for inferences is integrated within these lOFC microcircuits. As different cell-types may receive similar inputs, and thus potentially similar information, genetically distinct lOFC subpopulations could show functional homogeneity or differential representation of information used for inferences that guide adaptive behavior.

Here we investigated whether lOFC projection and local inhibitory populations are important for volitional action control. We used a self-paced instrumental task in which prior actions and the continuous context in which they occur are used to guide subsequent actions (Cazares et al., 2021; Schreiner et al., 2022). This allowed us to examine adjustments to action control while keeping broad action-outcome relationships stable. Mice learned to adjust lever press durations (i.e. an analog measure) to earn

rewards solely based on prior experiences, with no external, predictive information available to guide their ongoing behavior. Furthermore, lever pressing was goal-directed in that it was sensitive to shifts in action contingencies and outcome devaluation. We performed calcium-based fiber photometry of genetically distinct lOFC populations and found representation of volitional actions and action history in lOFC Calcium/calmodulin-dependent protein kinase II (CamKII+) projection neurons, and to a much lesser degree, in Parvalbumin (PV+) inhibitory interneurons. Behavior-dependent optogenetic perturbations to distinct lOFC populations showed lOFC activity encoded action-related information to guide future performance. Functional chronic loss of lOFC circuits produced a greater reliance on the most recently executed action despite a change in action contingencies. This suggests that a loss of lOFC resulted in recruitment of compensatory mechanisms and circuits that produced repetitive action control at the expense of integrating actions with broader experiential information for behavioral control. As such, we hypothesize that lOFC performs computations that contribute to the use of action history to guide adaptive behaviors.

Results

Mice learned to adjust self-generated lever presses using inferred action-related experience

Behavior is shaped in real time by its history. We adapted a lever-press hold down task that allowed us to investigate how experiential information influences subsequent action performance (Skinner, 1938; Platt et al., 1973; Yin, 2009; Fan et al., 2012; Cazares et al., 2021; Schreiner et al., 2022). Briefly, mice (C57BL/6J n = 23, 13 males, 10 females; PV^{cre} n = 14, 11 males, 3 females; no effect or interaction of

genotype or sex on any behavior measure so groups were combined in subsequent analyses) learned to hold down a lever press for longer than an arbitrary duration to earn a reward (Fig. 2.1a). Lever pressing was self-initiated, self-paced, and the lever remained extended into the chamber for the entire session. Importantly, there were no cues predictive of reward and mice received no feedback of performance success or failure until they terminated the lever press with reward delivered at offset.

After initial lever press pre-training, lever press duration criterion was set at >800 ms for five daily sessions, followed by five daily sessions with a >1600 ms duration criterion (Fig. 2.1b). A representative session from a well-trained mouse during a 1600 ms criteria day shows variability in the duration and frequency of lever presses made across the session (Fig. 2.1c). Examining the macroscopic aspects of lever press behavior showed mice reduced the number of total lever presses made (Fig. 2.1d, one-way RM ANOVAs for 800 ms and 1600 ms training durations, F's > 35.84, ps < 0.0001) and decreased response rates across each duration criteria (Fig. 2.1e, one-way RM ANOVAs Fs > 18.16, ps < 0.0001). Mice increased successful performance in the task within each duration criteria rule, as shown by an increase in the percentage of total presses made that exceeded the minimum duration criterion (Fig. 2.1f; one-way RM ANOVAs for 800 ms and 1600 ms training durations Fs > 31.32, ps < 0.0001). In addition, we observed rightward shifts in the distributions of press durations made when duration criteria shifted, from short durations made in pre training sessions (i.e. no duration requirement to earn a pellet reward) to longer durations made across the 800 ms and 1600 ms duration criterion sessions (Fig. 2.1g; two-way RM ANOVA, main effect of Duration Bin $F_{1.943, 69.96} = 336.5$, $p < 0.0001$, main effect of Criterion $F_{1.067,38.40} =$

Figure 2.1. *Mice learned to adjust self-paced, self-generated lever pressing actions across inferred contingency and outcome value changes.* **a** Behavior schematic demonstrating how mice must press and hold down a lever beyond a minimum duration to earn a food reward. **b** Training schedule for the lever press hold down task. Pretraining sessions were followed by sessions with a minimum duration criterion. Devaluation testing procedures occurred thereafter. **c** Representative data from one mouse showing variability of lever pressing and head entry behavior within a session. Dashed line indicates 1600 ms criterion. **d-f** Total lever presses (**d**), (**e**) lever pressing rate and (**f**) percentage of lever presses that exceeded the duration criterion across sessions. **g** Histogram of lever press durations (400 ms bins) averaged for all pretraining, 800 ms, and 1600 ms duration criterion sessions. **h** Normalized response rates (lever presses per minute) in valued and devalued states throughout devaluation testing. **i** Ratio of lever press duration Interquartile Range (IQR) and median during final 800 ms and 1600 ms duration criterion sessions. **j** Zoomed-in behavior from representative data shown in (c). k-n β coefficients of LME model relating current lever press duration (n) to prior (n - 1) press durations (**k**), press outcome (i.e. was lever press rewarded) (**l**), head entry (**m**), and interpress interval (IPI) (**n**) for actual and order shuffled data. 800 ms and 1600 ms refer to days where the criterion was >800 ms or >1600 ms. Data points represent mean ± SEM. Significance markers in k-n indicate comparisons to order shuffled data. Shuffled data are mean ± SEM of 1000 order shuffled β coefficients. *$p < 0.05$, ***$p < 0.001$, ****$p < 0.0001$ See also Supplementary Fig. 2.S1, Supplementary Table 2.S1, Supplementary Table 2.S2, Supplementary Table 2.S3.

Figure 2.1

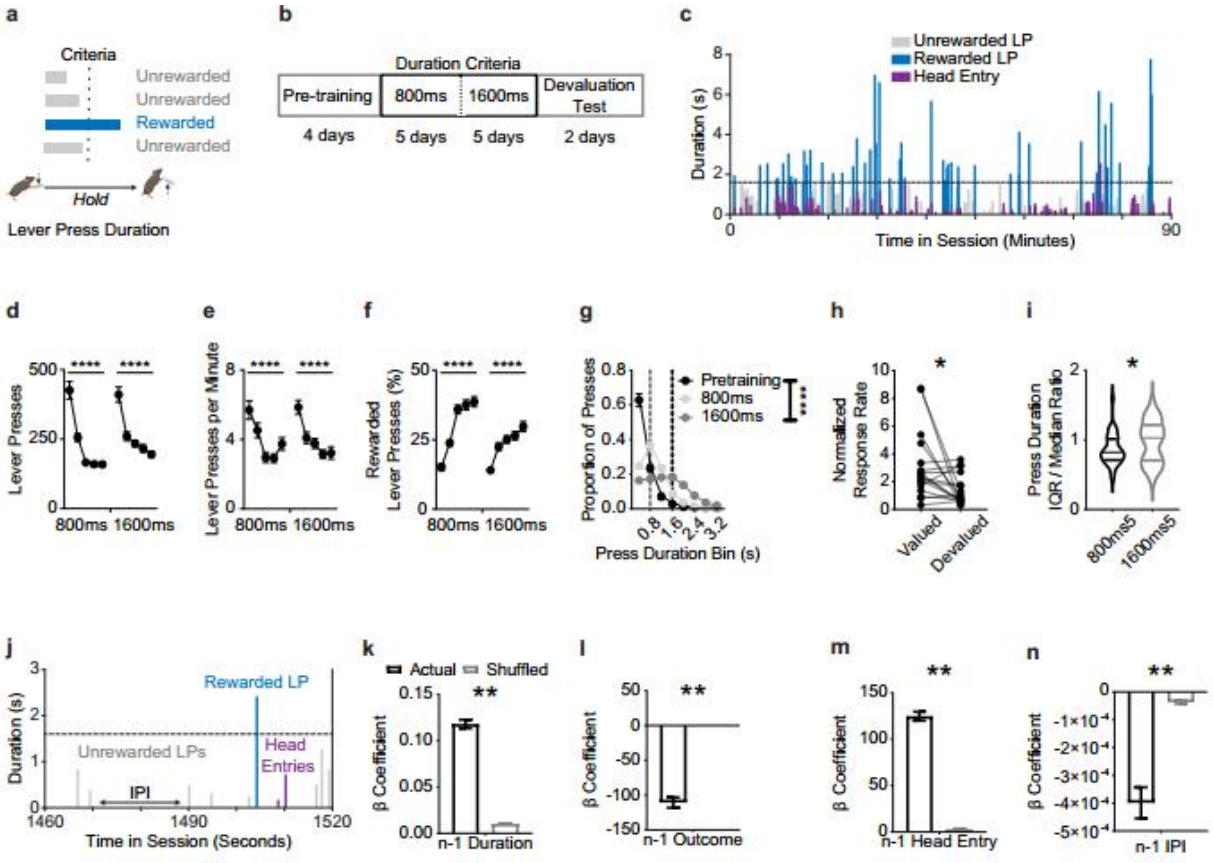
a
Criteria
Unrewarded
Unrewarded
Rewarded
Unrewarded
Hold
Lever Press Duration
b
Duration Criteria
Pre-training
800ms
1600ms
Devaluation Test
4 days
5 days
5 days
2 days
c
Unrewarded LP
Rewarded LP
Head Entry
Duration (s)
Time in Session (Minutes)
d
Lever Presses
800ms 1600ms
e
Lever Presses per Minute
800ms 1600ms
f
Rewarded Lever Presses (%)
800ms 1600ms
g
Pretraining
800ms
1600ms
Proportion of Presses
Press Duration Bin (s)
h
Normalized Response Rate
Valued
Devalued
i
Press Duration IQR / Median Ratio
800ms5
1600ms5
j
Rewarded LP
Unrewarded LPs
Head Entries
IPI
Duration (s)
Time in Session (Seconds)
k
Actual
Shuffled
β Coefficient
n-1 Duration
l
β Coefficient
n-1 Outcome
m
β Coefficient
n-1 Head Entry
n
β Coefficient
n-1 IPI

Figure 2.S1. *Devaluation testing procedures, performance, and LME models relating prior lever press durations to current press duration and overall session performance.* **a** Schematic showing counter-balanced devaluation testing procedures. Mice had 1 hour of free access to food pellets (devalued state) or a 20% sucrose solution (valued state) prior to a 10-minute 1600ms duration criterion session during which no reinforces were delivered. **b,c** Total lever presses (**b**) and percentage of lever presses (**c**) that exceeded the duration criterion in valued and devalued states throughout devaluation testing. Paired t tests revealed different patterns of lever pressing ($t_{16} = 2.408$, $p < 0.05$), but no difference in the percentage of lever presses ($t_{16} = 0.3536$, $p > 0.05$) that exceeded the duration criterion between valued and devalued states. **d** β coefficients of LME model relating current lever press duration (n) to prior (n – 10) press durations for actual and order shuffled data. **e** Linear regression for individual session data LME (n – 10) model described in (b), fitting (R^2) and percentage of lever presses that exceeded the duration criterion within that session. Dotted lines indicate 95% confidence interval of the best-fit line. Best-fit value slope = 0.001611 and Goodness of Fit (R^2) = 0.1120. Significant deviation from zero: $F_{1, 368} = 46.44$, $p < 0.0001$. **f** Linear regression for individual session data LME (n – 1) model described in (Fig. 1k-1n), fitting (R^2) and percentage of lever presses that exceeded the duration criterion within that session. Dotted lines indicate 95% confidence interval of the best-fit line. Best-fit value slope = 0.001062 and Goodness of Fit (R^2) = 0.05838. Significant deviation from zero: $F_{1, 368} = 22.81$, $p < 0.0001$. Significance markers in d indicate comparisons to order shuffled data. Shuffled data are mean ± SEM of 100 order shuffled β coefficients. * $p < 0.05$, *** $p < 0.001$, **** $p < 0.0001$. See also Supplementary Table 2.S1, Supplementary Table 2.S 2, Supplementary Table 2.S 3.

Figure 2.S1

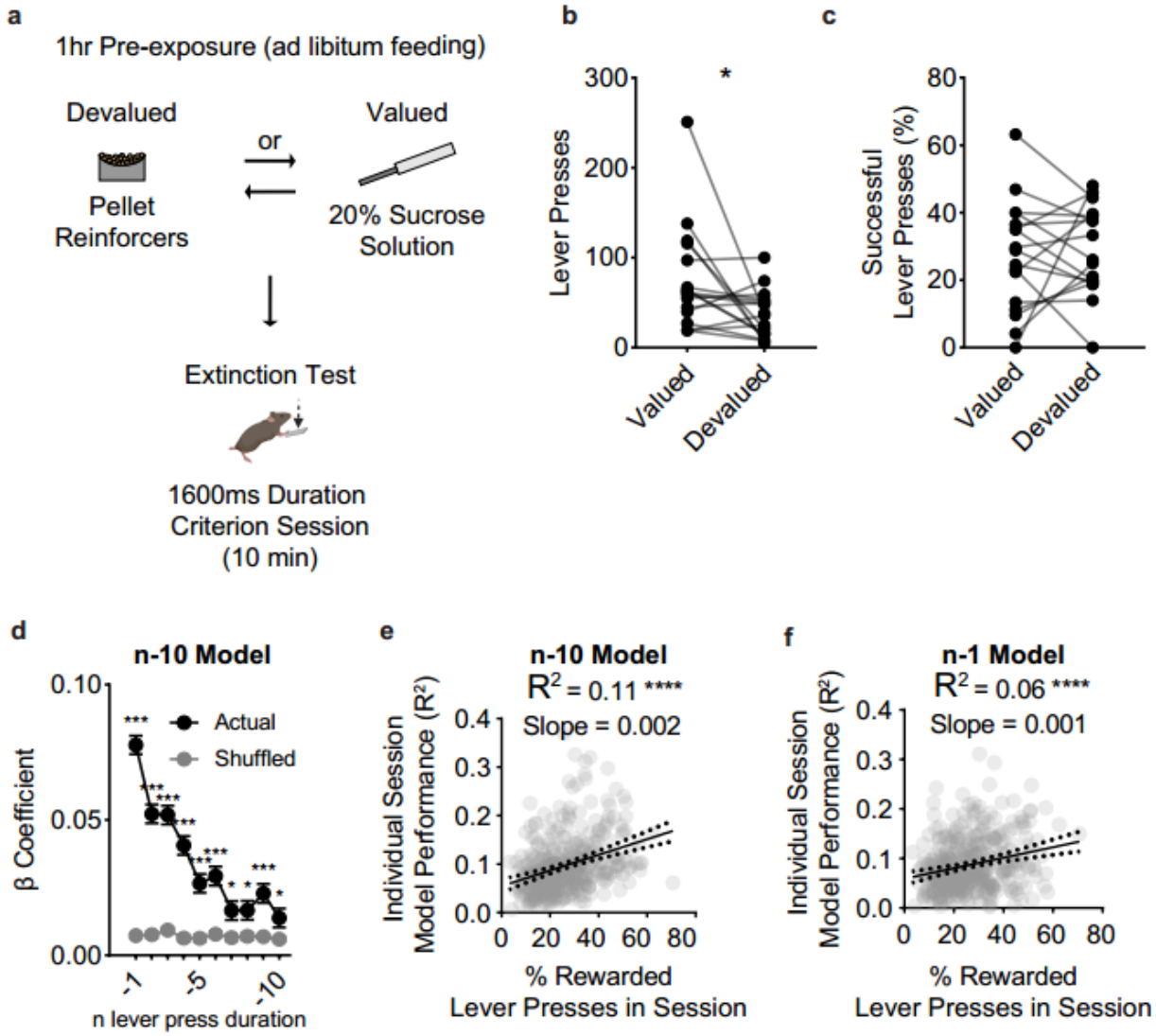
a
1hr Pre-exposure (ad libitum feeding)
Devalued
Pellet Reinforcers
or
Valued
20% Sucrose Solution
Extinction Test
1600ms Duration Criterion Session (10 min)
b
Lever Presses
300
200
100
0
*
Valued
Devalued
c
Successful Lever Presses (%)
80
60
40
20
0
Valued
Devalued
d
n-10 Model
β Coefficient
0.10
0.05
0.00
Actual
Shuffled
-1
-5
-10
n lever press duration
e
n-10 Model
R² = 0.11 ****
Slope = 0.002
Individual Session Model Performance (R²)
0.4
0.3
0.2
0.1
0.0
0 20 40 60 80
% Rewarded Lever Presses in Session
f
n-1 Model
R² = 0.06 ****
Slope = 0.001
Individual Session Model Performance (R²)
0.4
0.3
0.2
0.1
0.0
0 20 40 60 80
% Rewarded Lever Presses in Session

7.061, $p < 0.05$, and an interaction (Duration Bin * Criterion) $F_{2.622, 94.38} = 104.8$, $p < 0.0001$). Initiation of lever-press behavior in this task was goal-directed (Supplementary Fig. 2.S1a, see Materials and Methods), with outcome devaluation testing resulting in reduced normalized response rates in the devalued compared to valued states (Fig. 2.1h; Paired t-test, $t_{16} = 2.482$, $p < 0.05$) (Supplementary Fig. 2.S1b). Of note, the percentage of successful lever presses did not differ between valuation states (Supplementary Fig. 2.S1c), adding to prior findings that action initiation and performance in this task may be under different behavioral controllers (Cazares et al., 2021; Schreiner et al., 2022). Thus, broad behavioral performance measures suggested that mice used inferred contingency and expected outcome information to guide their lever press behavior.

However, it was unclear what information mice were using to adjust lever press performance. As previously reported (Schreiner et al., 2022), mice may not independently time lever press durations and their behavior violated the scalar property of timing (ratio of median and interquartile range (IQR) of lever press durations) (Fig. 2.1i; Paired t-test, $t_{36} = 2.588$, $p < 0.05$). The variable microstructure of ongoing behavior in our task (Fig. 2.1j) suggested that other sources of observable and inferred experiential information could influence lever press durations, such as prior lever press duration, prior reward delivery, prior checking behavior, as well as the time passed between lever presses (interpress-interval). To investigate whether these sources of experiential information influenced lever press behavior, we built linear mixed effect models (LMEs) that measured the predictive relationship of these behavioral events on the subsequent lever press duration (n). LME regression coefficients (β) from behavioral

covariates of interest were then compared against lever press order-shuffled data via permutation testing (see Materials and Methods).

We found that mice relied on prior experiential information to guide lever pressing. First, sequential lever press durations (n - 1) were related to one another (Fig. 2.1k; $p < 0.01$, Supplementary Table 2.S1), with the predictive relationship decaying up to the 10th prior (n - 10) lever press duration (Supplementary Fig. 2.S1d; $ps < 0.05$, Supplementary Table 2.S2), suggesting that mice inferred prior lever press durations to adjust future responding. Mice made shorter presses after reward delivery (n - 1 Outcome), potentially indicative of titrating lever press durations for performance success (Fig. 2.1l; $p < 0.01$) (Schreiner et al., 2022; Yin, 2009). Checking behavior, indexed via a head entry into the food receptacle, increased the subsequent lever press duration (Fig. 2.1m; $p < 0.01$). Furthermore, the longer the interval in between presses, the shorter the subsequent lever press duration (Fig. 2.1n; $p < 0.01$). Importantly, and in line with a prior report (Schreiner et al., 2022), we found that the relationship between sequential presses (β coefficient for n and n-1) was modified by whether the animal made a head entry (i.e. checking behavior) as well as how much time had elapsed (i.e. interpress interval) between presses (Supplementary Table 2.S3). In contrast, reward delivery did not alter the relationship between n and n - 1 lever press durations (Supplementary Table 2.S3), suggesting that the presence or absence of reward did not change how mice used prior lever press duration information to guide subsequent performance. The use of this experiential information improved performance. We tested LME model performance using individual session data and found a positive relationship between model R^2 for an individual and that individual's overall session performance

efficiency (Supplementary Fig. 2.S1e, 2.S1f). The above findings replicate previous results showing that when behavior is largely uninstructed, mice rely on numerous sources of experiential information to guide volitional action control (Schreiner et al., 2022), including inferences about prior action performance.

lOFC populations differentially encode actions and action-related information

We next sought to investigate whether OFC may reflect the use of such experiential information during decision-making, particularly lever press duration information. As head fixation can have large effects on context-dependent behaviors (Jovanovic et al., 2022), we monitored OFC population Ca^{2+} activity of CaMKII+ projection populations (rAAV5/PAAV-CaMKIIa-GCaMP6s) using *in vivo* fiber photometry in freely-moving mice (C57BL/6J, n = 9 mice, 6 males, 3 females) as they performed the lever-press hold down task during 1600 ms duration criterion training (Fig. 2.2a, Supplementary Fig. 2.S2). A perievent histogram of Ca^{2+}traces ordered by press duration revealed that CaMKII+ OFC projection population activity was modulated at select epochs relative to lever press initiation and execution (Fig. 2.2b). We segmented CaMKII+ fluorescence activity traces by whether or not the lever press was eventually rewarded. Group averaged CaMKII+ OFC projection population activity was modulated prior to the onset of a lever press, similarly to previously reported single-unit recordings (Gremel & Costa, 2013; Cazares et al., 2021). Permutation testing (Jean-Richard-dit-Bressel et al., 2020) revealed that pre onset lOFC Ca^{2+} activity differed with respect to its eventual outcome (Fig. 2.2c; ps < 0.05). Future success-related differences persisted during the lever press (Fig. 2.2d; ps < 0.05) and success-related differences were observed after the lever press release (Fig. 2.2e; ps < 0.05). Indeed, we observed

Figure 2.2. *$OFC^{CamKII+}$, but not OFC^{PV+}, Ca^{2+} activity encodes prior action information.* **a** (top)**, k** (bottom) Anatomical schematic and (bottom) representative histology of (**a**) $OFC^{CamKII+}$ or (**k**) OFC^{PV+} in vivo Ca^{2+} fiber photometry experiments. **b, l** Representative data heat map of (**b**) $OFC^{CamKII+}$ or (**l**) OFC^{PV+} normalized fluorescence changes relative to lever press initiation, ordered by lever press duration. Dashed white lines indicate 1600 ms session criterion window. Orange markers indicate the termination of an unrewarded lever press. Blue markers indicate the termination of rewarded lever press. **c-f, m-p** Ca^{2+} activity from (**c-f**) $OFC^{CamKII+}$ or (**m-p**) OFC^{PV+} populations z-scored normalized relative to a pre-lever press onset baseline period and aligned to (**c, m**) lever press onset, (**d, n**) lever press duration (presented as the relative percentage of total lever press duration), the (**e, o**) offset (i.e. termination) of a lever press, and the (**f, p**) first head entry made after a lever press. **g, q** Representative traces indicating changes in (**g**) $OFC^{CamKII+}$ or (**q**) OFC^{PV+} fluorescence over time. Shaded regions indicate the duration of the current (n) or prior (n - 1) lever press. Ca^{2+} activity magnitude predicted by LME models includes -2s to 0s before (Pre), during (Ongoing), or 0 to 2s after (Post) the current lever press. **h-j, r-t** β coefficients from LME models relating (**h-j**) $OFC^{CamKII+}$ or (**r-t**) OFC^{PV+} Ca^{2+} activity to current and prior durations for actual and order shuffled data (**h, r**) before press onset (Pre-LP Activity), (**i, s**) during the press (Ongoing LP Activity), and (**j, t**) after press offset (Post-LP Activity). LP = lever press, HE = Head Entry. Black lines in c-f, m-p indicate significant differences between Rewarded and Unrewarded lever presses via permutation testing ($p < 0.05$). Shuffled data are the mean ± SEM of 1000 order shuffled β coefficients. ** $p < 0.01$, *** $p < 0.001$. See also Supplementary Fig. 2.S2, Supplementary Table 2.S4, Supplementary Table 2.S5.

Figure 2.2

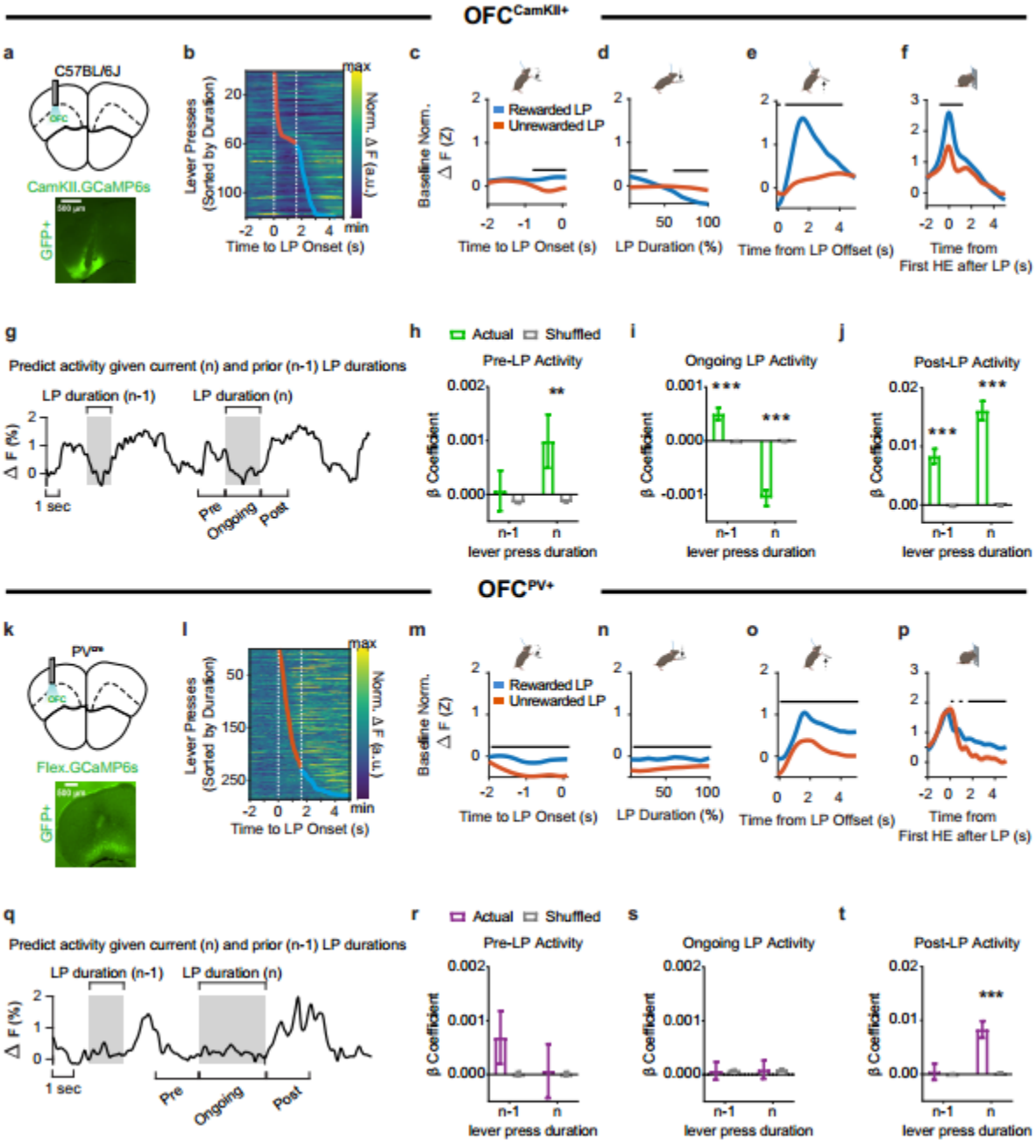
OFC CamKII+
a
C57BL/6J
OFC
CamKII.GCaMP6s
GFP+
b
Lever Presses (Sorted by Duration)
max
min
Norm. Δ F (a.u.)
Time to LP Onset (s)
c
Baseline Norm. Δ F (Z)
Rewarded LP
Unrewarded LP
Time to LP Onset (s)
d
LP Duration (%)
e
Time from LP Offset (s)
f
Time from First HE after LP (s)
g
Predict activity given current (n) and prior (n-1) LP durations
LP duration (n-1)
LP duration (n)
Δ F (%)
1 sec
Pre
Ongoing
Post
h
Actual
Shuffled
Pre-LP Activity
β Coefficient
lever press duration
i
Ongoing LP Activity
j
Post-LP Activity
OFC PV+
k
PV
Flex.GCaMP6s
l
m
n
o
p
q
r
s
t

Figure 2.S2. *Lever press performance throughout acquisition for fiber photometry experiments and representative OFC$^{CamKII+}$ Ca^{2+} activity.* **a** Training schedule for the lever press hold down task during fiber photometry experiments. Pretraining sessions were followed by sessions with a minimum duration criterion. **b-d** Total lever presses (**b**), (**c**) lever pressing rate and (**d**) percentage of lever presses that exceeded the duration criterion across sessions. One-way RM ANOVAs revealed a differences across 1600ms sessions for total lever presses ($F_{2.589, 41.43} = 5.739$, $p < 0.01$), lever pressing rate ($F_{2.652, 42.43} = 3.712$, $p < 0.05$), and percentage of lever presses that exceeded the duration criterion ($F_{2.959, 47.35} = 7.535$, $p < 0.001$). A Mixed-effects analysis revealed a difference across 800ms sessions for lever pressing rate only ($F_{2.650, 41.74} = 3.000$, $p < 0.05$). **e** Histogram of lever press durations (400ms bins) averaged for 800ms and 1600ms duration criterion sessions. A two-way Repeated Measures ANOVA (Bin * Criteria) on the proportion of presses across duration bins between the two duration criteria revealed a significant interaction: $F_{1.894, 30.30} = 9.954$, $p < 00.001$, a main effect of Bin: $F_{1.351, 21.61} = 95.29$, $p < 0.0001$, and a main effect of Criteria: $F_{1, 16} = 10.65$, $p < 0.01$). Post hoc comparisons showed significant differences between the duration criteria within the 0.4s ($p < 0.05$), 2.0s ($p < 0.05$), 2.4s ($p < 0.01$), 2.8s ($p < 0.01$) duration bins. **f** Representative trace showing the percentage of changes in baseline normalized Ca^{2+} activity over time. The region shaded in blue indicates a rewarded lever press duration. Green lines indicate head entries made. **g** Representative Ca^{2+} activity from a 1600ms duration criterion session aligned to lever press onset (i.e. initiation). Activity is z-score normalized to a pre-lever press onset baseline period. Blue indicates trace average of rewarded lever presses. Orange indicates trace average of unrewarded lever presses. LP = Lever Press. Data points represent mean ± SEM. * $p < 0.05$, ** $p < 0.01$, *** $p < 0.001$.

Figure 2.S2

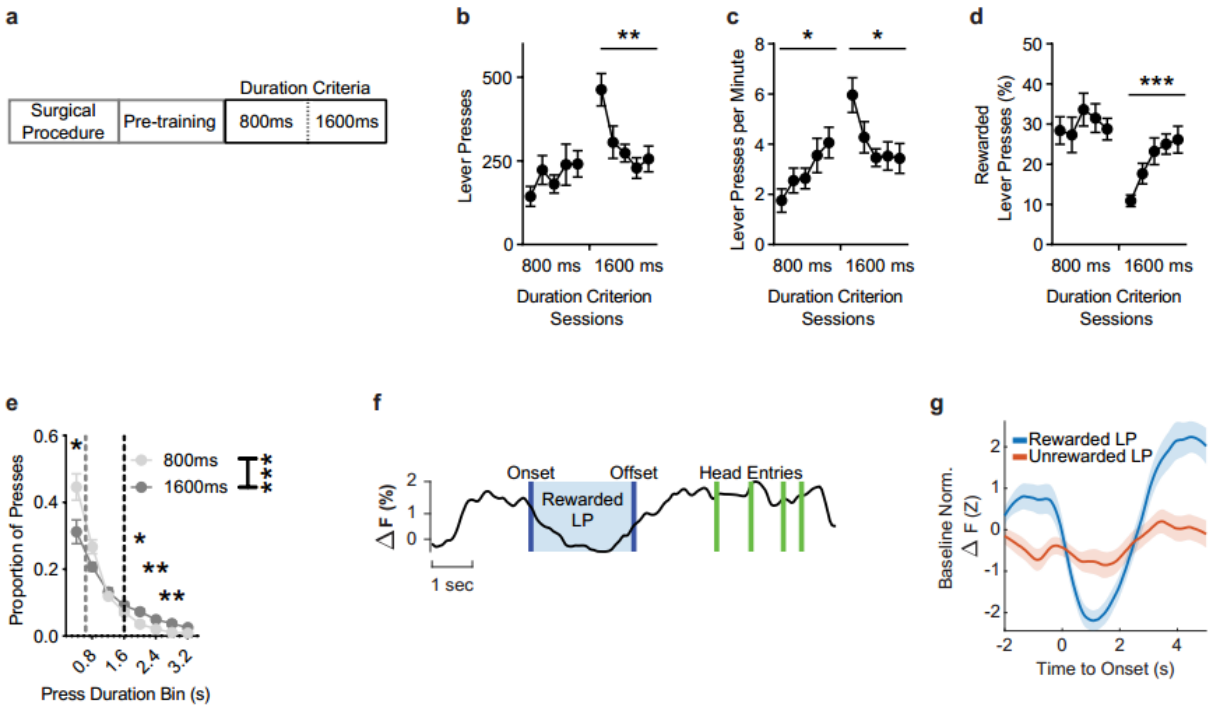
a
Duration Criteria
Surgical Procedure
Pre-training
800ms
1600ms
b
Lever Presses
500
250
0
**
800 ms
1600 ms
Duration Criterion
Sessions
c
Lever Presses per Minute
8
6
4
2
0
*
*
800 ms
1600 ms
Duration Criterion
Sessions
d
Rewarded Lever Presses (%)
50
40
30
20
10
0
***
800 ms
1600 ms
Duration Criterion
Sessions
e
Proportion of Presses
0.6
0.4
0.2
0.0
800ms
1600ms
*
*
**
**
**
0.8
1.6
2.4
3.2
Press Duration Bin (s)
f
ΔF (%)
2
1
0
Onset
Offset
Head Entries
Rewarded LP
1 sec
g
Baseline Norm. ΔF (Z)
2
1
0
-1
-2
Rewarded LP
Unrewarded LP
-2
0
2
4
Time to Onset (s)

greater levels of CaMKII+ OFC projection population activity in head entries that followed a successful lever press than in head entries following an unsuccessful lever press, corresponding to a time point during which mice had access to food pellet-related sensory and consummatory information (Fig. 2.2f; ps < 0.05).

Our results suggest that excitatory projection neurons in OFC can reflect information related to eventual performance outcomes before and throughout an instrumental action. To investigate whether this information originated from aspects of experiential information, we built LME models which aimed to predict lever press aligned changes in calcium activity given the current lever press duration and prior experiential information, with a focus on action-related information (Fig. 2.2g; see Materials and Methods). Prior to lever press onset, we found a significant relationship between CaMKII+ OFC projection population activity and the upcoming (n) lever press duration (Fig. 2.2h). This significant relationship was also found while the animals held down the lever (Fig. 2.2i) and was still present at termination of the lever press (Fig. 2.2j) (ps < 0.01). In other words, prior to lever press onset, greater increases in lOFC CaMKII+ activity were associated with longer durations of the upcoming action. However, during lever press execution, lower levels of activity corresponded to longer lever presses. At lever press offset, longer lever presses were associated with increased lOFC CamKII activity. When we examined whether lOFC CamKII+ activity reflected prior (n - 1) action-related information (i.e. prior press duration), we found a largely similar pattern, with significant relationships between current lOFC CamKII+ calcium activity and prior (n - 1) lever press duration during lever press execution (Fig 2i) as well as at lever press offset (Fig. 2.2j) (ps < 0.001). We also found that CaMKII+

OFC projection population activity during these lever press epochs was modulated by whether the prior lever press was rewarded or not, whether a checking head entry was made, as well as the time from prior lever press (Supplementary Table 2.S4). Together, our results suggest that current and prior action-related information as measured by lever press durations, as well as broader experiential information, is differentially encoded by CamKII+ projection populations in the OFC. This encoding occurred during action initiation and execution and further suggests that OFC projection circuits may be recruited to use action information from prior experiences during ongoing goal-directed actions.

OFC projection circuits do not act in isolation. Local GABAergic interneurons are crucial for the control of local circuit inhibition (Isaacson & Scanziani, 2011; Kepecs & Fishell, 2014; Ferguson & Cardin, 2020) with PV+ interneurons playing a critical role in tuning spike timing and synchronizing network oscillations (Sohal et al., 2009; Hu et al., 2014). As cortical projection and local inhibitory populations receive long-range cortical input (Zhang et al., 2016; Murphy & Deutch, 2018), it may be that PV+ lOFC inhibitory population activity reflects experiential information similar to that of CaMKII+ lOFC projection populations. However, it could also be that PV+ lOFC inhibitory population recruitment supports computations performed by local OFC projection populations independent of any specific type of information. Therefore we performed fiber photometry experiments monitoring Ca^{2+} activity of virally targeted PV+ lOFC interneuron populations (rAAV5/pAAV.CAG.Flex.GCaMP6s.WPRE.SV40) in freely moving PV^{cre} mice as they performed the lever-press hold down task (PV^{cre}, n = 8, 5 males, 3 females) (Fig. 2.2k). A peri-event histogram of baseline normalized PV+ traces

ordered by press duration suggested that PV+ lOFC interneuron population activity was modulated at select epochs relative to lever press initiation and execution, but with patterns that notably differed from CaMKII+ lOFC projection populations (Fig. 2.2l). Permutation testing revealed that group averaged lOFC PV+ Ca^{2+} activity was modulated prior to the onset of a lever press, with smaller reductions of activity observed with lever presses that would be rewarded (Fig. 2.2m; ps < 0.05). Reward-related differences in lOFC PV+ Ca^{2+} activity persisted during ongoing lever press execution (Fig. 2.2n; ps < 0.05) and after lever press offset (Figure 2.2o; ps < 0.05), increasing to a larger degree for rewarded than unrewarded press durations. In contrast to CaMKII+ lOFC projection populations, lOFC PV+ Ca^{2+} activity associated with head entries made following lever press release reached similar levels regardless of the presence of a reward (Fig. 2.2p; ps < 0.05).

To investigate whether PV+ lOFC inhibitory population activity is modulated by aspects of experiential information, we again built LME models which aimed to predict lever press aligned changes in PV+ Ca^{2+} activity given prior and current lever press durations, as well as other sources of experiential information (Fig. 2.2q). In contrast to the CaMKII+ lOFC projection population, PV+ lOFC interneuron population Ca^{2+} activity prior to (Fig. 2.2r) and throughout the lever press (Fig. 2.2s) was not predictive of ongoing (n) or prior (n - 1) lever press durations, prior checking behavior, nor the inter-press interval, but was predictive of whether the prior press was rewarded or not (Supplementary Table 2.S5). However, at lever press offset, PV+ lOFC interneuron population activity was predictive of the duration of the lever press that was just executed (n), as well as prior checking behavior and lever press outcome (Fig. 2.2t,

Supplementary Table 2.S5). Our results suggest that, unlike CamKII+ projection populations, PV+ inhibitory population activity in lOFC largely reflects outcome-related information during lever pressing and consequence-related information after lever press termination. Together, our results suggest that inferred action information is differentially encoded by lOFC sub-populations.

lOFC uses action-related information to modify behavior

That lOFC populations can reflect prior and current lever press durations suggests that lOFC activity may functionally contribute to the use of action information to adjust behavior. To test this hypothesis, we aimed to selectively disrupt local OFC activity in a temporally-specific manner during lever press execution. We used an optogenetic approach to bilaterally activate PV+ lOFC inhibitory populations with an excitatory opsin (rAAV5/Ef1a-DIO-hChR2(H134R)-eYFP), to inhibit local lOFC projection population activity (PV^{cre} ; n = 6 ChR2, 5 males, 1 female; n = 8 YFP, 5 males, 3 females) (Fig. 2.3a) (Baltz et al., 2018; Li et al., 2019). Optical stimulation of PV+ OFC inhibitory populations was behaviorally-dependent on the execution of a lever press, such that the initiation of every lever press, independent of their eventual duration, triggered light delivery (470 nm 20 Hz, 5 ms pulses) that continued until press termination (Fig. 2.3b). Stimulation days occurred after task acquisition (Fig. 2.3c). In days in which light was delivered, ChR2 mice maintained similar rates of responding (Fig. 2.3d; $p > 0.05$), but reduced the percentage of rewarded lever presses compared to fluorophore controls (Figure 2.3e; two-way RM ANOVA, main effect of Treatment only $F_{1, 12} = 4.990$, $p < 0.05$). Comparisons of lever press duration distributions suggested that light activation altered the distribution pattern of lever press durations in ChR2 mice

Figure 2.3. *Optogenetic excitation of OFC^{PV+} populations during action execution reduces rewarded performance and use of prior action information.* **a** (top) Schematic and (bottom) example histology of ChR2 optogenetic excitation of OFC^{PV+} neurons. **b** Behavior schematic demonstrating how 470 nm light delivery (20 Hz, 5 ms pulses) occurred for the duration of every lever press made. **c** Training schedule for optogenetic experiments. Pretraining sessions were followed by sessions with a minimum duration criterion. Sessions in which light was delivered occurred thereafter. **d-e** Lever pressing rate (**d**) and (**e**) percentage of lever presses that exceeded the duration criterion across sessions. Blue shaded region indicates the sessions in which light was delivered. **f** Histogram of lever press durations (400 ms bins) averaged for all 1600 ms duration criterion sessions during which light was delivered. **g** β coefficients of LME model relating current lever press duration (n) to prior (n - 1) press durations for YFP and ChR2 cohort actual data. Significance marker indicates comparisons to 1000 group shuffled data. 800 ms and 1600 ms refer to days where the criterion was >800 ms or >1600 ms. 1600 ms Stim On refers to days where criterion was >1600 ms and light was delivered. Data points represent mean ± SEM. *$p < 0.05$, **$p < 0.01$. See also Supplementary Table 2.S6.

Figure 2.3

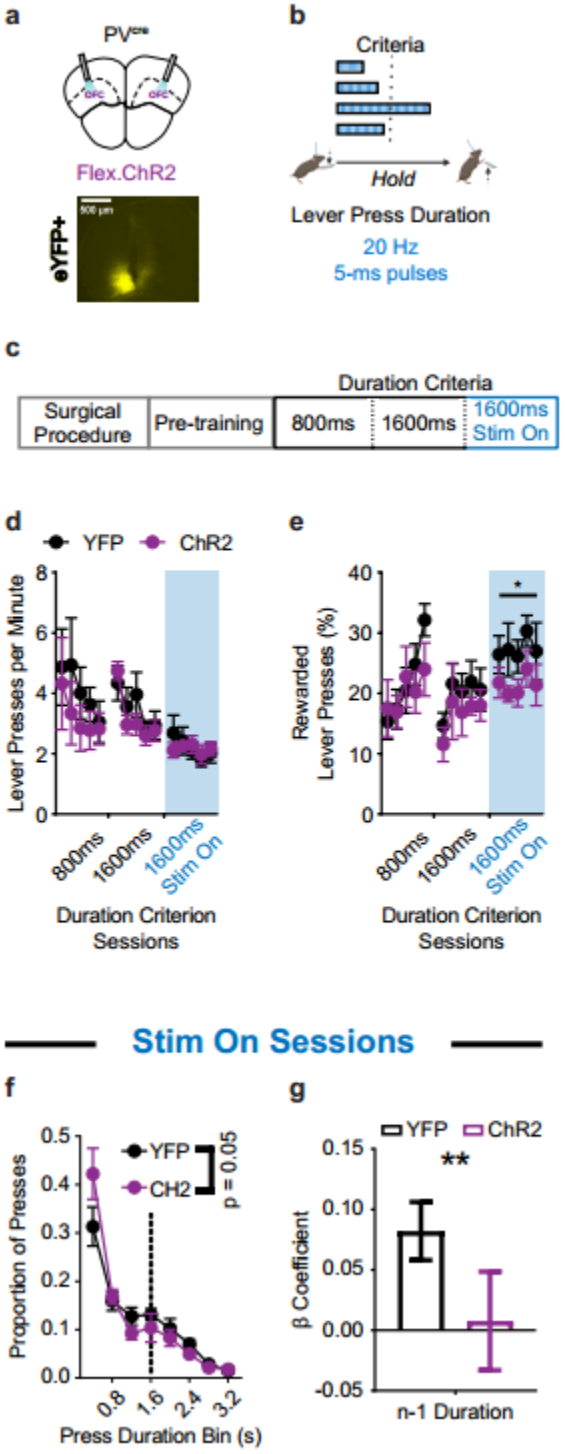
a
PV^Cre
Flex.ChR2
eYFP+
b
Criteria
Hold
Lever Press Duration
20 Hz
5-ms pulses
c
Duration Criteria
Surgical Procedure
Pre-training
800ms
1600ms
1600ms Stim On
d
YFP
ChR2
Lever Presses per Minute
800ms
1600ms
1600ms Stim On
Duration Criterion Sessions
e
Rewarded Lever Presses (%)
Duration Criterion Sessions
Stim On Sessions
f
Proportion of Presses
YFP
CH2
p = 0.05
Press Duration Bin (s)
g
YFP
ChR2
**
β Coefficient
n-1 Duration

(Fig. 2.3f; two-way RM ANOVA, main effect of Duration Bin $F_{1.813, 21.76} = 56.73$, $p = 0.0001$; marginally significant interaction (Duration Bin * Treatment) $F_{9, 108} = 1.967$, $p = 0.05$). The above data suggest disruption of lOFC activity during action execution impaired successful performance.

We next examined whether activation of lOFC PV+ inhibitory populations impaired performance in part by disrupting the predictive relationship between prior (n - 1) and ongoing (n) lever press durations. We added a term to our behavioral LME model that accounted for the presence or absence of the excitatory opsin (Treatment) in each animal. We found a significant interaction between the prior lever press duration and the presence of the opsin ($Duration_{n-1}$ * Treatment) in predicting subsequent lever press durations (Supplementary Table 2.S6; $p < 0.05$). A representation of group-segmented β coefficients showed a reduced relationship between prior (n - 1) and current (n) lever press durations in ChR2 animals compared to fluorophore controls (significant compared to 1000 group-shuffled data) (Fig. 2.3g, $p < 0.01$). The above suggests lOFC activity supports action-related information, such that its disruption during ongoing actions impairs the use of prior lever press duration information for behavioral control.

Disrupting lOFC activity during every lever press could have recruited compensatory mechanisms for task performance, such that these observed behavioral effects may not be directly attributable to a loss of lOFC function. Another possibility is that inhibiting lOFC during the lever press was akin to enhancing the general reduction in activity normally observed when the animal holds down the lever (Fig. 2.2d) (Cazares et al., 2021), thereby facilitating lOFC processes that could be competing with other

action-related processes and associated circuits. To directly investigate whether acute behavioral contributions of lOFC activity patterns support the use of action-related information, we bilaterally expressed an excitatory opsin in CamKII+ projection neurons (rAAV5/CamKII-hChR2(H134R)-eYFP-WPRE) to induce non-physiological increases in lOFC activity during lever pressing (i.e., when activity is normally decreased). We did this by pairing light activation to a subset of lever presses to determine how this perturbation would affect subsequent use of action-related information (C57BL/6J; n = 7 ChR2, 5 males, 2 females; n = 5 YFP, 2 males, 3 females) (Fig 2.4a). Specifically, light stimulation of CamKII+ projection populations was dependent on the execution of select lever presses, such that only every 7th lever press initiated light activation (470 nm 20 Hz, 5 ms pulses) that continued up until the lever press was terminated (Fig. 2.4b). As previously described, stimulation occurred post task-acquisition (Fig. 2.4c).

Both ChR2 and YFP mice reached similar rates of lever pressing and performance throughout training, including the 5 daily sessions during which light was delivered (Fig. 2.4d-f; ps > 0.05), suggesting that acute disruptions of lOFC activity during action execution on a subset of lever presses did not affect gross performance measures. A behavioral LME model that accounted for the presence or absence of the excitatory opsin in each animal found a significant interaction between the presence of the opsin and the predictive relationship between current and prior lever press durations ($Duration_{n-1}$ * Treatment) (Supplementary Table 2.S7, $p < 0.001$). To determine the direct effects of stimulation on the predictive relationship between prior (n - 1) and ongoing (n) lever press durations, we built a post-hoc LME model using either the ChR2 or YFP datasets that accounted for the presence or absence of light stimulation in each

Figure 2.4. *Selective optogenetic excitation of OFC$^{CamKII+}$ populations during action execution does not impair performance but affects use of prior action information.* **a** (top) Schematic and (bottom) example histology of ChR2 optogenetic excitation of OFC$^{CamKII+}$ neurons. **b** Behavior schematic demonstrating how 470 nm light delivery (20 Hz, 5 ms pulses) occurred for the duration of every 7th lever press made. **c** Training schedule for optogenetic experiments. Pretraining sessions were followed by sessions with a minimum duration criterion. Sessions in which light was delivered occurred thereafter. **d-e** Lever pressing rate (**d**) and (**e**) percentage of lever presses that exceeded the duration criterion across sessions. Blue shaded region indicates the sessions in which light was delivered. **f** Histogram of lever press durations (400 ms bins) averaged for all 1600 ms duration criterion sessions during which light was delivered. **g** β coefficients of post-hoc LME model relating current lever press duration (n) to prior (n - 1) or current (n) press durations for ChR2 cohort actual data. Significance marker indicates comparisons to 1000 order shuffled data. **h** Lever press durations of 1600 ms duration criterion sessions during which light was delivered on every 7th lever press, segmented by whether presses were paired with light activation or not. 800 ms and 1600 ms refer to days where the criterion was >800 ms or >1600 ms. 1600 ms Stim On refers to days where criterion was >1600 ms and light was delivered. Data points represent mean ± SEM. *$p < 0.05$, *** $p < 0.001$. See also Supplementary Table 2.S7, Supplementary Table 2.S8, Supplementary Table 2.S9.

Figure 2.4

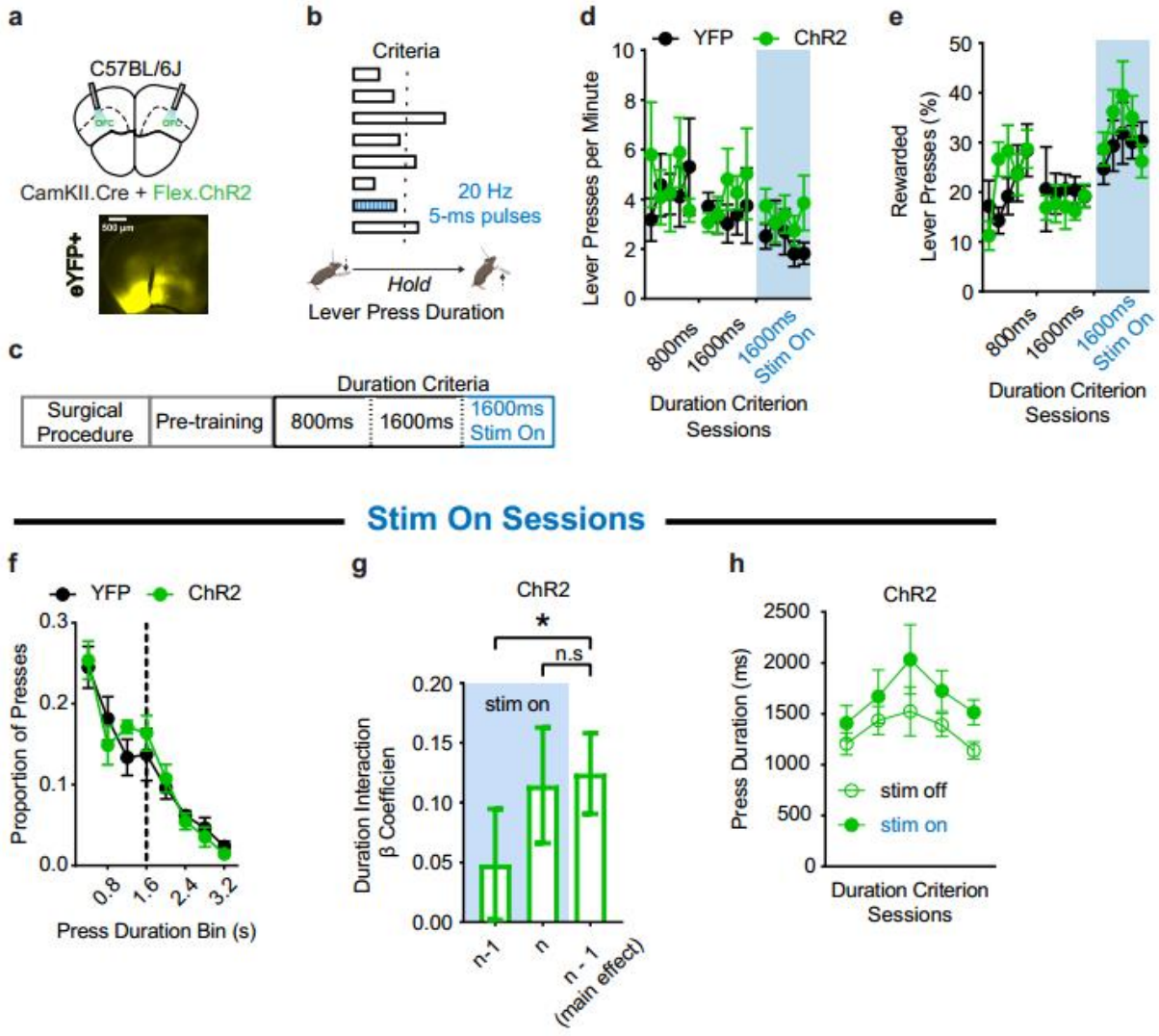
a
C57BL/6J
CamKII.Cre + Flex.ChR2
eYFP+
b
Criteria
20 Hz
5-ms pulses
Hold
Lever Press Duration
c
Duration Criteria
Surgical Procedure
Pre-training
800ms
1600ms
1600ms Stim On
d
YFP
ChR2
Lever Presses per Minute
800ms
1600ms
1600ms Stim On
Duration Criterion Sessions
e
Rewarded Lever Presses (%)
800ms
1600ms
1600ms Stim On
Duration Criterion Sessions
Stim On Sessions
f
YFP
ChR2
Proportion of Presses
Press Duration Bin (s)
g
ChR2
*
n.s
stim on
Duration Interaction β Coefficien
n-1
n
n - 1 (main effect)
h
ChR2
Press Duration (ms)
stim off
stim on
Duration Criterion Sessions

lever press. We found a significant interaction between prior press stimulation and the predictive relationship between current and prior press durations ($Duration_{n-1}$ * $Stimulation_{n-1}$) in ChR2-expressing mice that was absent in fluorophore control mice (Supplementary Table 2.S8, Supplementary Table 2.S9). Inspection of the LME model interaction β coefficients in ChR2 mice data showed light activation during the n - 1 lever press reduced the contribution of n-1 lever press duration to inform the ongoing (n) lever press ($p < 0.05$). However, light activation during the ongoing (n) lever press did not reduce that lever press's reliance on n - 1 duration information ($p > 0.05$) (Fig. 2.4g). These data suggest the proper patterning of lOFC activity supports processes related to the encoding (i.e. significant effect on n - 1 press activation), but not the retrieval and use (i.e. non-significant effect on n press activation) of action information to guide future action execution. To ensure that this decreased predictive relationship was not due to light activation inducing selective decreases or increases in the lever press duration itself, we confirmed that light activation did not change the duration of individual lever presses across sessions compared to non-light-activated presses (Fig. 2.4h; $p > 0.05$). In conjunction with our PV+ inhibitory population disruptions, these data suggest the proper patterning of lOFC activity supports processes related to the encoding of action information to guide future action execution, as lOFC perturbation does not disrupt ongoing performance but does disrupt the ability of prior lever press durations to inform future actions.

Loss of functional lOFC circuit increases reliance on immediate prior actions and outcomes

Different action strategies can be used to achieve the same goal (Dickinson, 1985; Balleine & Dickinson, 1998; Balleine & O'Doherty, 2010; Balleine, 2019); when one circuit is offline another may be recruited to support decision-making and adaptive behavior (H. H. Yin et al., 2006; Gremel & Costa, 2013; Li et al., 2016; Fresno et al., 2019). Within this framework, removal of OFC circuits could reveal compensatory or parallel mechanisms for volitional action control. To test how inactivation of lOFC projections impacted lever-press hold down task performance, prior to training we bilaterally ablated OFC CamKII+ neurons using a cre-dependent caspase approach that committed infected neurons to apoptosis (rAAV5/AAV-Flex-taCasP3-TEVP) (C57BL/6J; Lesion n = 16, 13 males, 3 females; Sham n = 23, 14 males, 9 females) (Fig. 2.5a-b, Supplementary Fig. 2.S3a) (Fink & Cookson, 2005; Yang et al., 2013).

lOFC lesioned mice had higher response rates than Sham mice during 1600 ms training (Fig. 2.5c; two-way RM ANOVA, main effect of Session $F_{1.912, 70.73} = 16.34$, $p < 0.0001$ and an interaction (Session * Treatment) $F_{4, 148} = 2.875$, $p < 0.05$). Lesion mice also had higher efficiency than Sham mice, with a higher percentage of rewarded lever presses (Fig. 2.5d; two-way RM ANOVA, main effect of Session $F_{2.347, 86.83} = 22.55$, $p < 0.0001$, and Treatment $F_{1, 37} = 6.804$, $p < 0.05$). Further, lOFC-lesioned mice showed a rightward shift in the distribution of lever press durations (Fig 2.5e; two-way RM ANOVA, main effect of Duration Bin $F_{2.872, 106.2} = 98.52$, $p < 0.0001$ and an interaction (Duration Bin * Treatment) $F_{9, 333} = 2.336$, $p < 0.05$) throughout the 1600 ms duration criterion sessions. A behavioral LME model that accounted for the presence or absence of the lesion in each animal found a significant interaction with treatment group altering the relationship between the current (n) and prior (n - 1) lever press durations

Figure 2.5. *Pretraining OFC$^{CamKII+}$ lesions increase rewarded performance and use of prior action information.* **a** (left) Schematic and (right) example histology of sham and Cre-dependent caspase lesion of OFC neurons. Red indicates AAV-EF1α-DIO-mCherry expression. Green indicates immunohistochemical reactions for neural nuclear protein NeuN. **b** Training schedule for lesion experiments. Pretraining sessions were followed by sessions with a minimum duration criterion. **c-d** Lever pressing rate (**c**) and (**d**) percentage of lever presses that exceeded the duration criterion across sessions. **e** Histogram of lever press durations (400 ms bins) averaged for all 800 ms and 1600 ms duration criterion sessions. Dotted lines indicate 800 ms (grey) and 1600 ms (black) duration criteria. **f-g** β coefficients of LME model relating current lever press duration (n) to prior (n - 1) press durations (**f**) and press outcome (i.e. was lever press rewarded) (**g**) for Sham and Lesion cohort actual data. Significance markers indicate comparisons to 1000 group shuffled data. **h-i** Lever pressing rate (**h**) and (**i**) percentage of lever presses that exceeded the 400 ms duration criterion across sessions. **j** Histogram of lever press durations (400 ms bins) averaged for all 400ms duration criterion sessions. Dotted line indicates 400 ms duration criteria. 400 ms, 800 ms,1600 ms refer to days where the criterion was >400 ms, >800 ms or >1600 ms. Data points represent mean ± SEM. *p <0 .05, ** p < 0.01, *** p < 0.001. See also Supplementary Table 2.S10.

Figure 2.5

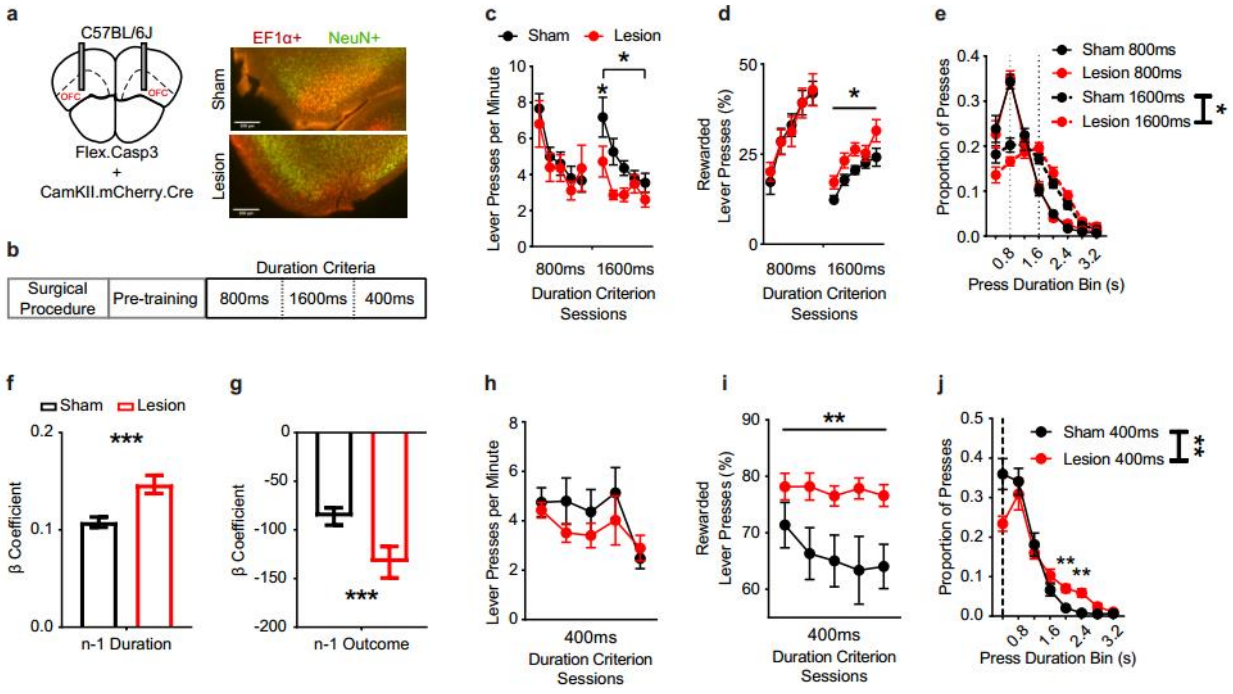
a
C57BL/6J
OFC
OFC
Flex.Casp3
+
CamKII.mCherry.Cre
EF1α+
NeuN+
Sham
Lesion
b
Duration Criteria
Surgical Procedure
Pre-training
800ms
1600ms
400ms
c
Sham
Lesion
Lever Presses per Minute
800ms 1600ms
Duration Criterion Sessions
d
Rewarded Lever Presses (%)
800ms 1600ms
Duration Criterion Sessions
e
Sham 800ms
Lesion 800ms
Sham 1600ms
Lesion 1600ms
Proportion of Presses
Press Duration Bin (s)
f
Sham
Lesion
β Coefficient
n-1 Duration
g
β Coefficient
n-1 Outcome
h
Lever Presses per Minute
400ms
Duration Criterion Sessions
i
Rewarded Lever Presses (%)
400ms
Duration Criterion Sessions
j
Sham 400ms
Lesion 400ms
Proportion of Presses
Press Duration Bin (s)

Figure 2.S3.

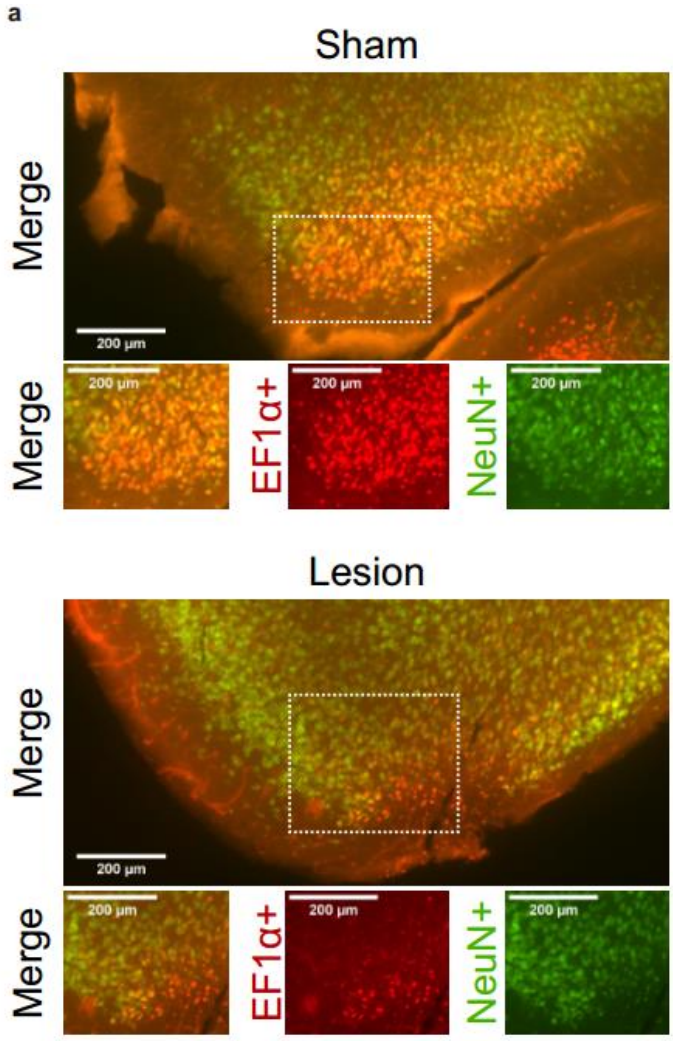

Figure 2.S3. ***Representative histology of sham and Cre-dependent caspase lesions of OFC$^{CamKII+}$ neurons.*** **a** Representative histology as shown in Fig. 5a of sham and Cre-dependent caspase lesions of OFC neurons, zoomed in for visual clarity. Red indicates AAV-EF1α-DIO-mCherry expression. Green indicates immunohistochemical reactions for neural nuclear protein NeuN. White dotted squares indicate zoomed-in regions. Slice taken approximately from Bregma: AP +2.7mm, L +1.65mm and V −2.6mm.

(Duration$_{n-1}$ * Treatment) (Supplementary Table 2.S10; $p < 0.0001$). A visual representation of treatment group-segmented β coefficients showed a larger positive relationship between prior and subsequent durations in Lesion animals compared to Sham controls (significant compared to 1000 group-shuffled data) (Fig. 2.5f, $p < 0.001$). We also found a significant interaction between the outcome of the prior lever press and lesion group (Outcome$_{n-1}$ * Treatment) (Supplementary Table 2.S10; $p = 0.0005$). A representation of treatment group-segmented β coefficients showed a greater negative relationship between prior outcome and subsequent durations in Lesion mice compared to Sham mice (significant when compared to 1000 group-shuffled data) (Fig. 2.5g, $p < 0.001$). Thus lOFC lesions prior to training resulted in mice performing actions more affected by immediate prior action performance and their immediate associated consequence.

lOFC lesions have been found to reduce behavioral flexibility and impair sensitivity to rule reversals (Bechara et al., 1999; Schoenbaum et al., 2002, 2003; Izquierdo et al., 2004; Stalnaker et al., 2007; Rhodes & Murray, 2013). We conducted an additional 5 daily sessions in which the duration criterion was reduced to 400 ms for a subset of animals (C57BL/6J; Lesion n = 16, 13 males, 3 females; Sham n = 8, 6 males, 2 females). We found that while Sham and Lesion mice showed similar rates of lever pressing (Fig. 2.5h; two-way RM ANOVA, main effect of Session only $F_{1.645, 36.20} = 4.274$, $p < 0.05$), Lesion mice performed more efficiently than Sham mice as indexed by a higher percentage of rewarded lever presses (Fig. 2.5i; Fig. 5h; two-way RM ANOVA, main effect of Treatment only $F_{1, 22} = 1.590$, $p < 0.01$) and showed a rightward shift in the distribution of lever press durations (Fig. 2.5j; two-way RM ANOVA, main effect of

Duration Bin $F_{2.369, 52.13} = 70.97$, $p < 0.0001$ and an interaction (Duration Bin * Treatment) $F_{9, 198} = 3.164$, $p < 0.01$). The above suggests mice with lOFC lesions did not adjust their performance to the same degree as sham animals when the duration contingency was reduced in duration. Instead, lOFC lesion mice continued to perform longer lever presses, a strategy that improved efficiency but differed from the exploration of effort that intact mice exhibited.

Discussion

Here we identify a role for lOFC in action control. By examining adjustments to actions within the continuous context in which they occur, we were able to separate control processes dictated by inferences about prior actions from those dictated by inferences of action-outcome contingency or expected outcome value. In doing so, we saw clear evidence that mice recruit and use lOFC activity to encode action-related information that can be used for inferences critical to adaptive control of behavior. A loss of lOFC circuits left mice more reliant on a strategy of repeating action execution to gain reward and impaired the updating of action contingencies. This raises the hypothesis that lOFC circuit disruptions seen in psychiatric disorders may give way to compensatory mechanisms that promote repetitive action control by exploiting the reliance on learned rules, even when disadvantageous.

There is increasing evidence of lOFC disruption in psychiatric disorders characterized by disrupted action control, including substance use disorders and compulsive disorders (Milad & Rauch, 2012; Pauls et al., 2014; Robbins et al., 2019; Lüscher et al., 2020), highlighting the need for a greater understanding of OFC's contribution to the use of action-related information. Actions made during decision-

making are often autonomous and unconstrained, occurring in contexts in which contingencies and associative structure of ongoing tasks are partially observable at best (Balleine, 2019; Costa, 2011; Murakami et al., 2014; Yoo et al., 2021). We show that eschewing trial-based, cued choice structure in task design has advantages for understanding how adaptive behavior is realized when actions are self-paced, self-generated, and solely reliant on inferences that recruit information from past experiences. The unstructured, self-paced nature of our task allowed us to identify patterns of lOFC activity that reflected prior action information as well as other sources of experience. As OFC populations have been shown to process Pavlovian-related and reward-predictive information (Jones et al., 2012; Stalnaker et al., 2014; Nogueira et al., 2017; Riceberg & Shapiro, 2017; Namboodiri et al., 2019; Sias et al., 2021; Hocker et al., 2021), our findings suggest that OFC can also represent and integrate action-related information to guide adaptive behavior depending on the behavioral context.

While prior single unit recordings from largely unclassified populations have shown lOFC neurons can reflect sensory, predictive, and outcome-related information (e.g., Padoa-Schioppa & Assad, 2006; Riceberg & Shapiro, 2017; Nogueira et al., 2017; Hocker et al., 2021), here we find that lOFC populations appear to be differentially recruited to support encoding of action-related information. CamKII+ projection neuron activity increased prior to the onset of the action, decreased during action execution, and ramped back up after the action was terminated (Fig. 2.2). These lOFC activity patterns were reminiscent of prior single-unit recording activity observations in rodents performing the same task (Cazares et al., 2021), suggesting single neuron population activity likely tracks population calcium activity. Furthermore, lOFC excitatory projection

neuron activity reflected current and prior action-related information during ongoing action execution. Temporally precise and behavioral dependent perturbation to these endogenous lOFC CamKII+ neuron activity patterns decreased reliance on action-related information. Intriguingly, these lOFC CamKII+ activity patterns differed in timing and magnitude compared to PV+ interneuron activity patterns. PV+ populations showed relatively performance-independent decreases in modulation prior to and through action execution, little outcome encoding during reward checking behaviors, and maintained little representation of action-related information. While the use of population calcium measurements may not capture individual neuron encoding of action-related information, these findings do suggest that action-related information is reflected in recruitment of lOFC CamKII+ populations and to a much lesser extent PV+ populations. Cortical GABAergic interneurons are thought to gate information flow within cortical microcircuits (Isaacson & Scanziani, 2011; Hu et al., 2014; Kepecs & Fishell, 2014; Ferguson & Cardin, 2020). Perhaps the observed differential patterns of lOFC activity are reflective of local microcircuit interactions that facilitate the flow of action-related information through this region.

OFC has been hypothesized to integrate and relay information from prior experiences to its broader circuits to support ongoing decision-making processes (Niv, 2019; Schuck et al., 2016). lOFC neurons have been shown to encode prior reward-predictive information before subsequent choices are made (Nogueira et al., 2017; Riceberg & Shapiro, 2017; Hocker et al., 2021). Here we observed lOFC CamKII+ activity reflected the future success or failure of the imminent and ongoing lever-press (Fig. 2.2). Furthermore, LME modeling showed that this activity maintained information

related to the prior lever press duration (Fig. 2.2). Indeed, optogenetic perturbation to lOFC populations during ongoing action execution revealed that this lOFC activity contributed to the execution of future responses. Specifically, we saw that optogenetic perturbation diminished performance efficacy and decreased reliance on duration-related information derived from the prior perturbed lever press, without directly affecting current lever press duration (Fig. 2.3, 2.4). These findings suggest that the encoding of prior actions by lOFC serves as a source of information that can contribute to adapting ongoing action execution. Such types of information within OFC populations has been hypothesized to be influenced by broader circuit innervation, such as the ventral tegmental area (Namboodiri et al., 2019) and the basolateral amygdala (Sias et al., 2021). Investigations examining what OFC relays to downstream targets suggests that lOFC terminals in the dorsal striatum convey both action and outcome-related information to influence ongoing behaviors (Ahmari et al., 2013; Burguière et al., 2013; Pascoli et al., 2018; Renteria et al., 2018; Groman et al., 2019). In addition, lOFC projections convey rule information to premotor cortical areas used to guide arbitration between rule exploration and exploitation (Johnson et al., 2016; Schreiner et al., 2022; Schreiner & Gremel, 2018). Whether broader circuit recruitment and downstream targets of these lOFC-based action representations involve the above-mentioned areas is unknown and should be explored.

The loss of lOFC CamKII+ projection neuron populations did not lead to a loss of efficacy in performance or action control. Instead, lesioned mice showed more efficacious performance and persisted in making longer lever presses despite the change to a shorter duration criterion for success (Fig. 2.5). Historically, OFC lesions

have been thought to spare behavior that relies on observable information while impairing behavior when task demands get more abstract and begin to rely on inference-based information (Wilson et al., 2014). Our results suggest a nuanced view of what lOFC may contribute to action control. While lOFC may not be necessary for direct action control per se, it does appear to be recruited when behavioral control necessitates the inclusion of action and outcome-related inferences, broad experiences, and the need for exploration (Hogeveen et al., 2022). Perhaps a functional loss of OFC circuits engaged compensatory mechanisms (e.g., recruitment of other circuits) that biased control of behavior to rely on more immediate sources of reward-related information (Dickinson, 1985; Daw et al., 2005; Balleine & O'Doherty, 2010; Doll et al., 2012; Drummond & Niv, 2020). In other words, lesioned animals may not have favored a shift in lever pressing strategy since long durations were still producing reward. In addition, lesioned mice may have reduced the degree of exploration normally exhibited. Both hypotheses suggest lOFC CamKII+ projection neuron lesions left mice repeating actions to exploit a known rule. We should note that it is not clear whether the behavioral effects in lesioned mice were mediated only by a loss of CamKII+ projection neuron populations or by other indirect consequences of cell death in the region, such as macrophage accumulation or inflammatory responses (Fink & Cookson, 2005). Thus activity originating from lOFC appears to support adaptive control of behaviors that in its absence facilitate action strategies that rely on similar behaviors if they had been previously successful.

OFC dysfunction is found in disease states associated with repetitive behaviors and disrupted action control, such as in obsessive compulsive disorder and substance

use disorders (Lüscher et al., 2020; Robbins et al., 2019). Investigating how information derived from past behaviors are integrated in OFC to influence subsequent actions can aid our understanding of how substances of abuse are sought out and consumed based on prior experience. In humans, repeated transcranial magnetic stimulation studies targeting OFC have been shown to be effective at reducing compulsivity (Nauczyciel et al., 2014; Price et al., 2021). Here we establish that population-specific activity originating in lOFC can reflect action-related information and can influence future action implementation. While OFC neurons have been shown to have less action-related recruitment and activity modulation during motor responding compared to some other cortical areas (Knudsen & Wallis 2022), discounting its role in processing action information in its entirety limits much needed investigations. The prior experimental discord over whether OFC contributes to action control may have arisen from the use of task parameters that were unable to isolate processes underlying action control from their relationship with associated outcomes or from examining choice behaviors that can readily use observable information. Such tasks may have also elicited a training-induced bias in recruitment of alternative mechanisms for action control. Thus, our findings support the hypothesis that lOFC circuits contribute to adaptive behaviors that rely on prior experience, and that their disruption may lead to an alteration of volitional action control biased towards excessive repetition.

Methods

Animals

C57BL/6J (n = 83, 58 males, 25 females) and PV^{cre} ($Pvalb^{tm1(cre)Arbr}$: n = 36, 26 males, 10 females) mice (>7 weeks/50 PND) (The Jackson Laboratory, Bar Harbour,

ME) were housed two to five per cage under a 14:10 hour light:dark and had access to water *ad libitum*. Prior to behavioral procedures, mice were food restricted to 85-90% of their baseline weight for at least 2 days, and were fed a minimum of one hour after daily training (Labdiet 5015). Exploratory analyses for sex and genotype differences in the behavioral cohort revealed similar levels of behavioral performance, and thus data was collapsed across sex and across genotype. Mice were at least 6 weeks of age prior to surgical procedures. All experiments were approved by the University of California San Diego Institutional Animal Care and Use Committee and were carried out in accordance with the National Institutes of Health (NIH) “Principles of Laboratory Care”. Investigators were not blind to the experimental groups. The Animal Care and Use Committee of the University of California, San Diego approved all experiments and experiments were conducted according to the National Institutes of Health (NIH) “Principles of Laboratory Care” guidelines.

Behavioral Procedures

Daily mouse training sessions occurred within sound attenuating operant chambers (Med-Associates, St Albans, VT) where lever presses (location counterbalanced, either left or right of the food magazine) were required for a reward outcome of regular ‘chow’ pellets (20 mg pellet per reinforcer, Bio-Serv formula F0071). On the first day of pre-training, mice were trained to retrieve pellets from the food magazine (no levers present) on a random time (RT) schedule, with a pellet outcome delivered on average every 120 seconds for 60 minutes. For the next 3 days of pre-training, lever presses were rewarded on a continuous reinforcement (CRF) schedule for up to 15 (CRF15), 30 (CRF30) or 60 (CRF60) pellet reward deliveries or until

90 minutes had passed. For surgical implant experiments, an additional CRF60 training day (for a total of 4 CRF days) was administered with the implant connected to habituate the animal to the tethered connection. Before each session in which the animal was tethered to a fiber optic cable, mice were exposed to a brief (< 60 seconds) bout of low-dose isoflurane anesthesia to connect the ferrule implant. To avoid confounding effects of anesthesia on brain activity, mice were then moved into the procedure room and monitored for a minimum of 30 min before placing them in the operant chamber and initiating the session. The start of each session triggered house-light illumination and the extension of the lever unless stated otherwise.

Following pre-training, mice were introduced to the hold down task. Lever presses now had a duration requirement, such that mice had to continue holding down the lever press for a fixed minimum amount of time in order to earn a pellet reward. Reward delivery occurred only after the termination of a lever press that exceeded the session's minimum duration criteria, which began with > 800 ms for 5 daily sessions, followed by > 1600 ms for another 5 daily sessions. Each session ended when 90 minutes had elapsed or the mouse had earned 60 total reinforcers, at which point the house light turned off and the lever was retracted. Each lever press onset and termination was timestamped at a 20 ms time resolution to calculate its duration, along with pellet delivery and the start and end of head entries into the food magazine.

Outcome Devaluation Testing

A subset of the behavioral cohort (n = 18, 10 males, 8 females) was habituated to a novel cage and 20% sucrose solution for 1 hour each day. Following the last day of hold down training, we performed sensory-specific satiation across 2 consecutive days,

consisting of counterbalanced valued and devalued days. For the valued day, the mice were allowed to freely consume 20% sucrose solution for 1 hour. For the devalued day, mice were allowed to freely consume for 1 hour the pellet outcome previously earned in the lever press hold down task. One mouse that did not consume enough pellets (< 0.1 g) or sucrose (< 0.1 ml) during this free-access period was excluded from subsequent analysis (giving final n = 17, 10 males). Immediately following the feeding period, mice were placed into their respective operant chamber for a 10 minute session during which the number and duration of lever presses made were recorded, but no pellet reward was delivered. Investigators were not blind to the experimental groups. Response rate comparisons between valued and devalued days were made by normalizing each mouse's test day response rate (RR) to the average response rate of their corresponding last 2 days of hold down training using the following formula:

$$RRTest\ Day\ \div\ mean(RR1600ms4 + RR1600ms5)$$

Surgical Procedures

Mice first underwent isoflurane anesthesia (1-2%) before stereotaxic-guided intracranial injections via 500 nl volume Hamilton syringes (Reno, NV). Viral vectors were infused at a rate of 100 nl/minute and the syringe was then left unperturbed for 5 minutes to allow for diffusion after delivery. Mice were allowed to recover for a minimum of two weeks before the start of behavioral procedures. At the end of behavioral procedures, mice were euthanized and their brains were extracted and fixed in 4% paraformaldehyde. Optic fiber placement and viral expression was qualified by examining tracts in 50- to 100-μm-thick brain slices under a macro fluorescence microscope (Olympus MVX10). All surgical and behavioral experiments were performed during the light portion of the cycle.

For fiber photometry experiments, OFC was unilaterally targeted for viral injections at the following stereotaxic coordinates from Bregma: AP +2.7mm, L +1.65mm and V −2.6mm, with optic fiber ferrule placed V -2.5mm from the skull. For C57BL/6J mouse experiments, n = 9 mice (n = 6 males, n = 3 females) were injected with 300 nl of rAAV5/PAAV-CaMKIIa-GCaMP6s to express GCaMP6s under control of the Ca^{2+} calmodulin dependent protein kinase IIα (CamKIIα) promoter. For PV^{cre} mouse experiments, n = 8 mice (n = 5 males, n = 3 females) were injected with 300 nl of rAAV5/pAAV.CAG.Flex.GCaMP6s.WPRE.SV40 to express GCaMP6s via a Cre-dependent CAG promoter in PV+ neurons. An additional bilateral craniotomy was made over the posterior cerebellum for placement of screws to anchor a dental cement enclosure at the base of the ferrule to the base of the skull.

For optogenetic experiments, OFC was bilaterally targeted for viral injections at the following stereotaxic coordinates from Bregma: AP +2.6mm, L +1.75mm and V −2.1mm, with optic fiber ferrules placed V -1.9mm from the skull at a +12 degree orientation. For C57BL/6J mouse experiments, n = 12 mice (n = 7 males, n = 5 females) were injected with 250 nl of rAAV5/CamKII-hChR2(H134R)-eYFP-WPRE to express ChR2 under the CaMKIIα promoter for optogenetic activation or a combination of 250 nL of rAAV5/Ef1a-DIO-EYFP and 250 nl of rAAV5/CamKII-GFP-Cre for CamKIIα promoter fluorophore controls. For PV^{cre} mouse experiments, n = 14 mice (n = 10 males, n = 4 females) were injected with 250 nl of rAAV5/Ef1a-DIO-hChR2(H134R)-eYFP to express cre-dependent ChR2 in PV+ neurons for optogenetic activation or 250 nL of rAAV5/Ef1a-DIO-EYFP for fluorophore controls.

For lesion experiments, OFC was bilaterally targeted for viral injections at the following stereotaxic coordinates from Bregma: AP +2.7mm, L +1.65mm and V −2.6mm. C57BL/6J mice (n = 39, n = 27 males, n = 12 females) were injected with a combination of 250 nl of rAAV5/Ef1a-DIO-mCherry and 250 nL of rAAV5/AAV-Flex-taCasP3-TEVP for cre-dependent apoptosis lesions or 250 nl of rAAV5/Ef1a-DIO-mCherry for sham lesion controls. To assess the presence and spread of lesions, brains were first cut into 50 um slices and store at 4C in .1% sodium azide PBS before undergoing NeuN staining procedures using Alexa Fluor 488 Conjugate ABN78A4 Anti-NeuN (rabbit) antibody (Sigma-Aldrich). Slices were washed 3 times for 10 minutes with 1x PBS and pre-incubated in 10% Horse Serum and 0.3% Triton-X-100-PBS with 1% BSA for 1 hour. After, slices were incubated for 48 hours at 4C with primary antibody (1:500) in 2% horse serum and 0.3% Triton X-100-PBS-1% BSA 2%. Slices were then washed for 10 minutes with 3x PBS and stored at 4C until imaging.

Fiber Photometry

After pre-training procedures, ferrule-implanted animals were unilaterally attached to bifurcated 400 um optical fiber tethers (Thorlabs, Newton, NJ) through which a 470nm LED (Thorlabs, Newton, NJ) excited virally expressed GCaMP6s (< 70 µW/mm2). Emitted fluorescence was monitored through the core of the bifurcated fiber using a 4x objective (Olympus, Shinjuku, Japan) focused onto a CMOS camera (FLIR Systems, Wilsonville, OR). Regions of interest demarcating each fiber fork were created within the fiber core using Bonsai software (Lopes et al., 2015) through which fluorescence intensity was captured at 20 Hz to produce two digitized signals, one for each animal connected to the bifurcated fiber. Analog behavioral timestamps for the

beginning and end of each lever press, head entry, and reinforcer delivery periods were simultaneously sent to Bonsai software via TTL Med-PC pulses using microprocessors (Arduino Duo, from Arduino, Sumerville, MA) containing custom code. After each session, Bonsai software saved photometry signals and behavioral timestamps within comma-separated value files (.csv) that were then imported into Matlab (Mathworks Inc., Natick, MA) for subsequent analysis using custom scripts (see Code Availability). Raw fluorescence intensity signals underwent running median (5th order) and low pass (high cutoff frequency of 1 Hz) filtering to reduce noise and electrical artifacts. To correct for photobleaching in which a signal captured from fluorophores degrades by continuous light exposure during the session, we high pass filtered the signal with a low cutoff frequency of 0.001Hz. Filtered fluorescence intensity signals subsequently underwent a quality check for low expression and fiber decoupling. Briefly, sessions that did not exceed a 15 second moving window calculation of the signal's 97.5 percentile by a minimum 1% fluorescence change were excluded from further analyses (Markowitz et al., 2018). Peri-event changes in fluorescence intensity were then calculated via z-score normalization to each corresponding pre-lever press onset period (i.e. -5 seconds to -2 seconds prior to lever press). These z-scored fluorescence traces were then combined across all mice within a group to preserve the variance seen within a subject. Activity during the ongoing lever press duration was modified using Akima interpolation via MATLAB's *interp1* function, excluding any lever press that was fewer than 2 samples (i.e. 100 ms) in duration that would invalidate interpolation. Comparisons between rewarded and unrewarded lever press traces were made using running permutation tests (1000 shuffles) that required at least 5 consecutive samples (or 3 consecutive

samples for interpolated activity) to be different from one another (Jean-Richard-dit-Bressel et al., 2020). Population Ca^{2+} activity traces were then smoothed with MATLAB's Savitzky–Golay *smoothdata* method using a 20 sample (or 1 sample for interpolated activity) sliding window for visual display purposes only.

Optogenetic Excitation

Optogenetic excitation occurred only in the additional 5 sessions (days 6-10) during which the minimum duration criteria was 1600 ms. LEDs (470nm, Thorlabs) used for optogenetic excitation experiments were triggered by TTL pulses emitted from Med-PC operant chambers via Arduino Duos programmed with custom code. Sheathed (200 uM) optic fiber cables were coupled to bilaterally implanted ferrules (>= 1mW output at ferrule tip) through which a closed-loop system delivered light at 20 Hz (5 ms pulses) throughout the entirety of each (or every 7th) lever press duration.

Data Analysis

Linear Mixed Effects Models of Behavior

Linear Mixed Effects (LME) models were built to investigate the predictive relationship between the duration of individual lever presses (n) and the lever press occurring immediately prior to it (n - 1) (Schreiner et al., 2022). Random intercept terms for mouse and training day were included to account for the repeated, non-independent structure of the aggregated session data. To account for variance explained by the overall performance within a session, fixed terms included the overall percentage of rewarded lever presses as well as the timestamps of each lever press. To test how predictive relationships were contingent upon their sequential order, beta coefficient outputs pertaining to each behavioral measurement of interest were compared to a 100

order shuffled distribution of beta coefficients using permutation testing (Supplementary Table 2.S1). Importantly, shuffling occurred within individual sessions/mice to preserve overall performance statistics (e.g. total lever presses made), and the order shuffling for each behavioral covariate occurred independently from each other. Thus the LME model for the behavioral cohort consisted of the following formula:

$$D_n = \beta_0 + \beta_D D_{n-1} + \beta_O O_{n-1} + \beta_{HE} HE_{n-1} + \beta_{IPI} IPI_{n-1} + \beta_t(t) + \beta_{\%}(\%) + (1|M) + (1|D) + \varepsilon_i$$

Where D_n is the current lever press duration, D_{n-1} is the prior lever press duration (in ms), O_{n-1} is the outcome of the prior lever press (binary 1 for reward, 0 for no reward), HE_{n-1} is the indicator of whether a head entry was made between the current and prior lever press (binary 1 for head entry made, 0 for no head entry made), IPI_{n-1} is the interpress interval (in ms), and B_x is the linear regression coefficient for each corresponding behavioral covariate term x (β_0 being the intercept term). Covariates for lever press timestamps (t, in ms) and overall percentage of rewarded lever presses (%) were included alongside random intercept terms for mouse (M) and day (D).

To determine how far back the predictive relationship existed between press n and any particular n-back press, we built and shuffled-order tested a similar LME model that included additional variables accounting for the duration of lever press n and n-back (n - 1 through n - 10) lever press durations as follows (Supplementary Table 2.S2):

$$n = \beta_0 + \beta_{n-1} n_{-1} + \beta_{n-2} n_{-2} + \ldots + \beta_{n-10} n_{-10} + \beta_t(t) + \beta_{\%}(\%) + (1|M) + (1|D) + \varepsilon_i$$

We built an additional LME model that included interaction terms to determine how prior behavioral variables (i.e. prior reward, checking, and interpress interval) compounded their effect on the subsequent lever press duration (Supplementary Table 2.S3):

$$D_n = \beta_0 + \beta_D D_{n-1} + \beta_O O_{n-1} + \beta_{HE} HE_{n-1} + \beta_{IPI} IPI_{n-1} + \beta_{O*D} O_{n-1}*D_{n-1} + \beta_{HE*D} HE_{n-1}*D_{n-1} + \beta_{IPI*D} IPI_{n-1}*D_{n-1} + \beta_t(t) + \beta_{\%}(\%) + (1|M) + (1|D) + \varepsilon_i$$

Regression coefficient terms β_x and shuffled-order testing procedures were as previously described, with the added covariates for main effects of prior duration (D_{n-1}, lever press duration in ms) and its interactions with prior lever press outcome ($O_{n-1}*D_{n-1}$), prior presence of a head entry ($HE_{n-1}*D_{n-1}$), and interpress interval ($IPI_{n-1}*D_{n-1}$).

To determine how the predictive relationship of behavioral covariates for current lever press durations were affected by experimental manipulations (e.g. optogenetic excitation via ChR2), we built and 1000 shuffled-order tested similar LME models that included additional variables accounting for treatment group main effects and interactions as follows (Supplementary Table 2.S6, Supplementary Table 2.S7, Supplementary Table 2.S8, Supplementary Table 2.S9, Supplementary Table 2.S10):

$$D_n = \beta_0 + \beta_D D_{n-1} + \beta_O O_{n-1} + \beta_{HE} HE_{n-1} + \beta_{IPI} IPI_{n-1} + \beta_t(t) + \beta_{\%}(\%) + \beta_{Tx}(Tx) + \beta_{D*Tx} D_{n-1}*Tx + \beta_{O*Tx} O_{n-1}*Tx + \beta_{HE*Tx} HE_{n-1}*Tx + \beta_{IPI*Tx} IPI_{n-1}*Tx + (1|M) + (1|D) + \varepsilon_i$$

Regression coefficient terms β_x in these models were as previously described, with the added covariates for main effects of treatment (Tx, binary 1 for experimental and 0 for control groups) and its interactions with prior lever press duration ($D_{n-1}*Tx$), prior outcome ($O_{n-1}*Tx$), prior presence of a head entry ($HE_{n-1}*Tx$), and interpress interval ($IPI_{n-1}*Tx$). For the optogenetic excitation experiment in which only every 7th lever press triggered light delivery, a post-hoc LME model was tested using only the ChR2 group. In this case, however, the treatment main effect term Tx (and associated interaction terms) instead indicated the presence or absence of optogenetic stimulation for each individual lever press.

Linear Mixed Effects Models of Ca^{2+} Activity

For OFC Ca^{2+} fluorescence activity monitoring experiments, LME models were built to predict Ca^{2+} activity within peri-event epochs given current and prior lever press durations alongside other behavioral variables. For these models, only data collected from the 1600 ms minimum duration criterion days were used. The mean area under the curve of activity traces during each of three epochs (-1s to 0s before lever press onset, lever press duration, and 0s to +1s after lever press release) was calculated to predict activity at each of these three time points using the following formula (Supplementary Table 2.S4, Supplementary Table 2.S5):

$$A_n = \beta_0 + \beta_D D_n + \beta_{D\text{-}1} D_{n-1} + \beta_O O_{n-1} + \beta_{HE} HE_{n-1} + \beta_{IPI} IPI_{n-1} + \beta_t(t) + \beta_{\%}(\%) + \beta_A A_{n-1} + (1|M) + (1|D) + \varepsilon_i$$

Where A_n is Ca^{2+} activity associated with the current lever press epoch (pre-onset, duration, or post-offset). Regression coefficient terms β_x in these models were as previously described, with the added covariates for main effects of current duration (D_n, in ms) and prior lever press activity (A_{n-1}) during that epoch to control for Ca^{2+} activity autocorrelation. LME regression coefficients for behavior measures of interest were compared to 1000 order shuffled datasets to test whether their predictive ability was due to the subsequent relationship.

Quantification and Statistical Analysis

All analyses were two-tailed and statistical significance was defined as an α of $p < 0.05$. Statistical analysis was performed using GraphPad Prism 8.3.0 (GraphPad Software) and custom MATLAB R2019a (MathWorks) scripts using a PC desktop with Windows 10. Acquisition data, including lever presses, response rate, and percentage

of lever presses that were rewarded were analyzed using one-way or two-way repeated measures ANOVAs with Greenhouse-Geisser corrections and Šidák corrections for post-hoc multiple comparisons unless otherwise noted. For outcome devaluation testing, a paired parametric t-test was performed to examine whether sensory-specific satiety reduced lever press responses on the devalued day compared to the valued day. For each LME model, we report the average regression coefficient (β), which measures the effect size and indicates how much a change in a predictor variable will change the output (e.g. lever press duration). Unless stated otherwise, significant predictors underwent follow-up permutation test comparisons for β coefficient values against a distribution of 1000 order or group shuffled versions of the same variable. For Ca^{2+} activity comparisons (i.e. reward vs no reward), permutation testing required 5 consecutive samples (or 3 consecutive samples for interpolated activity) that passed the threshold for significance. Lever presses longer than 10 seconds were excluded from all Ca^{2+} activity analyses. Data are presented as mean ± SEM.

Data Availability

The data reported in this paper will be shared by the lead contact upon request.

Code Availability

Data analysis code is freely available online at https://github.com/gremellab/OFC-Action-Inference

All scripts/functions were executed using Matlab 2019a.

Acknowledgements

Chapter 2, is, in full, a reprint of the material submitted to *Neuron* (2022). This work was funded by DGE-1650112 (C.C.), F99-NS120434 (C.C.), F31AA027439 (D.C.S.), R01AA026077 (C.M.G.), and a Whitehall Foundation Award (C.M.G).

Author Contributions

C.C.: Conceptualization, Formal analysis, Funding acquisition, Investigation, Methodology, Visualization, Writing - original draft, Writing - review and edition. D.C.S.: Formal analysis and Writing - review and editing. M.L.V.: Investigation and Writing - review and editing. C.M.G.: Conceptualization, Methodology, Supervision, Funding acquisition, Project administration, Visualization, Writing - original draft, Writing - review and editing.

References

Ahmari, S. E., Spellman, T., Douglass, N. L., Kheirbek, M. A., Simpson, H. B., Deisseroth, K., Gordon, J. A., & Hen, R. (2013). Repeated cortico-striatal stimulation generates persistent OCD-like behavior. *Science (New York, N.Y.)*, *340*(6137), 1234–1239. https://doi.org/10.1126/science.1234733

Balleine, B. W. (2019). The Meaning of Behavior: Discriminating Reflex and Volition in the Brain. *Neuron*, *104*(1), 47–62. https://doi.org/10.1016/j.neuron.2019.09.024

Balleine, B. W., & Dickinson, A. (1998). Goal-directed instrumental action: Contingency and incentive learning and their cortical substrates. *Neuropharmacology*, *37*(4–5), 407–419. https://doi.org/10.1016/s0028-3908(98)00033-1

Balleine, B. W., & O'Doherty, J. P. (2010). Human and rodent homologies in action control: Corticostriatal determinants of goal-directed and habitual action. *Neuropsychopharmacology: Official Publication of the American College of Neuropsychopharmacology*, *35*(1), 48–69. https://doi.org/10.1038/npp.2009.131

Baltz, E. T., Yalcinbas, E. A., Renteria, R., & Gremel, C. M. (2018). Orbital frontal cortex updates state-induced value change for decision-making. *ELife*, *7*, e35988. https://doi.org/10.7554/eLife.35988

Barreiros, I. V., Panayi, M. C., & Walton, M. E. (2021). Organization of Afferents along the Anterior-posterior and Medial-lateral Axes of the Rat Orbitofrontal Cortex. *Neuroscience*, *460*, 53–68. https://doi.org/10.1016/j.neuroscience.2021.02.017

Bechara, A., Damasio, H., Damasio, A. R., & Lee, G. P. (1999). Different Contributions of the Human Amygdala and Ventromedial Prefrontal Cortex to Decision-Making. *Journal of Neuroscience*, *19*(13), 5473–5481. https://doi.org/10.1523/JNEUROSCI.19-13-05473.1999

Bouton, M. E., & Balleine, B. W. (2019). Prediction and control of operant behavior: What you see is not all there is. *Behavior Analysis (Washington, D.C.)*, *19*(2), 202–212. https://doi.org/10.1037/bar0000108

Bradfield, L. A., Dezfouli, A., van Holstein, M., Chieng, B., & Balleine, B. W. (2015). Medial Orbitofrontal Cortex Mediates Outcome Retrieval in Partially Observable Task Situations. *Neuron*, *88*(6), 1268–1280. https://doi.org/10.1016/j.neuron.2015.10.044

Burguière, E., Monteiro, P., Feng, G., & Graybiel, A. M. (2013). Optogenetic Stimulation of Lateral Orbitofronto-Striatal Pathway Suppresses Compulsive Behaviors. *Science*, *340*(6137), 1243–1246. https://doi.org/10.1126/science.1232380

Burke, K. A., Franz, T. M., Miller, D. N., & Schoenbaum, G. (2008). The role of the orbitofrontal cortex in the pursuit of happiness and more specific rewards. *Nature*, *454*(7202), 340–344. https://doi.org/10.1038/nature06993

Burke, K. A., Takahashi, Y. K., Correll, J., Brown, P. L., & Schoenbaum, G. (2009). Orbitofrontal inactivation impairs reversal of Pavlovian learning by interfering with disinhibition of responding for previously unrewarded cues. *The European Journal of Neuroscience*, *30*(10), 1941–1946. https://doi.org/10.1111/j.1460-9568.2009.06992.x

Cai, X., & Padoa-Schioppa, C. (2014). Contributions of Orbitofrontal and Lateral Prefrontal Cortices to Economic Choice and the Good-to-action Transformation. *Neuron*, *81*(5), 1140–1151. https://doi.org/10.1016/j.neuron.2014.01.008

Camille, N., Tsuchida, A., & Fellows, L. K. (2011). Double Dissociation of Stimulus-Value and Action-Value Learning in Humans with Orbitofrontal or Anterior Cingulate Cortex Damage. *Journal of Neuroscience*, *31*(42), 15048–15052. https://doi.org/10.1523/JNEUROSCI.3164-11.2011

Cavada, C., Compañy, T., Tejedor, J., Cruz-Rizzolo, R. J., & Reinoso-Suárez, F. (2000). The Anatomical Connections of the Macaque Monkey Orbitofrontal Cortex. A Review. *Cerebral Cortex*, *10*(3), 220–242. https://doi.org/10.1093/cercor/10.3.220

Cazares, C., Schreiner, D. C., & Gremel, C. M. (2021). Different Effects of Alcohol Exposure on Action and Outcome-Related Orbitofrontal Cortex Activity. *ENeuro*, *8*(2). https://doi.org/10.1523/ENEURO.0052-21.2021

Costa, R. M. (2011). A selectionist account of de novo action learning. *Current Opinion in Neurobiology*, *21*(4), 579–586. https://doi.org/10.1016/j.conb.2011.05.004

Daw, N. D., Niv, Y., & Dayan, P. (2005). Uncertainty-based competition between prefrontal and dorsolateral striatal systems for behavioral control. *Nature Neuroscience*, *8*(12), 1704–1711. https://doi.org/10.1038/nn1560

Daw, N. D., O'Doherty, J. P., Dayan, P., Seymour, B., & Dolan, R. J. (2006). Cortical substrates for exploratory decisions in humans. *Nature*, *441*(7095), 876–879. https://doi.org/10.1038/nature04766

Dickinson, A. (1985). Actions and Habits: The Development of Behavioural Autonomy. *Philosophical Transactions of the Royal Society of London Series B*, *308*, 67. https://doi.org/10.1098/rstb.1985.0010

Doll, B. B., Simon, D. A., & Daw, N. D. (2012). The ubiquity of model-based reinforcement learning. *Current Opinion in Neurobiology*, *22*(6), 1075–1081.

https://doi.org/10.1016/j.conb.2012.08.003

Drummond, N., & Niv, Y. (2020). Model-based decision making and model-free learning. *Current Biology*, *30*(15), R860–R865. https://doi.org/10.1016/j.cub.2020.06.051

Duan, L. Y., Horst, N. K., Cranmore, S. A. W., Horiguchi, N., Cardinal, R. N., Roberts, A. C., & Robbins, T. W. (2021). Controlling one's world: Identification of sub-regions of primate PFC underlying goal-directed behavior. *Neuron*, *109*(15), 2485-2498.e5. https://doi.org/10.1016/j.neuron.2021.06.003

Fan, D., Rossi, M. A., & Yin, H. H. (2012). Mechanisms of action selection and timing in substantia nigra neurons. *The Journal of Neuroscience: The Official Journal of the Society for Neuroscience*, *32*(16), 5534–5548. https://doi.org/10.1523/JNEUROSCI.5924-11.2012

Fellows, L. K. (2011). Orbitofrontal contributions to value-based decision making: Evidence from humans with frontal lobe damage. *Annals of the New York Academy of Sciences*, *1239*, 51–58. https://doi.org/10.1111/j.1749-6632.2011.06229.x

Ferguson, K. A., & Cardin, J. A. (2020). Mechanisms underlying gain modulation in the cortex. *Nature Reviews. Neuroscience*, *21*(2), 80–92. https://doi.org/10.1038/s41583-019-0253-y

Fink, S. L., & Cookson, B. T. (2005). Apoptosis, Pyroptosis, and Necrosis: Mechanistic Description of Dead and Dying Eukaryotic Cells. *Infection and Immunity*, *73*(4), 1907–1916. https://doi.org/10.1128/IAI.73.4.1907-1916.2005

Fresno, V., Parkes, S. L., Faugère, A., Coutureau, E., & Wolff, M. (2019). A thalamocortical circuit for updating action-outcome associations. *ELife*, *8*, e46187. https://doi.org/10.7554/eLife.46187

Furuyashiki, T., Holland, P. C., & Gallagher, M. (2008). Rat Orbitofrontal Cortex Separately Encodes Response and Outcome Information during Performance of Goal-Directed Behavior. *Journal of Neuroscience*, *28*(19), 5127–5138. https://doi.org/10.1523/JNEUROSCI.0319-08.2008

Gallagher, M., McMahan, R. W., & Schoenbaum, G. (1999). Orbitofrontal Cortex and Representation of Incentive Value in Associative Learning. *Journal of Neuroscience*, *19*(15), 6610–6614. https://doi.org/10.1523/JNEUROSCI.19-15-06610.1999

Gardner, M. P. H., & Schoenbaum, G. (2021). The orbitofrontal cartographer. *Behavioral Neuroscience*, *135*(2), 267–276. https://doi.org/10.1037/bne0000463

Gourley, S. L., Olevska, A., Zimmermann, K. S., Ressler, K. J., DiLeone, R. J., & Taylor, J. R. (2013). The orbitofrontal cortex regulates outcome-based decision-making via the lateral striatum. *The European Journal of Neuroscience*, *38*(3). https://doi.org/10.1111/ejn.12239

Grattan, L. E., & Glimcher, P. W. (2014). Absence of Spatial Tuning in the Orbitofrontal Cortex. *PLOS ONE*, *9*(11), e112750. https://doi.org/10.1371/journal.pone.0112750

Gremel, C. M., Chancey, J. H., Atwood, B. K., Luo, G., Neve, R., Ramakrishnan, C., Deisseroth, K., Lovinger, D. M., & Costa, R. M. (2016). Endocannabinoid Modulation of Orbitostriatal Circuits Gates Habit Formation. *Neuron*, *90*(6), 1312–1324. https://doi.org/10.1016/j.neuron.2016.04.043

Gremel, C. M., & Costa, R. M. (2013). Orbitofrontal and striatal circuits dynamically encode the shift between goal-directed and habitual actions. *Nature Communications*, *4*, 2264. https://doi.org/10.1038/ncomms3264

Groman, S. M., Keistler, C., Keip, A. J., Hammarlund, E., DiLeone, R. J., Pittenger, C., Lee, D., & Taylor, J. R. (2019). Orbitofrontal Circuits Control Multiple Reinforcement-Learning Processes. *Neuron*, *103*(4), 734-746.e3. https://doi.org/10.1016/j.neuron.2019.05.042

Haggard, P. (2008). Human volition: Towards a neuroscience of will. *Nature Reviews Neuroscience*, *9*(12), 934–946. https://doi.org/10.1038/nrn2497

Hocker, D. L., Brody, C. D., Savin, C., & Constantinople, C. M. (2021). Subpopulations of neurons in lOFC encode previous and current rewards at time of choice. *ELife*, *10*, e70129. https://doi.org/10.7554/eLife.70129

Hogeveen, J., Mullins, T. S., Romero, J. D., Eversole, E., Rogge-Obando, K., Mayer, A. R., & Costa, V. D. (2022). The neurocomputational bases of explore-exploit decision-making. *Neuron*. https://doi.org/10.1016/j.neuron.2022.03.014

Hu, H., Gan, J., & Jonas, P. (2014). Fast-spiking, parvalbumin+ GABAergic interneurons: From cellular design to microcircuit function. *Science*, *345*(6196). https://doi.org/10.1126/science.1255263

Inagaki, H. K., Chen, S., Ridder, M. C., Sah, P., Li, N., Yang, Z., Hasanbegovic, H., Gao, Z., Gerfen, C. R., & Svoboda, K. (2022). A midbrain-thalamus-cortex circuit reorganizes cortical dynamics to initiate movement. *Cell*, *185*(6), 1065-1081.e23. https://doi.org/10.1016/j.cell.2022.02.006

Isaacson, J. S., & Scanziani, M. (2011). How Inhibition Shapes Cortical Activity. *Neuron*, *72*(2), 231–243. https://doi.org/10.1016/j.neuron.2011.09.027

Izquierdo, A., Suda, R. K., & Murray, E. A. (2004). Bilateral Orbital Prefrontal Cortex Lesions in Rhesus Monkeys Disrupt Choices Guided by Both Reward Value and Reward Contingency. *The Journal of Neuroscience*, *24*(34), 7540–7548. https://doi.org/10.1523/JNEUROSCI.1921-04.2004

Jean-Richard-dit-Bressel, P., Clifford, C. W. G., & McNally, G. P. (2020). Analyzing Event-Related Transients: Confidence Intervals, Permutation Tests, and Consecutive Thresholds. *Frontiers in Molecular Neuroscience*, *13*. https://www.frontiersin.org/article/10.3389/fnmol.2020.00014

Johnson, C. M., Peckler, H., Tai, L.-H., & Wilbrecht, L. (2016). Rule learning enhances structural plasticity of long-range axons in frontal cortex. *Nature Communications*, *7*, 10785. https://doi.org/10.1038/ncomms10785

Jones, J. L., Esber, G. R., McDannald, M. A., Gruber, A. J., Hernandez, A., Mirenzi, A., & Schoenbaum, G. (2012). Orbitofrontal cortex supports behavior and learning using inferred but not cached values. *Science (New York, N.Y.)*, *338*(6109), 953–956. https://doi.org/10.1126/science.1227489

Jovanovic, V., Fishbein, A. R., de la Mothe, L., Lee, K.-F., & Miller, C. T. (2022). Behavioral context affects social signal representations within single primate prefrontal cortex neurons. *Neuron*, *110*(8), 1318-1326.e4. https://doi.org/10.1016/j.neuron.2022.01.020

Kepecs, A., & Fishell, G. (2014). Interneuron cell types are fit to function. *Nature*, *505*(7483), 318–326. https://doi.org/10.1038/nature12983

Klaus, A., Alves da Silva, J., & Costa, R. M. (2019). What, If, and When to Move: Basal Ganglia Circuits and Self-Paced Action Initiation. *Annual Review of Neuroscience*, *42*(1), 459–483. https://doi.org/10.1146/annurev-neuro-072116-031033

Li, N., Chen, S., Guo, Z. V., Chen, H., Huo, Y., Inagaki, H. K., Chen, G., Davis, C., Hansel, D., Guo, C., & Svoboda, K. (2019). Spatiotemporal constraints on optogenetic inactivation in cortical circuits. *ELife*, *8*, e48622. https://doi.org/10.7554/eLife.48622

Li, N., Daie, K., Svoboda, K., & Druckmann, S. (2016). Robust neuronal dynamics in premotor cortex during motor planning. *Nature*, *532*(7600), 459–464. https://doi.org/10.1038/nature17643

Lopatina, N., Sadacca, B. F., McDannald, M. A., Styer, C. V., Peterson, J. F., Cheer, J. F., & Schoenbaum, G. (2017). Ensembles in medial and lateral orbitofrontal cortex construct cognitive maps emphasizing different features of the behavioral landscape. *Behavioral Neuroscience*, *131*(3), 201–212. https://doi.org/10.1037/bne0000195

Lopes, G., Bonacchi, N., Frazão, J., Neto, J. P., Atallah, B. V., Soares, S., Moreira, L., Matias, S., Itskov, P. M., Correia, P. A., Medina, R. E., Calcaterra, L., Dreosti, E., Paton, J. J., & Kampff, A. R. (2015). Bonsai: An event-based framework for processing and controlling data streams. *Frontiers in Neuroinformatics*, *9*. https://www.frontiersin.org/article/10.3389/fninf.2015.00007

Luk, C.-H., & Wallis, J. D. (2013). Choice Coding in Frontal Cortex during Stimulus-Guided or Action-Guided Decision-Making. *Journal of Neuroscience*, *33*(5), 1864–1871. https://doi.org/10.1523/JNEUROSCI.4920-12.2013

Lüscher, C., Robbins, T. W., & Everitt, B. J. (2020). The transition to compulsion in addiction. *Nature Reviews. Neuroscience*, *21*(5), 247–263. https://doi.org/10.1038/s41583-020-0289-z

Malvaez, M., Shieh, C., Murphy, M. D., Greenfield, V. Y., & Wassum, K. M. (2019). Distinct cortical-amygdala projections drive reward value encoding and retrieval. *Nature Neuroscience*, *22*(5), 762–769. https://doi.org/10.1038/s41593-019-0374-7

Milad, M. R., & Rauch, S. L. (2012). Obsessive-compulsive disorder: Beyond segregated cortico-striatal pathways. *Trends in Cognitive Sciences*, *16*(1), 43–51. https://doi.org/10.1016/j.tics.2011.11.003

Morrison, S. E., & Salzman, C. D. (2011). Representations of appetitive and aversive information in the primate orbitofrontal cortex. *Annals of the New York Academy of Sciences*, *1239*, 59–70. https://doi.org/10.1111/j.1749-6632.2011.06255.x

Murakami, M., Vicente, M. I., Costa, G. M., & Mainen, Z. F. (2014). Neural antecedents of self-initiated actions in secondary motor cortex. *Nature Neuroscience*, *17*(11), 1574–1582. https://doi.org/10.1038/nn.3826

Murphy, M. J. M., & Deutch, A. Y. (2018). Organization of afferents to the orbitofrontal cortex in the rat. *The Journal of Comparative Neurology*, *526*(9), 1498–1526. https://doi.org/10.1002/cne.24424

Namboodiri, V. M. K., Otis, J. M., van Heeswijk, K., Voets, E. S., Alghorazi, R. A., Rodriguez-Romaguera, J., Mihalas, S., & Stuber, G. D. (2019). Single-cell activity tracking reveals that orbitofrontal neurons acquire and maintain a long-term memory to guide behavioral adaptation. *Nature Neuroscience*, *22*(7), 1110–1121. https://doi.org/10.1038/s41593-019-0408-1

Nauczyciel, C., Le Jeune, F., Naudet, F., Douabin, S., Esquevin, A., Vérin, M., Dondaine, T., Robert, G., Drapier, D., & Millet, B. (2014). Repetitive transcranial magnetic stimulation over the orbitofrontal cortex for obsessive-compulsive disorder: A double-blind, crossover study. *Translational Psychiatry*, *4*, e436.

https://doi.org/10.1038/tp.2014.62

Niv, Y. (2019). Learning task-state representations. *Nature Neuroscience*, *22*(10), 1544–1553. https://doi.org/10.1038/s41593-019-0470-8

Nogueira, R., Abolafia, J. M., Drugowitsch, J., Balaguer-Ballester, E., Sanchez-Vives, M. V., & Moreno-Bote, R. (2017). Lateral orbitofrontal cortex anticipates choices and integrates prior with current information. *Nature Communications*, *8*(1), 1–13. https://doi.org/10.1038/ncomms14823

Ostlund, S. B., & Balleine, B. W. (2007). Orbitofrontal cortex mediates outcome encoding in Pavlovian but not instrumental conditioning. *The Journal of Neuroscience: The Official Journal of the Society for Neuroscience*, *27*(18), 4819–4825. https://doi.org/10.1523/JNEUROSCI.5443-06.2007

Padoa-Schioppa, C., & Assad, J. A. (2006). Neurons in the orbitofrontal cortex encode economic value. *Nature*, *441*(7090), 223–226. https://doi.org/10.1038/nature04676

Panayi, M. C., & Killcross, S. (2018). Functional heterogeneity within the rodent lateral orbitofrontal cortex dissociates outcome devaluation and reversal learning deficits. *ELife*, *7*, e37357. https://doi.org/10.7554/eLife.37357

Parkes, S. L., Ravassard, P. M., Cerpa, J.-C., Wolff, M., Ferreira, G., & Coutureau, E. (2018). Insular and Ventrolateral Orbitofrontal Cortices Differentially Contribute to Goal-Directed Behavior in Rodents. *Cerebral Cortex (New York, N.Y.: 1991)*, *28*(7), 2313–2325. https://doi.org/10.1093/cercor/bhx132

Pascoli, V., Hiver, A., Zessen, R. V., Loureiro, M., Achargui, R., Harada, M., Flakowski, J., & Lüscher, C. (2018). Stochastic synaptic plasticity underlying compulsion in a model of addiction. *Nature*, *564*(7736), 366. https://doi.org/10.1038/s41586-018-0789-4

Pauls, D. L., Abramovitch, A., Rauch, S. L., & Geller, D. A. (2014). Obsessive-compulsive disorder: An integrative genetic and neurobiological perspective. *Nature Reviews. Neuroscience*, *15*(6), 410–424. https://doi.org/10.1038/nrn3746

Platt, J. R., Kuch, D. O., & Bitgood, S. C. (1973). Rats' lever-press durations as psychophysical judgements of time. *Journal of the Experimental Analysis of Behavior*, *19*(2), 239–250. https://doi.org/10.1901/jeab.1973.19-239

Price, J. L. (2007). Definition of the orbital cortex in relation to specific connections with limbic and visceral structures and other cortical regions. *Annals of the New York Academy of Sciences*, *1121*, 54–71. https://doi.org/10.1196/annals.1401.008

Price, R. B., Gillan, C. M., Hanlon, C., Ferrarelli, F., Kim, T., Karim, H. T., Renard, M.,

Kaskie, R., Degutis, M., Wears, A., Vienneau, E. P., Peterchev, A. V., Brown, V., Siegle, G. J., Wallace, M. L., & Ahmari, S. E. (2021). Effect of Experimental Manipulation of the Orbitofrontal Cortex on Short-Term Markers of Compulsive Behavior: A Theta Burst Stimulation Study. *The American Journal of Psychiatry*, *178*(5), 459–468. https://doi.org/10.1176/appi.ajp.2020.20060821

Renteria, R., Baltz, E. T., & Gremel, C. M. (2018). Chronic alcohol exposure disrupts top-down control over basal ganglia action selection to produce habits. *Nature Communications*, *9*(1), 211. https://doi.org/10.1038/s41467-017-02615-9

Rhodes, S. E. V., & Murray, E. A. (2013). Differential Effects of Amygdala, Orbital Prefrontal Cortex, and Prelimbic Cortex Lesions on Goal-Directed Behavior in Rhesus Macaques. *The Journal of Neuroscience*, *33*(8), 3380–3389. https://doi.org/10.1523/JNEUROSCI.4374-12.2013

Riceberg, J. S., & Shapiro, M. L. (2017). Orbitofrontal Cortex Signals Expected Outcomes with Predictive Codes When Stable Contingencies Promote the Integration of Reward History. *Journal of Neuroscience*, *37*(8), 2010–2021. https://doi.org/10.1523/JNEUROSCI.2951-16.2016

Rich, E. L., & Wallis, J. D. (2016). Decoding subjective decisions from orbitofrontal cortex. *Nature Neuroscience*, *19*(7), 973–980. https://doi.org/10.1038/nn.4320

Robbins, T. W., Vaghi, M. M., & Banca, P. (2019). Obsessive-Compulsive Disorder: Puzzles and Prospects. *Neuron*, *102*(1), 27–47. https://doi.org/10.1016/j.neuron.2019.01.046

Roesch, M. R., Taylor, A. R., & Schoenbaum, G. (2006). Encoding of Time-Discounted Rewards in Orbitofrontal Cortex Is Independent of Value Representation. *Neuron*, *51*(4), 509–520. https://doi.org/10.1016/j.neuron.2006.06.027

Rolls, E. T. (2004). The functions of the orbitofrontal cortex. *Brain and Cognition*, *55*(1), 11–29. https://doi.org/10.1016/S0278-2626(03)00277-X

Rudebeck, P. H., Behrens, T. E., Kennerley, S. W., Baxter, M. G., Buckley, M. J., Walton, M. E., & Rushworth, M. F. S. (2008). Frontal Cortex Subregions Play Distinct Roles in Choices between Actions and Stimuli. *Journal of Neuroscience*, *28*(51), 13775–13785. https://doi.org/10.1523/JNEUROSCI.3541-08.2008

Rudebeck, P. H., & Murray, E. A. (2008). Amygdala and orbitofrontal cortex lesions differentially influence choices during object reversal learning. *The Journal of Neuroscience: The Official Journal of the Society for Neuroscience*, *28*(33), 8338–8343. https://doi.org/10.1523/JNEUROSCI.2272-08.2008

Sadacca, B. F., Wied, H. M., Lopatina, N., Saini, G. K., Nemirovsky, D., & Schoenbaum, G. (2018). Orbitofrontal neurons signal sensory associations underlying model-

based inference in a sensory preconditioning task. *ELife*, *7*, e30373. https://doi.org/10.7554/eLife.30373

Schoenbaum, G., Nugent, S. L., Saddoris, M. P., & Setlow, B. (2002). Orbitofrontal lesions in rats impair reversal but not acquisition of go, no-go odor discriminations. *Neuroreport*, *13*(6), 885–890. https://doi.org/10.1097/00001756-200205070-00030

Schoenbaum, G., Setlow, B., Nugent, S. L., Saddoris, M. P., & Gallagher, M. (2003). Lesions of orbitofrontal cortex and basolateral amygdala complex disrupt acquisition of odor-guided discriminations and reversals. *Learning & Memory (Cold Spring Harbor, N.Y.)*, *10*(2), 129–140. https://doi.org/10.1101/lm.55203

Schreiner, D. C., Cazares, C., Renteria, R., & Gremel, C. M. (2022). Information normally considered task-irrelevant drives decision-making and affects premotor circuit recruitment. *Nature Communications*, *13*(1), 2134. https://doi.org/10.1038/s41467-022-29807-2

Schreiner, D. C., & Gremel, C. M. (2018). Orbital Frontal Cortex Projections to Secondary Motor Cortex Mediate Exploitation of Learned Rules. *Scientific Reports*, *8*(1), 10979. https://doi.org/10.1038/s41598-018-29285-x

Schreiner, D. C., Yalcinbas, E. A., & Gremel, C. M. (2021). A Push For Examining Subjective Experience in Value-Based Decision-Making. *Current Opinion in Behavioral Sciences*, *41*, 45–49. https://doi.org/10.1016/j.cobeha.2021.03.020

Schuck, N. W., Cai, M. B., Wilson, R. C., & Niv, Y. (2016). Human Orbitofrontal Cortex Represents a Cognitive Map of State Space. *Neuron*, *91*(6), 1402–1412. https://doi.org/10.1016/j.neuron.2016.08.019

Sias, A. C., Morse, A. K., Wang, S., Greenfield, V. Y., Goodpaster, C. M., Wrenn, T. M., Wikenheiser, A. M., Holley, S. M., Cepeda, C., Levine, M. S., & Wassum, K. M. (2021). A bidirectional corticoamygdala circuit for the encoding and retrieval of detailed reward memories. *ELife*, *10*, e68617. https://doi.org/10.7554/eLife.68617

Simon, N. W., Wood, J., & Moghaddam, B. (2015). Action-outcome relationships are represented differently by medial prefrontal and orbitofrontal cortex neurons during action execution. *Journal of Neurophysiology*, *114*(6), 3374–3385. https://doi.org/10.1152/jn.00884.2015

Skinner, B. F. (1938). *The behavior of organisms: An experimental analysis* (p. 457). Appleton-Century.

Sohal, V. S., Zhang, F., Yizhar, O., & Deisseroth, K. (2009). Parvalbumin neurons and gamma rhythms enhance cortical circuit performance. *Nature*, *459*(7247), 698–702. https://doi.org/10.1038/nature07991

Stalnaker, T. A., Cooch, N. K., McDannald, M. A., Liu, T.-L., Wied, H., & Schoenbaum, G. (2014). Orbitofrontal neurons infer the value and identity of predicted outcomes. *Nature Communications*, *5*, 3926. https://doi.org/10.1038/ncomms4926

Stalnaker, T. A., Franz, T. M., Singh, T., & Schoenbaum, G. (2007). Basolateral Amygdala Lesions Abolish Orbitofrontal-Dependent Reversal Impairments. *Neuron*, *54*(1), 51–58. https://doi.org/10.1016/j.neuron.2007.02.014

Wikenheiser, A. M., & Schoenbaum, G. (2016). Over the river, through the woods: Cognitive maps in the hippocampus and orbitofrontal cortex. *Nature Reviews Neuroscience*, *17*(8), 513–523. https://doi.org/10.1038/nrn.2016.56

Wilson, R. C., Takahashi, Y. K., Schoenbaum, G., & Niv, Y. (2014). Orbitofrontal cortex as a cognitive map of task space. *Neuron*, *81*(2), 267–279. https://doi.org/10.1016/j.neuron.2013.11.005

Yalcinbas, E. A., Cazares, C., & Gremel, C. M. (2021). Call for a more balanced approach to understanding orbital frontal cortex function. *Behavioral Neuroscience*, *135*(2), 255–266. https://doi.org/10.1037/bne0000450

Yang, C. F., Chiang, M. C., Gray, D. C., Prabhakaran, M., Alvarado, M., Juntti, S. A., Unger, E. K., Wells, J. A., & Shah, N. M. (2013). Sexually dimorphic neurons in the ventromedial hypothalamus govern mating in both sexes and aggression in males. *Cell*, *153*(4), 896–909. https://doi.org/10.1016/j.cell.2013.04.017

Yin, H. (2009). The role of the murine motor cortex in action duration and order. *Frontiers in Integrative Neuroscience*, *3*. https://www.frontiersin.org/article/10.3389/neuro.07.023.2009

Yin, H. H., Knowlton, B. J., & Balleine, B. W. (2006). Inactivation of dorsolateral striatum enhances sensitivity to changes in the action-outcome contingency in instrumental conditioning. *Behavioural Brain Research*, *166*(2), 189–196. https://doi.org/10.1016/j.bbr.2005.07.012

Yoo, S. B. M., Hayden, B. Y., & Pearson, J. M. (2021). Continuous decisions. *Philosophical Transactions of the Royal Society B: Biological Sciences*, *376*(1819), 20190664. https://doi.org/10.1098/rstb.2019.0664

Zhang, S., Xu, M., Chang, W.-C., Ma, C., Hoang Do, J. P., Jeong, D., Lei, T., Fan, J. L., & Dan, Y. (2016). Organization of long-range inputs and outputs of frontal cortex for top-down control. *Nature Neuroscience*, *19*(12), 1733–1742. https://doi.org/10.1038/nn.4417

CONCLUSION

The ability to adapt our behavior when circumstances change is crucial to our daily lives. We're constantly adjusting when to act, what action to perform, and when to perform it. When the ability to adapt behavior breaks down, we engage in repetitive behaviors. Psychiatric disorders, like substance use disorders, are debilitating illnesses in which repetitive behaviors are recurrent and persistent. For example, a patient suffering from addiction may not change their actions for seeking and consuming a drug even when it is no longer as pleasurable as it was before. Unless we investigate the specific brain cells that support adaptive behavior, we will not know exactly what brain processes break down in addiction, and therefore existing therapies will remain limited and non-specific.

Chapters 1 and 2 of this dissertation focused on investigating the OFC, a brain region that is shown to be dysfunctional in alcohol dependence. Chapter 1 of this dissertation showed the impact of alcohol-dependence on OFC activity related to self-initiated actions and their associated outcomes. Chapter 2 revealed that activity from different neuron populations in the orbitofrontal cortex can represent action information and that disrupting this activity can make actions less reliant on prior performance. Before the experiments detailed in Chapter 2, it was not fully understood if OFC used information from prior actions to guide behavior. Chapter 2 also contributed to furthering our understanding of specifically what types of brain cells in the OFC may be dysfunctional in alcohol use disorder patients, as different cell-types were shown to process action and outcome-related information differently throughout action execution. Altogether, the findings from the experiments detailed in this dissertation showed that

adaptive behavior can be shaped by how the OFC represents action-related information and further support the OFC as a target brain region for the intervention of repetitive behaviors in neuropsychiatric disorders.

OFC Circuits are disrupted in Alcohol Dependence

The disruptions to behavioral flexibility observed in AUD (Sjoerds et al., 2013) suggest that continued alcohol abuse and relapse in these patient populations may be a consequence of an inability to change control of drug-seeking and drug-taking behaviors (Belin et al., 2013; Everitt and Robbins, 2005; Hogarth, 2020). While dependence-induced behavioral dysfunction can continue well into drug-abstinence, cases of long-term recovery seen in patient populations disprove a permanent loss of function (Dawson et al., 2005). Thus, an increased understanding of how alcohol dependence changes the neural circuits controlling adaptive behavior has been proposed to be leveraged in therapeutic approaches aimed at restoring appropriate adaptive behavior processes. The use of animal models has led to better characterization of circuits impacted by AUD and other substance-use disorders and raise the possibility of restoring behavioral flexibility in these disorders by targeting associated circuits (Lovinger and Gremel, 2021). Targeting these cortical circuits to treat AUD patients has grown in feasibility as intracranial brain stimulation therapies begin to show some level of success at treating impulsivity (Nauczyciel et al., 2014; Price et al., 2021).

Circuit-based approaches to understanding the impact of AUD on behavior have largely focused on investigating its effects on two competing systems for behavioral control (Everitt and Robbins, 2016; Gremel and Lovinger, 2017): associative circuits

shown to be essential for response-outcome associations and goal-directed control of actions (Balleine and Dickinson, 1998; Yin and Knowlton, 2006) and sensorimotor circuits known to produce stimulus-response associations and habitual actions (Yin and Knowlton, 2006). Within the associative circuitry lies OFC, which in preclinical work has been shown to be altered in relation to alcohol-dependence (Nimitvilai et al., 2016, 2017; Renteria et al., 2018), including specific alterations found in its projections to the dorsal striatum (Renteria et al., 2018, 2021). As the main input nucleus of the basal ganglia, dependence disruptions to OFC-DS projections are hypothesized to contribute in part to the loss of behavioral flexibility observed in substance-use disorder patients (Gillan et al., 2016; Lovinger and Gremel, 2021). The experiments detailed in Chapter 1 further support how alcohol dependence induces alterations to activity originating from OFC during adaptive behavior. That we found alterations in both outcome and action encoding indicate that alcohol dependence not only disrupts processing of information related to rewards (McMurray et al., 2016), but also to information specifically tied to actions even moments before its associated outcome is known. While outcome-related information has been shown to be transmitted by OFC to its distributed targets (Lichtenberg et al., 2017; Schoenbaum et al., 1998, 2003), such as the BLA (Sias et al., 2021), it remains to be seen whether action-related information is similarly transmitted to other motor circuits as a way to guide changes in behavior. A potential candidate region to examine this would be secondary motor cortex (M2), as its reciprocal connections to OFC (Zingg et al., 2014) and its vulnerability to the long-lasting effects of alcohol dependence (Morris et al., 2018) suggest behavioral control impairments seen in AUD patients may originate in part from disruptions to this circuit.

OFC Uses Action-Related Information for Behavioral Control

When we act to achieve a goal, we can create a conscious memory of our actions, such as whether performing those acts led to a failure or success. These memories can be used to adapt our actions the next time we perform the same task in the future. But we don't solely rely on our ability to recall explicit experiences related to performance. What sorts of other types of information derived from experience, in addition to information retrieved from memory, is being used to guide behavior? Given OFC's large role in encoding aspects of behavior such as the value of cued choices (Hocker et al., 2021; Nogueira et al., 2017; Riceberg and Shapiro, 2017; Roesch et al., 2006; Rudebeck and Murray, 2008; Schoenbaum et al., 2003), there has been an increased interest in investigating the capacity for OFC to maintain and update task-relevant information across performance. In one study, clusters of lOFC neurons during cued choice behaviors have been shown to encode a variety of task variables, including reward attributes and the animal's choices (Hocker et al., 2021). Importantly, when this study examined activity from these clusters before an upcoming choice was made, strong representations of prior reward outcomes were found right up to when the choice response was executed. This representation of outcome-related information from prior experiences aligns with other work demonstrating lOFC neuron sensitivity to reward history (Nogueira et al., 2017; Riceberg and Shapiro, 2017). For example, reward history integration by OFC neurons was shown to be dependent on consecutive reward episodes, suggesting that lOFC is recruited when reward history stabilizes and is predictive of future success (Riceberg and Shapiro, 2017). This integration of prior and current information is not limited to reward nor choices; sensory-related information

associated with specific stimuli were shown to be represented by lOFC neuron activity prior to the upcoming choice (Nogueira et al., 2017). Thus, it appears that lOFC plays a role in representing information from prior choices and outcomes to guide behavior, but what other sources of information could be at play? Given the constrained nature of the tasks used in these studies, the question remained whether information explicitly tied to the response itself, independent of observable and outcome-related information, can similarly be represented by lOFC populations during volitional behavior.

Debate over whether OFC is recruited for action-control processes comes from non-human primate studies investigating OFC's role in Pavlovian-related control of value-based behaviors (Knudsen and Wallis, 2022; Padoa-Schioppa, 2011). Through the use of *in vivo* recordings, these studies describe several features of OFC neurons that are largely uncontested, such as their ability to encode the expected value of outcomes (Padoa-Schioppa and Assad, 2006; Rich and Wallis, 2014) and choices (Kennerley et al., 2009, 2011; Rich and Wallis, 2016). That these studies found few OFC neurons selectively recruited during motor responses made in these tasks has led some to hypothesize that motor signals contribute little to OFC processes used for guiding value-based behavior (Knudsen and Wallis, 2022; Padoa-Schioppa, 2011). However, OFC's role in processing action-related information to shape adaptive behavior should not be discounted due to the quantity of neurons recruited in these studies. For example, a larger representation of value related information in these recordings does not necessitate the absence of other types of information being represented, especially when these studies have in fact found a small percentage of neurons that are active during motor responses alongside outcome and choice

representation (Kennerley et al., 2009; Padoa-Schioppa and Assad, 2006). While neuroanatomical evidence indicates OFC is less connected to regions directly involved in motor control (Barreiros et al., 2021; Cavada et al., 2000), such as M2 (Zingg et al., 2014), than other autonomic control regions, these sparse projections may nonetheless be contributing significantly to ongoing action-related processes. Thus, while non-human primate work supports how OFC processes outcome-related information to guide value-based, it would be remiss to discount OFC's role in processing action-related information in its entirety.

Chapters 1 and 2 provide direct evidence for lOFC supporting adaptive behavior in relation to the actions made to achieve a desired outcome. In Chapter 1, we show that lOFC activity is modulated with respect to an un-cued action. We also show that modulation tied to outcomes is affected by alcohol dependence. In Chapter 2, we show that action-related modulation by OFC is cell-type specific, and that features of prior actions are maintained by these populations during ongoing action execution. When we disrupted this activity, behavioral control changed and future actions relied less on prior performance. Disparities between our findings and prior reports may be due to our use of a task in which we disambiguated processes as they relate to actions independently from those of their associated outcomes. Nonetheless, our work does seem to suggest that lOFC encoding of action information is recruited for behavioral control within a specific context in which actions cannot rely solely on external sources of information like sensory cues.

Future Directions

Call for an Exploratory Approach to the Functional Dissection of OFC Circuitry

As is the case for the OFC, other brain regions have also historically been studied in the context of their cell populations with defined projection targets. Often attempts to map OFC anatomy have been guided by functional definitions that rely on circuit manipulations at a time when OFC heterogeneity is still not fully understood, resulting in different orders of segmentation that altogether paint a highly complex picture. Nonetheless, cross-species histological findings appear to agree on the idea that the OFC is made up of anatomically distinct sub-regions whose differences primarily lie on the basis of their cytoarchitectural organization, and more recently, the hypothesized function of its input and output projections. However, the cognitive or behavioral function that these projections in and out of these OFC subregions support does not always translate across species, largely due to technical limitations and differences in task design for assessing OFC function in humans and non-human primates.

In rodents, OFC is understood to be generally composed of three segments (medial, central, and lateral) with each of these segments having been further divided based on their position within an established circuit (i.e.. medial, ventral, lateral, dorsolateral), with some receiving greater attention than others due to a growing interest in their contributions to learning and value-based decision-making. For example, reciprocal connections between the lateral OFC and the BLA transmit reward-related information critical for decision-making behavior (Lichtenberg et al., 2017; Malvaez et al., 2019; Schoenbaum et al., 1998; Sias et al., 2021; Stalnaker et al., 2007). Other work has similarly highlighted how lateral OFC projections to the striatum carry value-based information supporting decision-making actions (Hirokawa et al., 2019; Renteria

et al., 2018). In contrast, monkey OFC neurons have been reported to not encode decision-making actions directly, but rather the value of expected outcomes from those actions (Kennerley et al., 2009). Nonetheless, structural and functional homologies across species do exist, as disrupting amygdala-OFC connectivity has been reported to alter value-based decision-making in monkeys (Fiuzat et al., 2017) and rodents (Sias et al., 2021). However, these examples of what is known about OFC functional connectivity and the types of information the region can represent, have all relied on a priori assumptions about known OFC input-output mappings, and all primarily centered around excitatory projection neurons. Given the vast complexity of the circuit mechanisms that support OFC function, unbiased approaches can pose an advantage for an increased understanding of OFC-dependent behavior.

Identification of OFC circuit changes that contribute to psychiatric disease has been constrained by a lack of robust exploratory methodology. For example, most research focused on OFC circuit function has relied on a priori assumptions about its known input-output mappings. Given the vast complexity of the circuit mechanisms that support OFC function, unbiased approaches can pose an advantage for identifying the functional changes that result in pathological OFC-dependent behavior. Monosynaptic rabies tracing is one such exploratory technique that allows for the whole-brain identification of the direct inputs to specific cell types (Callaway and Luo, 2015). This tool has been previously used to successfully map input changes onto cell populations across a variety of brain circuits and to subsequently guide functional manipulations in behaving animals (Tian et al., 2016). For example, previous use of this monosynaptic input mapping technique has revealed how drugs of abuse can redistribute OFC input

connectivity to genetically identified neuronal subpopulations critical for experience-dependent behaviors (Beier et al., 2017). Follow-up work further revealed how these cocaine-induced input changes result in a preferential strengthening of connections between neurons activated by cocaine exposure (Wall et al., 2019).

However, the scope of these studies extended well beyond investigating OFC input-output connectivity, and to date there have been no similar assessments made with other drugs of abuse. In addition, the efficiency of rabies spread across synapses remains uncertain, raising questions over the proportion of input neurons that are labeled by the virus. Nonetheless, use of this technique could elevate the direct quantification of the heterogeneity of orbitofrontal circuit connectivity across excitatory and inhibitory populations to the robust degree seen in other archetypical neuronal circuits, such as in the vision and motor systems. In revealing OFC input-output connectivity we will achieve a greater understanding of what types of information processed by OFC is sent to its distributed network for control of behavior. As seen in Chapter 2, OFC populations differentially contribute to actions. OFC projects to M2 (Zingg et al., 2014) and this circuit has been similarly implicated in compulsive disorders and repetitive behaviors, including AUD (Duka et al., 2011; Morris et al., 2018). Future work should examine how a history of alcohol dependence may result in a redistribution of input connectivity from OFC to M2 and investigate whether any observed changes in connectivity are also associated with how action-related information critical for behavioral control is relayed in this projection.

Call for Investigating OFC Function Outside of Instructed Behavior

What we do know about OFC functional connectivity underscores the region as a key node in the bottom-up integration and top-down control of sensory information for the modulation of behavioral output (Liu et al., 2020; Wang et al., 2020). These integrative functions, largely investigated within the context of the OFC's canonical role in value assignment and value-based behaviors, warrants further exploration to the same level of scrutiny as its sensory input regions have received (e.g., primary visual cortex). For example, the vast majority of work ascribing function to the OFC has focused on using behavioral tasks or instructed movements (e.g. lever press or spout lick) to investigate the dynamics of the region's contributions to cognitive processes. With the ongoing development of technology that allows for large-scale data acquisition of cortical activity and behavior, spontaneous, non-task related activity can now be broadly investigated outside of two-dimensional measures, as typically seen with pupil diameter and its association with arousal states. For instance, considerable progress has been made in understanding the function of non-task related spontaneous activity occurring within the visual cortex (Stringer et al., 2019). The brain is never at rest, and in this vein, ongoing spontaneous activity in the visual cortex has been found to signal information firmly associated with multidimensional behavioral and cognitive states not fully captured by uninstructed locomotion or pupil diameter alone.

The vast majority of work ascribing function to the OFC has focused on using constrained and rigid tasks to investigate the dynamics of the region's contributions to behavioral control processes. Future work could benefit from taking a step back and asking, what does the OFC do with incoming sensory information in the absence of elicited behavioral output? If the integration of spontaneous sensory information with

non-task related motor actions can manifest as early as the primary visual cortex, how do the higher-order cortices process this spontaneous activity outside of a task-related context? Through the use of wide-field calcium imaging, uninstructed movements have been found to influence the single-trial variability of cortex-wide activity occurring on the dorsal surface of the brain as mice performed a decision-making task (Musall et al., 2019). The advent of gradient refractive index lenses and miniaturized head-mounted microendoscopes should allow for similar investigations exploring the function of spontaneous OFC activity outside of the context of instructed behavior (Flusberg et al., 2008). There's a lot we may be missing by ignoring what's happening in OFC that challenges the notion of this region being exclusively contributing to control of value-based behaviors.

References

Balleine, B.W., and Dickinson, A. (1998). Goal-directed instrumental action: contingency and incentive learning and their cortical substrates. Neuropharmacology *37*, 407–419. https://doi.org/10.1016/s0028-3908(98)00033-1.

Barreiros, I., Ishii, H., Walton, M., and Panagi, M.C. (2021). Defining an orbitofrontal compass: functional and anatomical heterogeneity across anterior-posterior and medial-lateral axes. Behavioral Neuroscience.

Beier, K.T., Kim, C.K., Hoerbelt, P., Hung, L.W., Heifets, B.D., DeLoach, K.E., Mosca, T.J., Neuner, S., Deisseroth, K., Luo, L., et al. (2017). Rabies screen reveals GPe control of cocaine-triggered plasticity. Nature *549*, 345–350. https://doi.org/10.1038/nature23888.

Belin, D., Belin-Rauscent, A., Murray, J.E., and Everitt, B.J. (2013). Addiction: failure of control over maladaptive incentive habits. Current Opinion in Neurobiology *23*, 564–572. https://doi.org/10.1016/j.conb.2013.01.025.

Callaway, E.M., and Luo, L. (2015). Monosynaptic Circuit Tracing with Glycoprotein-Deleted Rabies Viruses. J. Neurosci. *35*, 8979–8985. https://doi.org/10.1523/JNEUROSCI.0409-15.2015.

Cavada, C., Compañy, T., Tejedor, J., Cruz-Rizzolo, R.J., and Reinoso-Suárez, F. (2000). The Anatomical Connections of the Macaque Monkey Orbitofrontal Cortex. A Review. Cereb Cortex *10*, 220–242. https://doi.org/10.1093/cercor/10.3.220.

Dawson, D.A., Grant, B.F., Stinson, F.S., Chou, P.S., Huang, B., and Ruan, W.J. (2005). Recovery from DSM-IV alcohol dependence: United States, 2001–2002. Addiction *100*, 281–292. https://doi.org/10.1111/j.1360-0443.2004.00964.x.

Duka, T., Trick, L., Nikolaou, K., Gray, M.A., Kempton, M.J., Williams, H., Williams, S.C.R., Critchley, H.D., and Stephens, D.N. (2011). Unique Brain Areas Associated with Abstinence Control Are Damaged in Multiply Detoxified Alcoholics. Biol Psychiatry *70*, 545–552. https://doi.org/10.1016/j.biopsych.2011.04.006.

Everitt, B.J., and Robbins, T.W. (2005). Neural systems of reinforcement for drug addiction: from actions to habits to compulsion. Nat Neurosci *8*, 1481–1489. https://doi.org/10.1038/nn1579.

Everitt, B.J., and Robbins, T.W. (2016). Drug Addiction: Updating Actions to Habits to Compulsions Ten Years On. Annu Rev Psychol *67*, 23–50. https://doi.org/10.1146/annurev-psych-122414-033457.

Fiuzat, E.C., Rhodes, S.E.V., and Murray, E.A. (2017). The Role of Orbitofrontal–Amygdala Interactions in Updating Action–Outcome Valuations in Macaques. J Neurosci *37*, 2463–2470. https://doi.org/10.1523/JNEUROSCI.1839-16.2017.

Flusberg, B.A., Nimmerjahn, A., Cocker, E.D., Mukamel, E.A., Barretto, R.P.J., Ko, T.H., Burns, L.D., Jung, J.C., and Schnitzer, M.J. (2008). High-speed, miniaturized fluorescence microscopy in freely moving mice. Nat Methods *5*, 935–938. https://doi.org/10.1038/nmeth.1256.

Gillan, C.M., Kosinski, M., Whelan, R., Phelps, E.A., and Daw, N.D. (2016). Characterizing a psychiatric symptom dimension related to deficits in goal-directed control. Elife *5*. https://doi.org/10.7554/eLife.11305.

Gremel, C.M., and Lovinger, D.M. (2017). Associative and sensorimotor cortico-basal ganglia circuit roles in effects of abused drugs. Genes, Brain and Behavior *16*, 71–85. https://doi.org/10.1111/gbb.12309.

Hirokawa, J., Vaughan, A., Masset, P., Ott, T., and Kepecs, A. (2019). Frontal cortex neuron types categorically encode single decision variables. Nature *576*, 446–451. https://doi.org/10.1038/s41586-019-1816-9.

Hocker, D.L., Brody, C.D., Savin, C., and Constantinople, C.M. (2021). Subpopulations of neurons in lOFC encode previous and current rewards at time of choice. ELife *10*, e70129. https://doi.org/10.7554/eLife.70129.

Hogarth, L. (2020). Addiction is driven by excessive goal-directed drug choice under negative affect: translational critique of habit and compulsion theory. Neuropsychopharmacol. *45*, 720–735. https://doi.org/10.1038/s41386-020-0600-8.

Kennerley, S.W., Dahmubed, A.F., Lara, A.H., and Wallis, J.D. (2009). Neurons in the frontal lobe encode the value of multiple decision variables. J Cogn Neurosci *21*, 1162–1178. https://doi.org/10.1162/jocn.2009.21100.

Kennerley, S.W., Behrens, T.E.J., and Wallis, J.D. (2011). Double dissociation of value computations in orbitofrontal and anterior cingulate neurons. Nat Neurosci *14*, 1581–1589. https://doi.org/10.1038/nn.2961.

Knudsen, E.B., and Wallis, J.D. (2022). Taking stock of value in the orbitofrontal cortex. Nat Rev Neurosci 1–11. https://doi.org/10.1038/s41583-022-00589-2.

Lichtenberg, N.T., Pennington, Z.T., Holley, S.M., Greenfield, V.Y., Cepeda, C., Levine, M.S., and Wassum, K.M. (2017). Basolateral Amygdala to Orbitofrontal Cortex Projections Enable Cue-Triggered Reward Expectations. J. Neurosci. *37*, 8374–8384. https://doi.org/10.1523/JNEUROSCI.0486-17.2017.

Liu, S., Ye, M., Pao, G.M., Song, S.M., Jhang, J., and Han, S. (2020). Identification of a novel breathing circuit that controls pain and anxiety. BioRxiv 2020.01.09.900738. https://doi.org/10.1101/2020.01.09.900738.

Lovinger, D.M., and Gremel, C.M. (2021). A circuit-based information approach to substance abuse research. Trends in Neurosciences *44*, 122–135. https://doi.org/10.1016/j.tins.2020.10.005.

Malvaez, M., Shieh, C., Murphy, M.D., Greenfield, V.Y., and Wassum, K.M. (2019). Distinct cortical-amygdala projections drive reward value encoding and retrieval. Nat Neurosci *22*, 762–769. https://doi.org/10.1038/s41593-019-0374-7.

McMurray, M.S., Amodeo, L.R., and Roitman, J.D. (2016). Consequences of Adolescent Ethanol Consumption on Risk Preference and Orbitofrontal Cortex Encoding of Reward. Neuropsychopharmacology *41*, 1366–1375. https://doi.org/10.1038/npp.2015.288.

Morris, L.S., Baek, K., Tait, R., Elliott, R., Ersche, K.D., Flechais, R., McGonigle, J., Murphy, A., Nestor, L.J., Orban, C., et al. (2018). Naltrexone ameliorates functional network abnormalities in alcohol-dependent individuals. Addict Biol *23*, 425–436. https://doi.org/10.1111/adb.12503.

Musall, S., Kaufman, M.T., Juavinett, A.L., Gluf, S., and Churchland, A.K. (2019). Single-trial neural dynamics are dominated by richly varied movements. Nat Neurosci *22*, 1677–1686. https://doi.org/10.1038/s41593-019-0502-4.

Nauczyciel, C., Le Jeune, F., Naudet, F., Douabin, S., Esquevin, A., Vérin, M., Dondaine, T., Robert, G., Drapier, D., and Millet, B. (2014). Repetitive transcranial magnetic stimulation over the orbitofrontal cortex for obsessive-compulsive disorder: a double-blind, crossover study. Transl Psychiatry *4*, e436. https://doi.org/10.1038/tp.2014.62.

Nimitvilai, S., Lopez, M.F., Mulholland, P.J., and Woodward, J.J. (2016). Chronic Intermittent Ethanol Exposure Enhances the Excitability and Synaptic Plasticity of Lateral Orbitofrontal Cortex Neurons and Induces a Tolerance to the Acute Inhibitory Actions of Ethanol. Neuropsychopharmacology *41*, 1112–1127. https://doi.org/10.1038/npp.2015.250.

Nimitvilai, S., Uys, J.D., Woodward, J.J., Randall, P.K., Ball, L.E., Williams, R.W., Jones, B.C., Lu, L., Grant, K.A., and Mulholland, P.J. (2017). Orbitofrontal Neuroadaptations and Cross-Species Synaptic Biomarkers in Heavy-Drinking Macaques. J. Neurosci. *37*, 3646–3660. https://doi.org/10.1523/JNEUROSCI.0133-17.2017.

Nogueira, R., Abolafia, J.M., Drugowitsch, J., Balaguer-Ballester, E., Sanchez-Vives, M.V., and Moreno-Bote, R. (2017). Lateral orbitofrontal cortex anticipates choices

and integrates prior with current information. Nat Commun *8*, 1–13. https://doi.org/10.1038/ncomms14823.

Padoa-Schioppa, C. (2011). Neurobiology of economic choice: a good-based model. Annu Rev Neurosci *34*, 333–359. https://doi.org/10.1146/annurev-neuro-061010-113648.

Padoa-Schioppa, C., and Assad, J.A. (2006). Neurons in the orbitofrontal cortex encode economic value. Nature *441*, 223–226. https://doi.org/10.1038/nature04676.

Price, R.B., Gillan, C.M., Hanlon, C., Ferrarelli, F., Kim, T., Karim, H.T., Renard, M., Kaskie, R., Degutis, M., Wears, A., et al. (2021). Effect of Experimental Manipulation of the Orbitofrontal Cortex on Short-Term Markers of Compulsive Behavior: A Theta Burst Stimulation Study. Am J Psychiatry *178*, 459–468. https://doi.org/10.1176/appi.ajp.2020.20060821.

Renteria, R., Baltz, E.T., and Gremel, C.M. (2018). Chronic alcohol exposure disrupts top-down control over basal ganglia action selection to produce habits. Nat Commun *9*. https://doi.org/10.1038/s41467-017-02615-9.

Renteria, R., Cazares, C., Baltz, E.T., Schreiner, D.C., Yalcinbas, E.A., Steinkellner, T., Hnasko, T.S., and Gremel, C.M. (2021). Mechanism for differential recruitment of orbitostriatal transmission during actions and outcomes following chronic alcohol exposure. Elife *10*, e67065. https://doi.org/10.7554/eLife.67065.

Riceberg, J.S., and Shapiro, M.L. (2017). Orbitofrontal Cortex Signals Expected Outcomes with Predictive Codes When Stable Contingencies Promote the Integration of Reward History. J. Neurosci. *37*, 2010–2021. https://doi.org/10.1523/JNEUROSCI.2951-16.2016.

Rich, E.L., and Wallis, J.D. (2014). Medial-lateral organization of the orbitofrontal cortex. J Cogn Neurosci *26*, 1347–1362. https://doi.org/10.1162/jocn_a_00573.

Rich, E.L., and Wallis, J.D. (2016). Decoding subjective decisions from orbitofrontal cortex. Nat. Neurosci. *19*, 973–980. https://doi.org/10.1038/nn.4320.

Roesch, M.R., Taylor, A.R., and Schoenbaum, G. (2006). Encoding of Time-Discounted Rewards in Orbitofrontal Cortex Is Independent of Value Representation. Neuron *51*, 509–520. https://doi.org/10.1016/j.neuron.2006.06.027.

Rudebeck, P.H., and Murray, E.A. (2008). Amygdala and orbitofrontal cortex lesions differentially influence choices during object reversal learning. J Neurosci *28*, 8338–8343. https://doi.org/10.1523/JNEUROSCI.2272-08.2008.

Schoenbaum, G., Chiba, A.A., and Gallagher, M. (1998). Orbitofrontal cortex and basolateral amygdala encode expected outcomes during learning. Nature Neuroscience *1*, 155–159. https://doi.org/10.1038/407.

Schoenbaum, G., Setlow, B., Saddoris, M.P., and Gallagher, M. (2003). Encoding Predicted Outcome and Acquired Value in Orbitofrontal Cortex during Cue Sampling Depends upon Input from Basolateral Amygdala. Neuron *39*, 855–867. https://doi.org/10.1016/S0896-6273(03)00474-4.

Sias, A.C., Morse, A.K., Wang, S., Greenfield, V.Y., Goodpaster, C.M., Wrenn, T.M., Wikenheiser, A.M., Holley, S.M., Cepeda, C., Levine, M.S., et al. (2021). A bidirectional corticoamygdala circuit for the encoding and retrieval of detailed reward memories. Elife *10*, e68617. https://doi.org/10.7554/eLife.68617.

Sjoerds, Z., de Wit, S., van den Brink, W., Robbins, T.W., Beekman, A.T.F., Penninx, B.W.J.H., and Veltman, D.J. (2013). Behavioral and neuroimaging evidence for overreliance on habit learning in alcohol-dependent patients. Transl Psychiatry *3*, e337. https://doi.org/10.1038/tp.2013.107.

Stalnaker, T.A., Franz, T.M., Singh, T., and Schoenbaum, G. (2007). Basolateral amygdala lesions abolish orbitofrontal-dependent reversal impairments. Neuron *54*, 51–58. https://doi.org/10.1016/j.neuron.2007.02.014.

Stringer, C., Pachitariu, M., Steinmetz, N., Reddy, C.B., Carandini, M., and Harris, K.D. (2019). Spontaneous behaviors drive multidimensional, brainwide activity. Science *364*, 255. https://doi.org/10.1126/science.aav7893.

Tian, J., Huang, R., Cohen, J.Y., Osakada, F., Kobak, D., Machens, C.K., Callaway, E.M., Uchida, N., and Watabe-Uchida, M. (2016). Distributed and Mixed Information in Monosynaptic Inputs to Dopamine Neurons. Neuron *91*, 1374–1389. https://doi.org/10.1016/j.neuron.2016.08.018.

Wall, N.R., Neumann, P.A., Beier, K.T., Mokhtari, A.K., Luo, L., and Malenka, R.C. (2019). Complementary Genetic Targeting and Monosynaptic Input Mapping Reveal Recruitment and Refinement of Distributed Corticostriatal Ensembles by Cocaine. Neuron *104*, 916-930.e5. https://doi.org/10.1016/j.neuron.2019.10.032.

Wang, F., Schoenbaum, G., and Kahnt, T. (2020). Interactions between human orbitofrontal cortex and hippocampus support model-based inference. PLOS Biology *18*, e3000578. https://doi.org/10.1371/journal.pbio.3000578.

Yin, H.H., and Knowlton, B.J. (2006). The role of the basal ganglia in habit formation. Nat Rev Neurosci *7*, 464–476. https://doi.org/10.1038/nrn1919.

Zingg, B., Hintiryan, H., Gou, L., Song, M.Y., Bay, M., Bienkowski, M.S., Foster, N.N., Yamashita, S., Bowman, I., Toga, A.W., et al. (2014). Neural Networks of the

Mouse Neocortex. Cell *156*, 1096–1111.
https://doi.org/10.1016/j.cell.2014.02.023.